AD_____

Award Number: W81XWH-11-1-0150

TITLE: Protection by Purines in Toxin Models of Parkinson's Disease

PRINCIPAL INVESTIGATOR: Michael A. Schwarzschild, MD PhD

CONTRACTING ORGANIZATION:
MASSACHUSETTS GENERAL HOSPITAL
BOSTON MA 02114-2554

REPORT DATE: July 2013

TYPE OF REPORT: Final Year 2

PREPARED FOR: U.S. Army Medical Research and Materiel Command
Fort Detrick, Maryland 21702-5012

DISTRIBUTION STATEMENT:

☑ Approved for public release; distribution unlimited

The views, opinions and/or findings contained in this report are those of the author(s) and should not be construed as an official Department of the Army position, policy or decision unless so designated by other documentation.

REPORT DOCUMENTATION PAGE

Form Approved
OMB No. 0704-0188

Public reporting burden for this collection of information is estimated to average 1 hour per response, including the time for reviewing instructions, searching existing data sources, gathering and maintaining the data needed, and completing and reviewing this collection of information. Send comments regarding this burden estimate or any other aspect of this collection of information, including suggestions for reducing this burden to Department of Defense, Washington Headquarters Services, Directorate for Information Operations and Reports (0704-0188), 1215 Jefferson Davis Highway, Suite 1204, Arlington, VA 22202-4302. Respondents should be aware that notwithstanding any other provision of law, no person shall be subject to any penalty for failing to comply with a collection of information if it does not display a currently valid OMB control number. **PLEASE DO NOT RETURN YOUR FORM TO THE ABOVE ADDRESS.**

1. REPORT DATE *(DD-MM-YYYY)*
July 2013

2. REPORT TYPE
Final Year 2

3. DATES COVERED *(From - To)*
17-JAN-2011 - 14 Jun 2013

4. TITLE AND SUBTITLE
Protection by Purines in Toxin Models of Parkinson's Disease

5a. CONTRACT NUMBER

5b. GRANT NUMBER
W81XWH-11-1-0150

5c. PROGRAM ELEMENT NUMBER

5d. PROJECT NUMBER
W23RYX0285N601

5e. TASK NUMBER

5f. WORK UNIT NUMBER

6. AUTHOR(S)
Michael A. Schwarzschild, MD PhD (principal investigator)
email: michaels@helix.mgh.harvard.edu

7. PERFORMING ORGANIZATION NAME(S) AND ADDRESS(ES)
Massachusetts General Hospital
Boston, MA 02114-2554

8. PERFORMING ORGANIZATION REPORT NUMBER

9. SPONSORING / MONITORING AGENCY NAME(S) AND ADDRESS(ES)
US ARMYMEDICAL RESEARCH ACQUISITION ACT
Director
820 CHANDLER STREET
FORT DETRICKMD 21702-5014

10. SPONSOR/MONITOR'S ACRONYM(S)
USAMRAA

11. SPONSOR/MONITOR'S REPORT NUMBER(S)

12. DISTRIBUTION / AVAILABILITY STATEMENT Approved for public release (distribution unlimited)

13. SUPPLEMENTARY NOTES

14. ABSTRACT

In Year 2 of the project substantial progress has been made toward our original Specific Aims (SAs) and broader central goal of elucidating the neuroprotective potential and mechanisms of purines implicated in the neurodegeneration of Parkinson's disease (PD). Major published findings during Year 2 included our demonstrations that α-synuclein toxicity in a mouse model of PD depends upon caffeine's putative molecular target, the adenosine A_{2A} receptor (**SA1**); that raising or lowering endogenous urate (through knockout [KO] of the *urate oxidase* [*UOx*] gene or its transgenic overexpression) attenuates or exacerbates, respectively, toxin-induced dopaminergic neuron degeneration in mouse models of PD (**SA2**); and that urate confers protection against oxidative toxins in cellular models of PD in a strikingly astrocyte-dependent manner (**SA3**). We also published methodological and collaborative progress in support of all three SAs. Recently we have obtained preliminary data identifying released glutathione as a likely candidate for the astrocytic protective factor. In addition in year 2 we have begun to characterize a conditional *UOx* KO to obviate developmental confounds of the initially reported constitutive *UOx* KO. Together our findings strengthen the rationale for pursuing purine targets as candidate neuroprotective strategies for PD, and have epidemiological and military as well as translational significance.

15. SUBJECT TERMS
urate, tri-oxy-purine, synuclein, neuroprotection, neurotoxin, Parkinson's disease

16. SECURITY CLASSIFICATION OF:			17. LIMITATION OF ABSTRACT	18. NUMBER OF PAGES	19a. NAME OF RESPONSIBLE PERSON
					USAMRMC
a. REPORT	b. ABSTRACT	c. THIS PAGE			19b. TELEPHONE NUMBER *(inc area code)*
U	U	U	UU	71	

Standard Form 298 (Rev. 8-98)
Prescribed by ANSI Std. Z39.18

Table of Contents

Cover…… 1

SF 298/abstract……..…... 2

Table of Contents……..……... 3

Introduction…… 4

Body……. 5-11

Key Research Accomplishments…….…... 11

Reportable Outcomes…….……...… 12-13

Conclusions/Plans/Significance……..… 13-14

Appendices

Year 2 Journal Publications (*acknowledging DoD/W81XWH--1-0150*)

A: Kachroo A & Schwarzschild MA. 2012 [*Arch. Neurol.*]

B: Schwarzschild MA. 2012 [*Neurology*]

C: Burdett T *et al*, 2013 [*Biomed Chromatogr.*]

D: Chen X, Wu G & Schwarzschild MA. 2012 [*Curr Neurol Neurosci.*]

E: Cipriani S *et al*, 2012a [*PLoS One*]

F: Cipriani S *et al*, 2012b [*J. Neurochem.*]

G: Chen X *et al.* 2013 [*Proc Natl Acad Sci USA*]

H: Salamone J *et al*, 2012 [*Eur. Neuropsychopharmacol.*]

Introduction (unchanged from proposal SOW)

The overarching aim of the proposed work is to characterize the ***mechanisms and neuroprotective potential of purines linked to better outcomes in Parkinson's disease*** *(PD)*. We will pursue 3 Specific Aims (SAs) outlined in Section 3 below, and schematized in Figure 1 in the context of purine metabolism and dopaminergic neuron death. **SA1** seeks to determine the effects of the adenosine A_{2A} receptor antagonist caffeine as well as of neuronal A_{2A} receptor knockout (KO) in unilateral toxin models of PD. The potential role of excitotoxic glutatmate release will be investigated. **SA2** will assess the effects of the antioxidant urate (a.k.a. uric acid) on neurotoxicity *in vivo* using complementary pharmacologic and genetic approaches. Inosine, a therapeutically relevant urate precusor, will be tested along with genetic manipulations of urate metabolism, including global KO or conditional KO (cKO) of the *urate oxidase* (*UOx*) or *xanthine oxidoreductase* (*XOR*) genes. **SA3** will explore oxidative and α-synuclein mechanisms of urate protection in a neuronal cell culture models of PD. We propose to systematically pursue the following work on each SA with completion times indicated in brackets.

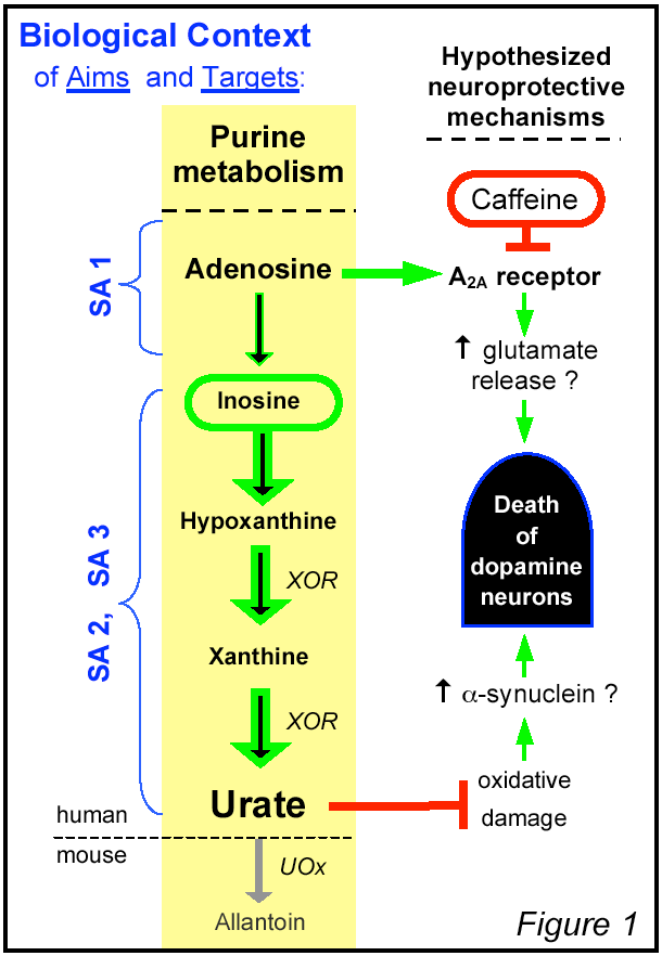

Figure 1

SA 1: **Mechanisms of protection by caffeine in toxin models of PD *in vivo***

Aim 1a: After establishing a 2,4-dichlorophenoxyacetic acid (2,4-D) model in mice [**Yr 1**], comparing the effects of systemic caffeine on 2,4-D *vs* 6-OHDA toxicities [**Yr 2**].

Aim 1b: Caffeine effects on toxin-induced glutamate release assessed by microdialysis [**Yr 3**].

Aim 1c: A_{2A} receptor dependence of caffeine effects on protection [**Yr 4**] and release [**Yr 5**].

SA 2: **Neruoprotection by urate in a unilateral toxin model of PD *in vivo*.**

Aim 2a: Determine *UOx* KO phenotype [**Yr 1**] and superimposed inosine effect in *UOx* KO [**Yr 2**].

Aim 2b: Localize the influence of increased urate on neurotoxicity using *UOx* cKO (Cre/*loxP* system) mice to elevate urate discretely in dopaminergic neurons [**Yr 3**] *vs* astrocytes [**Yr 4**].

Aim 2c: Assess for protection by *XOR* cKO (Cre/*loxP* system) with low urate in dopaminergic neurons [**Yr 4**] *vs* astrocytes [**Yr 5**], after completing floxed *XOR* mouse generation [**Yr 3**].

SA 3: **Mechanisms of protection by urate in toxin models of PD in neuronal cultures.**

Aim 3a: Determine inosine and urate effects on neurotoxicity and associated oxidative damage, MAPK pathway activation and α-synuclein expression [**Yr 1**].

Aim 3b: Effects of endogenous urate increase in *UOx* KO [**Yr 2**] and decrease in *XOR* KO [**Yr 4**].

Aim 3c: Effects of local urate increase in *UOx* cKO [**Yr 3**] and decrease in *XOR* cKO [**Yr 5**].

Body of the Report:

We report substantial progress during Year 2 on all three of our original SAs, particularly SA 2 and 3 focused on exploring the role urate in PD models *in vivo* and in cell culture, respectively. Our progress is highlighted by and detailed in 8 publications in Year 2, which are attached as Appendices A-H. Four of these publications represent achievement of major components of SA's as follows:

SA 1: **Caffeine and adenosine A_{2A} antagonism in models of PD *in vivo***

Kachroo A & Schwarzschild MA. (2012)
Adenosine A_{2A} receptor gene disruption protects in an α-synuclein model of Parkinson's disease.
Annals Neurol. 71:278-82. (**Appendix A**)

- First demonstration that α-synuclein toxicity in a mouse model of PD depends upon caffeine's putative molecular target, the adenosine A_{2A} receptor.
- The findings suggest that caffeine and more specific antagonists of the adenosine A_{2A} receptor may confer protection against dopaminergic neuron degeneration induced by an established genetic contributor to PD pathophysiology, and strengthen further the rationale for clinical trials designed to assess the disease-modifying potential of these agents in PD.

SA 2: **Neuroprotection by urate in a unilateral toxin model of PD *in vivo*.**

Chen X, Burdett TC, Desjardins CA, Logan R, Cipriani S, Xu Y & Schwarzschild MA. (2013)
Disrupted and transgenic urate oxidase alter urate and dopaminergic neurodegeneration.
Proc Natl Acad Sci U S A. 110(1):300-5. (**Appendix G**)

- First demonstration that genetic manipulations raising and lowering brain urate levels can prevent and exacerbate dopaminergic neuron degeneration *in vivo*, respectively.
- Findings strengthen the rationale for ongoing efforts to develop a urate-elevating drug as a candidate neuroprotective strategy in PD.

SA 3: **Mechanisms of protection by urate in toxin models of PD in neuronal cultures.**

Cipriani S, Desjardins CA, Burdett TC, Xu Y, Xu K, Schwarzschild MA. (2012)
Urate and its transgenic depletion modulate neuronal vulnerability in a cellular model of Parkinson's disease.
PLoS One. 7:e37331. (**Appendix E**)

- First demonstration that exogenous urate or manipulation of endogenous urate (by transgenic over-expression of *urate oxidase*) can modulate dopaminergic neuron degeneration in a cellular model of PD.

Cipriani S, Desjardins CA, Burdett TC, Xu Y, Xu K, Schwarzschild MA. (2012)
Protection of dopaminergic cells by urate requires its accumulation in astrocytes.
J Neurochem. 123:172-81. (**Appendix F**)

- Identifies an astrocyte-dependent mechanism underlying neuroprotection by urate in cultured dopaminergic neuron model of PD.

- Demonstrates a critical role for the transport of urate in its neuroprotective effect, highlighting the therapeutic potential of targeting urate transporters as an alternative approach to CNS urate elevation that may avoid potetnail adverse effects of systemic urate elevation.

Also in Year 2 our laboratory published (**Appendix C**) key bioanalytical methodological developed to support the purine studies central to the project. The methods will facilitate the investigation of CNS purine mechanisms by other groups.

Our group also published two manuscripts reviewing the protective potential of caffeine (**Appendix B**) and urate (**Appendix D**) in PD reflecting concepts pursed under SAs 1 and 2/3, respectively.

In addition to completing/reporting these milestones under our original SA's in Year 2, we also have made preliminary and as yet unpublished progress this past year. In addition to progress and challenges summarized in our quarterly reports to Grants Officer's Representative Dr. Steve Grate and USAMRAA, below is a summary of Year 2 progress not covered in the past year's publications.

SA 1: **Mechanisms of protection by caffeine in toxin models of PD *in vivo*.**

In addition to publication of our findings that, "Adenosine A_{2A} receptor gene disruption protects in an α-synuclein model of Parkinson's" (attached as Appendix A), we have now also published collaborative findings (under SA 1b/c) of adenosine A_{2A} receptor roles in a model of parkinsonian tremors with colleagues at the University at the University of Connecticut (as above; Salamone et al., 2012; Appendix H). We demonstrated that either pharmacological blockade or genetic depletion of the adenosine A_{2A} receptor attenuated pilocarpine-induced jaw tremors, which share features of parkinsonian tremors. The studies strengthen further the broad therapeutic potential of adenosine A_{2A} receptor antagonism in Parkinson's disease (PD) – both as potential neuroprotective (possibly anti-excitotoxic and anti-synucleinopathic) as well as a symptomatic (including anti-tremor) strategies for PD.

During Year 2 we also experienced a setback in our effort to establishing a 2,4-D model in mice (under SA1a). Sectioning and immunohistochemical staining of the mouse brains processed in Yr 1 in preparation for stereological assessment of the nigral dopaminergic neuronal counts was complicated by technical problems during the tissue fixation steps. Unfortunately no additional brain sections from these mice were suitable for stereological analysis to complete this portion of the experiment. Results for the behavioral and neurochemical (striatal dopamine) components of the experiment had been published in preliminary form in Year 1 of the project. Repeating the 2,4-D treatment on a fresh set of mice for a complete analysis including stereological counts of nigral dopaminergic neurons may be pursued later in the project period depending on priorities/resources.

Lastly with respect to SA 1 we have successfully pursued recruitment of an advanced research fellow to purse SA's 1b and 1c, which employ *in vivo* microdialysis to explore the role of adenosine A_{2A} receptors in mouse models of PD. Dr. Marco Orru is joining our laboratory at MGH this month (February 2013). He has considerable expertise in both adenosine A_{2A}

receptor biology and *in vivo* microdialysis and has just completed a highly productive fellowship under Dr. Sergi Ferre at the NIH/NIDA. The increase in project effort is facilitated by accelerated support during Year 2 with early execution of Option Yr 2 for the project (based on our success in achieving early SA goals ahead of schedule as above.)

SA 2: Neruoprotection by urate in a unilateral toxin model of PD *in vivo*.

Aim 2a: Determine UOx KO phenotype [Yr 1] and superimposed inosine effect in UOx KO
Aim 2b: Localize the influence of increased urate on neurotoxicity using UOx cKO (Cre/loxP system) mice to elevate urate discretely in dopaminergic neurons vs astrocytes.

To investigate effects of postnatal *UOx* KO, *UOx* conditional KO mice have been generated using the Cre/*loxP* system based on (tamoxifen) inducible ubiquitously expressed *cre* transgene (*UBC*-cre). We then mated *UOx*$^{flox/flox}$ mice with transgenic (Tg) *UBC-cre* mice (obtained from the Jackson Laboratory) to generate *UBC-cre UOx*$^{flox/+}$ mice. These are now being crossed with *UOx*$^{flox/flox}$ mice to produce offspring comprising *UBC-cre UOx*$^{flox/flox}$ mice and their non-transgenic (NTg) littermate controls (NTg *UOx*$^{flox/flox}$ mice).

We have now conducted an initial characterization of the first set of these mice. Recombination was induced by 75 mg/kg tamoxifen (20 mg/ml in corn oil) i.p. injection once daily for 5 days. Mice were sacrificed 7 days or 28 days after the last injection. Tamoxifen injections appeared well-tolerated without evidence of general toxicity. There was no difference in body weight between *UBC-cre UOx*$^{flox/flox}$ mice and NTg *UOx*$^{flox/flox}$ littermate controls over the entire experimental courses.

UOx protein expression in *UBC-cre UOx*$^{flox/flox}$ and control NTg *UOx*$^{flox/flox}$ mice treated with tamoxifen

UOx protein was detected in liver in NTg *UOx*$^{flox/flox}$ control mice by Western Blot. Its expression in *UBC-cre UOx*$^{flox/flox}$ mice was significantly lower at both 7 and 28 days after completing tamoxifen administration (Fig. 2), suggesting successful induction of *cre* expression and resultant Cre-catalyzed recombination and knockout of *UOx*. The variability within *UBC-cre UOx*$^{flox/flox}$ group is likely due to low solubility and uneven suspension of tamoxifen that we observed at the time of its injection. To address this technical difficulty we will either lower concentration of tamoxifen solution or sonicate solution well to ensure equal dosing among animals.

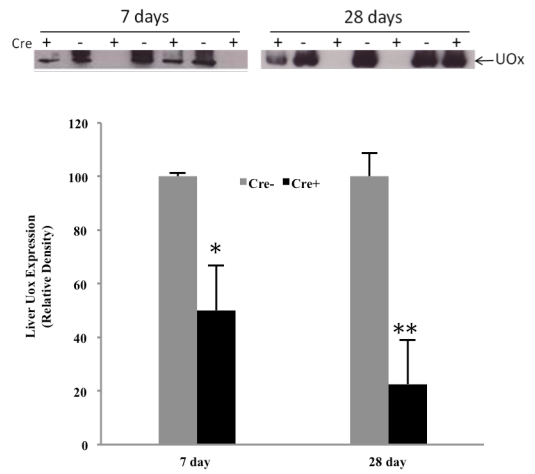

Fig 2. UOx protein in *UBC-cre UOx*$^{flox/flox}$ and control NTg *UOx*$^{flox/flox}$ mice treated with tamoxifen. *UBC-cre UOx*$^{flox/flox}$ and control NTg *UOx*$^{flox/flox}$ were injected with tamoxifen. Mice were sacrificed 7 days or 28 days after the last injection. UOx protein in liver was detected by Western blot. Band density was analyzed using Image J. Results were expressed as relative density to loading control. n=3 Cre- (NTg) and n=4 Cre+ both 7 day and 28 day time points. * p=0.05; **p=0.01

Levels of urate in *UBC-cre UOx*$^{flox/flox}$ and control NTg *UOx*$^{flox/flox}$ mice treated with tamoxifen

Animals were sacrificed and urate levels in blood and brain (striatum) were determined by HPLC-ECD. There are trends towards increased urate in both blood and brain in *UBC-cre UOx*$^{flox/flox}$ mice at both 7 and 28 days after tamoxifen treatment (Fig. 3). The inconsistency within *UBC-cre UOx*$^{flox/flox}$ mice correlates well and is likely caused by observed variability in UOx protein expression in this group of mice (Fig. 3).

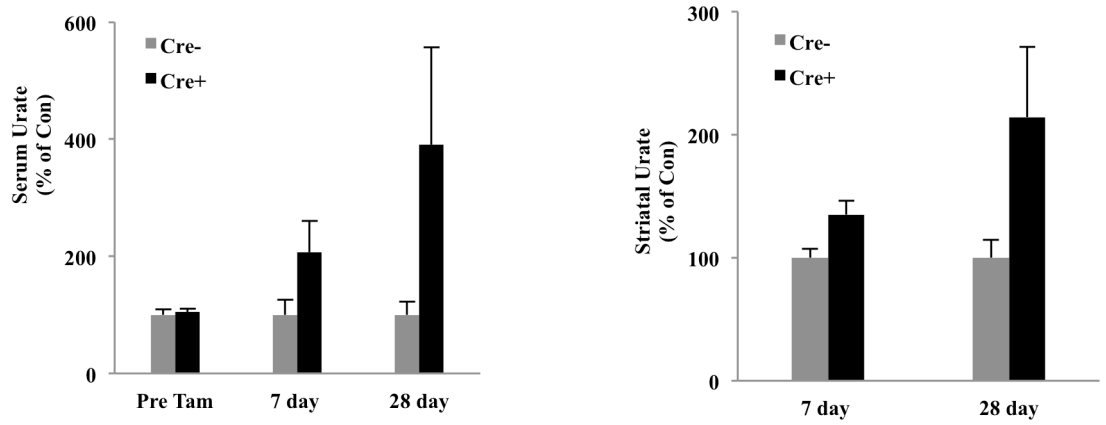

Fig 3. Blood and brain urate in *UBC-cre UOx*$^{flox/flox}$ and control NTg *UOx*$^{flox/flox}$ mice treated with tamoxifen. *UBC-cre UOx*$^{flox/flox}$ and control NTg *UOx*$^{flox/flox}$ were injected with 75 mg/kg tamoxifen (in corn oil) i.p. once daily for 5 days. Mice were sacrificed 7 days or 28 days after the last injection. Blood and brain urate levels were determined by HPLC-ECD. n=3 Cre- (NTg) and n=4 Cre+ both 7 day and 28 day time points.

Protein carbonyls in *UBC-cre UOx*$^{flox/flox}$ and control NTg *UOx*$^{flox/flox}$ mice treated with tamoxifen

Mice were sacrificed and protein carbonyls in liver and brain samples were determined by Oxyblot as an index of oxidative damage. There is no statistical difference between *UBC-cre UOx*$^{flox/flox}$ and control NTg *UOx*$^{flox/flox}$ mice in liver or brain at either sacrifice time points (Fig. 4). Due to limited sample size and large viability, it is unclear whether changes in urate levels by

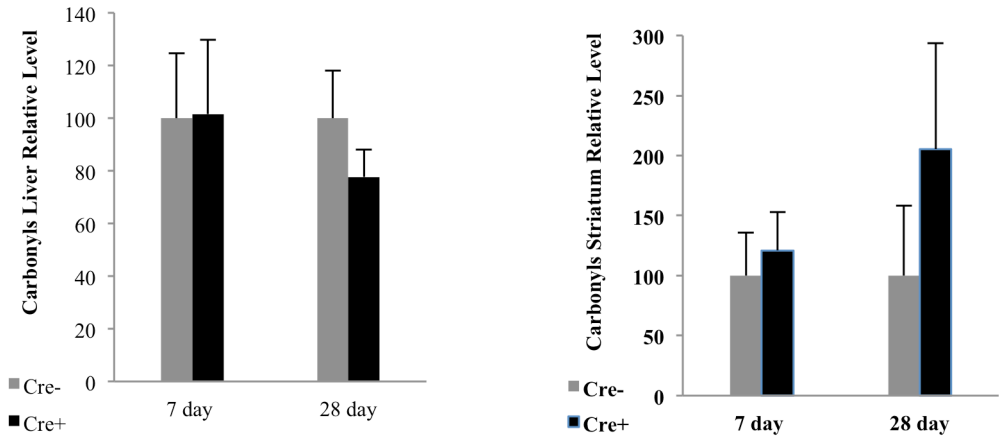

Fig 4. Protein carbonyls in *UBC-cre UOx*$^{flox/flox}$ and control NTg *UOx*$^{flox/flox}$ mice treated with tamoxifen. *UBC-cre UOx*$^{flox/flox}$ and control NTg *UOx*$^{flox/flox}$ were injected with 75 mg/kg tamoxifen (in corn oil) ip once daily for 5 days. Mice were sacrificed 7 days or 28 days after the last injection. Protein carbonyls were determined by Oxyblot. Band density was analyzed using Image J. Results were expressed as relative density to ponceau staining. n=3 Cre- and n=4 Cre+ both 7 day and 28 day time points.

conditional *UOx* KO might alter protein carbonyls in periphery or in CNS. We will further characterize these mice when more animals are available, and will include longer time points after tamoxifen treatment given uncertainty over protein carbonyl turnover rates.

SA #3: Protection by urate in cellular models of PD: anti-oxidant and α−synuclein mechanisms.

1. Protection of dopaminergic cells by urate requires its accumulation in astrocytes.

We have recently confirmed protective properties of urate in cellular models of PD. To date these models have been based on spontaneous cell death or that produced by oxidative and mitochondrial toxins, including H2O2, rotenone, MPP+, 6-hydroxydopamine (6-OHDA), glutamate and iron ions. In our recent studies, we also found that urate produced much of its protective effect indirectly via astrocytes (see Appendices E and F). They in turn release a potent neuroprotective factor, which differs from urate because incubation of medium conditioned by urate-treated astrocytes with commercially obtained urate oxidase (UOx) eliminates urate but not the protective influence.

To further characterize the mechanisms underlying the astrocyte-dependence of urate's neuroprotection in cellular models of PD, we have employed complementary biochemical techniques and targeted screens to identify the putative protective factor(s) released by urate-stimulated astrocytes. The MES 23.5 dopaminergic cell line, which is hybrid of murine neuroblastoma-glioma N18TG2 cells with rat mesencephalic neurons is used to assay the protective effect of urate or of conditioned medium from urate-treated astrocytes. We treated enriched astroglial cultures with varying concentrations of urate, or vehicle. Twenty-four hours later conditioned media is collected and immediately used for the following experiments or stored at -20ºC for later experiments. The MES 23.5 cells are pre-treated with increasing proportions of conditioned medium and then exposed to toxins. For cell viability evaluation, as shown in Figure 5A, Annexin–V–FITC (BD-Pharmingen) and propidium iodide (PI, Sigma) staining is followed by flow cytometry analysis using FACScan (BD Biosciences). Urate treated conditioned medium from astrocytes is significantly more protective against H_2O_2 induced MES 23.5 cell death (Figure 5).

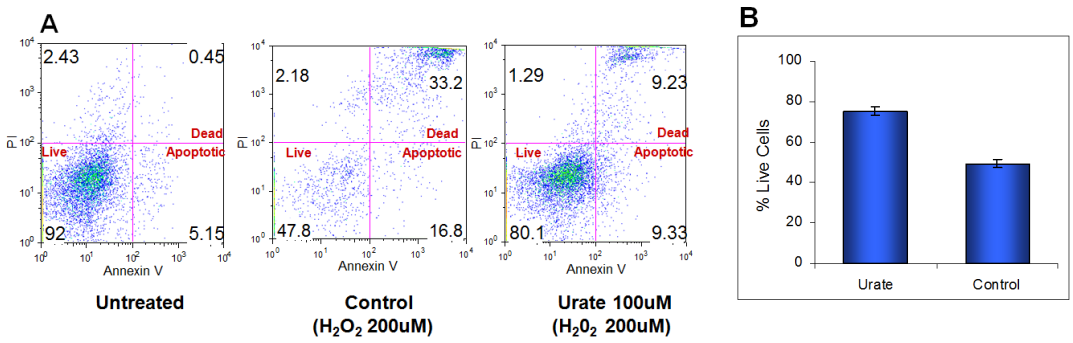

Figure 5. *Urate protects MES 23.5 cells from H_2O_2 induced cell death via conditioned medium from urate-treated astrocytes. (A) FACS analysis showing cell viability using PI/Annexin V staining. Percentages of PI+/Annexin V+ (necrotic), PI-/Annexin V+ (apoptotic) and PI−/Annexin V− (vital) staining is shown in MES 23.5 cells treated with conditioned medium from control or urate-treated astrocytes followed by H_2O_2 exposure. (B) Graphical representation of number of live cells in urate treated conditioned medium compared to vehicle control (n=3).*

2. ***Urate treatment causes release of glutathione (GSH) from astrocytes.***

Since we have shown a significant protective effect of conditioned medium from urate-treated astrocytes on MES 23.5 cell viability in presence of 200 uM H_2O_2, we have initiated targeted screens to identify the putative neuroprotective factor in the conditioned medium from urate-treated (versus untreated) astrocyte using commercially available ELISA-based assay kits. We have assayed for prespecified established neuroprotective factors including glial-derived neurotrophic factor (GDNF), brain-derived neurotrophic factor (BDNF), interleukin 6 (IL6) and glutathione (GSH). We identified GSH) as a primary candidate for the putative neuroprotective factor that is released from urate-treated astrocytes because it was the only one of the screened candidate neuroprotectants to be detected at a higher concentration in conditioned medium from urate-treated (compared to control) astrocytes (Fig 6).

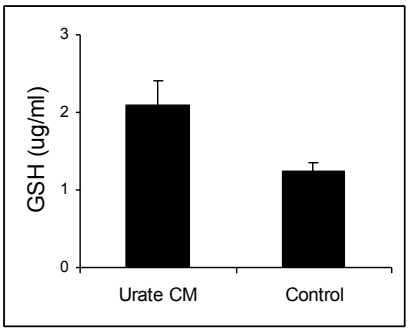

Figure 6. *Total GSH content was significantly increased in conditioned medium from urate-treated (versus untreated) astrocyte using commercially available ELISA kit (Abcam).*

We are currently pursuing validation of GSH as a candidate mediator of urate's neuroprotective effect by conducting a) parallel ELISA- and HPLC-based assays of lysates from urate- vs vehicle-treated astrocytes, and b) experiments on the effect of inhibiting GSH synthesis in conditioned media from urate-treated astrocytes in order to definitively assess its role in neuroprotection conveyed by the conditioned medium. We block GSH function in the conditioned media by targeting its synthesis or its uptake by neuronal cells. **L-Buthionine-sulfoximine (BSO)** inhibits GSH synthesis thus reducing cellular GSH level (Figure 7). **Acivicin** is an antibiotic that inhibits g-glutamyl transpeptidase and transmembrane glutathione transport. The effects of using these two drugs on the cell viability experiments (as described above) are presently being pursued.

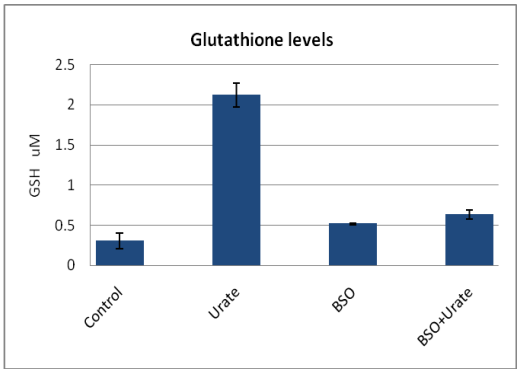

Figure 7. *Total GSH content was significantly increased in urate-treated (versus untreated) astrocyte cell lysates. L-Buthionine-sulfoximine (BSO) inhibits GSH synthesis thus reducing cellular GSH levels.*

3. Gene expression analysis in urate treated astrocytes to assess the differential expression of glutathione synthesis genes.

To further investigate the molecular mechanisms of urate-induced, astrocyte-dependent neuroprotection, we are preparing to analyze the differential expression of key enzymes in the glutathione biosynthesis pathway in urate- or vehicle-treated astrocytes. Total RNA from urate-treated and control astrocytes were extracted and reverse transcribed into cDNA (Invitrogen) and will be used for quantitative PCR (qPCR) assay. The following key antioxidant genes would be assessed for their expression.

Symbol	**Name**	**Function**
GCLC	Glutamate—cysteine ligase catalytic	glutathione synthesis
GCLM	Glutamate--cysteine ligase regulatory	glutathione synthesis
HO-1	Heme oxygenase 1	Antioxidant, heme metabolism
ACTB	Beta-actin	Housekeeping
LAM	Lamin	Housekeeping

Key Research Accomplishments (Year 2)

- Publication demonstrating that mutant α -synuclein-induced neurodegeneration in mice requires adenosine A_{2A} receptors, providing evidence of a gene-environment interactions influencing the putative protective effects of adenosine A_{2A} antagonists like caffeine. (See Appendix A.)
- Completion and publication of studies demonstrating that systematic (knockout and transgenic *urate oxidase*) genetic evidence for a critical role for endogenous urate as a neuroprotectant in a standard toxin model of Parkinson's disease. (See Appendix G.)
- Provided evidence that *urate oxidase* mutations during human evolution may have conferred a mechanism for neuroprotection. (See Appendix G.)
- Publication demonstrating a robust neuroprotective and antioxidant properties of urate in cellular models of Parkinson's disease. (See Appendices E and F.)
- Publication demonstrating of an astrocyte-dependent mechnanism of neuroprotection by urate in cellular models of PD. (See Appendices E and F.)
- Publication demonstrating that urate induces astrocytes to release a neuroprotective factor. (See Appendices F.)
- Publication of first evidence that urate transporters may be targeted as a novel neuroprotective strategy for Parkinson's disease. (See Appendices F.)
- Preliminary characterization of advanced genetic probe of *urate oxidase* function in PD models based on Cre/*loxP* conditional KO methodology. (See unpublished data, above.)
- Preliminary identification of glutathione (GSH) as the urate-induced neuroprotective factor released by astrocytes. (See unpublished data, above.)

Reportable Outcomes

In Year 2 of the project we have published 9 manuscripts reflecting progress on the project (and in all cases explicitly acknowledging grant support from the DoD/NEPTR/W81XWH-11-1-0150) as follows, with relevant SA's noted in **bold**:

Kachroo A, Schwarzschild MA. (2012) Adenosine A_{2A} receptor gene disruption protects in an α-synuclein model of Parkinson's disease. *Annals Neurol*. 71:278-82. – **SA 1** (**Appendix A**)

Schwarzschild MA. (2012) Caffeine in Parkinson disease: better for cruise control than snooze patrol? *Neurology*. 79:616-8. [editorial/review] – **SA 1** (**Appendix B**)

Burdett TC, Desjardins CA, Logan R, McFarland NR, Chen X, Schwarzschild MA. (2013) Efficient determination of purine metabolites in brain tissue and serum by high-performance liquid chromatography with electrochemical and UV detection. *Biomed Chromatogr*. 27(1):122-9. – **SA 2/3** (**Appendix C**)

Chen X, Wu G, Schwarzschild MA. (2012) Urate in Parkinson's disease: more than a biomarker? Curr *Neurol Neurosci Rep*. 12(4):367-75. [review] – **SA 2/3** (**Appendix D**)

Cipriani S, Desjardins CA, Burdett TC, Xu Y, Xu K, Schwarzschild MA. (2012) Urate and its transgenic depletion modulate neuronal vulnerability in a cellular model of Parkinson's disease. *PLoS One*. 7:e37331. – **SA 3** (**Appendix E**)

Cipriani S, Desjardins CA, Burdett TC, Xu Y, Xu K, Schwarzschild MA. (2012) Protection of dopaminergic cells by urate requires its accumulation in astrocytes. *J Neurochem*. 123:172-81 – **SA 3** (**Appendix F**)

Chen X, Burdett TC, Desjardins CA, Logan R, Cipriani S, Xu Y, Schwarzschild MA. (2013) Disrupted and transgenic urate oxidase alter urate and dopaminergic neurodegeneration. *Proc Natl Acad Sci USA*. 110(1):300-5. – **SA 2** (**Appendix G**)

Salamone JD, Collins-Praino LE, Pardo M, Podurgiel SJ, Baqi Y, Müller CE, Schwarzschild MA, Correa M. (2012) Conditional neural knockout of the adenosine A_{2A} receptor and pharmacological A_{2A} antagonism reduce pilocarpine-induced tremulous jaw movements: Studies with a mouse model of parkinsonian tremor. *Eur Neuropsychopharmacol*. 2012 Sep 1. [Epub ahead of print] – **SA 1** (**Appendix H**)

Presentations (given by PI; *acknowledging W81XWH--1-0150 / NETPR / DoD*) included:

- May 23, 2012 – (Stockholm, Sweden) The Karolinska Institute – seminar speaker, "Epidemiological Clues to Purine Targets in PD: caffeine, adenosine & urate".
- June 2, 2012 – (Fukuoka, Japan) International Symposium on Adenine Nucleosides and Nucleotides in Biomedicine – symposium speaker, "Caffeine & Urate as Neuroprotectants: Evolution, Epidemiology & Trials".
- June 17, 2012 – (Dublin, Ireland) 14th International Congress of Parkinson's Disease and Movement Disorders – syposium speaker, "Novel non-dopaminergic targets for the motor symptoms of Parkinson's disease".

- June 28, 2012 – (New York, NY) Department of Defense/NETPR Symposium on Parkinson's Disease Models, Biomarkers & Biochemical Pathways – session speaker, "*Protective Potential of Purines against Neurodegeneration of PD*".
- October 17, 2012 – (Boston, MA) Massachusetts General Hospital Dept. of Neurology Neuroscience Residents Research Series – seminar speaker, "Integrating Epidemiological, Basic and Clinical Neurosciences to Develop Parkinson's Trials".
- October 24, 2012 – (North Chicago, IL) Cellular & Molecular Pharmacology Seminar Series, The Chicago Medical School, Rosalind Franklin University of Medicine & Science – seminar speaker, "Epidemiology and Neuroprotective Potential of Urate in Parkinson's Disease".

Funding Applied for Based on the Work Supported by this Award includes:

NIH (NINDS) 1K24 NS060991 (competing renewal for career/mentoring award; Schwarzschild, PI) 2013-2018 "*Pursuing Puringergic Pathways to Clinical Trials for Parkinson's Disease*" [pending].

NIH (NINDS/NIA) R21 in response to FOA PA-11-261, "NIH Exploratory /Developmental Research Grant Program" (new application; Schwarzschild and DK Simon, dual-PIs) 2013-2015 "Role of urate in protecting mitochondrial function in the brain" [pending].

NIH (NINDS) RFA-AI-12-021 (new application; Schwarzschild, US PI): "U.S.-China Program for Biomedical Collaborative Research (R01)" (Schwarzschild, PI) 2014-2016 *"Neuroprotective potential of Urate in Parkinson's Disease"* [pending].

Conclusions/Plans/Signficance

In the second year of the project we have made substantial progress toward each of the original SA's as documented in multiple research manuscripts generated (appendices). The results help establish that multiple purines (adenosine antagonists, inosine and urate) can confer neuroprotection in mouse models of Parkinson's disease. They provide a solid foundation on which to build our subsequent experiments, including those outlined in the SOW.

Plans – Major plans in Yr 3 include initiation of microdialysis experiments over caffeine and A_{2A} receptor regulation of glutamate (and possibly α-synuclein) release in toxin models of PD (SA 1). We will also build on our above preliminary data characterizing our newly generated inducible/conditional (post-natal) knockout (KO) of *UOx* by exploring its phenotype in a toxin model of PD. This conditional KO obviates the confounding developmental phenotype of the constitutive *UOx* knockout described in Appendix G (SA2). We will seek to confirm the identity of GSH as the neuroprotective factor released by astrocytes in response to urate treatment in cellular models of PD (SA3).

Significance -- Our characterization of the roles of these purines in mouse models of PD neurodegeneration through this preclinical project remains well positioned to inform and potentially accelerate the conduct of phase III clinical trials of neuroprotective candidates for the disease. In parallel with our progress made on these laboratory studies in Yr 1 and 2, human studies are under way investigating adenosine- and urate-targeted strategies in patients with PD. Recently caffeine itself (http://clinicaltrials.gov/show/NCT01738178) as well as more specific antagonism of the adenosine A_{2A} receptor (http://clinicaltrials.gov/ct2/show/NCT01155479) has entered clinical development in PD trials designed to assess disease-modifying effects. Similarly our own clinical development of inosine as a urate precursor targeted as a candidate neuroprotective strategy is progressing (http://clinicaltrials.gov/ct2/show/NCT00833690).

In addition to its high translational impact, our exploration of purines in preclinical models of PD has substantial epidemiological and military significance. The mechanistic insights pursued under this project reflect a prototypic interaction between putative environmental protectants (e.g., caffeine, urate) and toxins.

Adenosine A_{2A} Receptor Gene Disruption Protects in an α-Synuclein Model of Parkinson's Disease

Anil Kachroo, MD, PhD, and
Michael A. Schwarzschild, MD, PhD

To investigate the putative interaction between chronic exposure to adenosine receptor antagonist caffeine and genetic influences on Parkinson's disease (PD), we determined whether deletion of the adenosine A_{2A} receptor in knockout (KO) mice protects against dopaminergic neuron degeneration induced by a mutant human α-synuclein (*hm²-αSYN*) transgene containing both A53T and A30P. The A_{2A} KO completely prevented loss of dopamine and dopaminergic neurons caused by the mutant α-synuclein transgene without altering levels of its expression. The adenosine A_{2A} receptor appears required for neurotoxicity in a mutant α-synuclein model of PD. Together with prior studies the present findings indirectly support the neuroprotective potential of caffeine and more specific A_{2A} antagonists.

ANN NEUROL 2012;71:278–282

Adenosine A_{2A} receptor antagonists are emerging as promising candidates for nondopaminergic therapy for Parkinson's disease (PD) in part due to symptomatic effects on motor deficits in preclinical models, and selective expression of the A_{2A} receptor within the basal ganglia. Consumption of caffeine a nonspecific A_{2A} receptor antagonist has been consistently linked to reduced risk of developing PD.[1] Caffeine protects against dopaminergic nigrostriatal toxicity in a number of PD models.[2–5] Similar protective effects are consistently observed with specific A_{2A} antagonists[6] and in mice lacking the A_{2A} receptor due to global[2] or neuronal knockout (KO)[7] of its gene. Recently, polymorphisms in the human A_{2A} receptor gene (*ADORA2A*) have been linked to a reduced risk of PD.[8] To explore the effect of chronically disrupting adenosine A_{2A} receptor signaling in a progressive genetic model of neurodegeneration in PD, we crossed A_{2A} KO mice with 1 of the few transgenic α-synuclein lines that feature progressive loss of dopamine (DA) and dopaminergic neurons characteristic of the disease.[9,10] Assessments of the integrity of the dopaminergic nigrostriatal system of their offspring in late life indicated an essential role of adenosine A_{2A} receptors in the neurodegenerative effect of mutant α-synuclein in a mouse model of PD.

Subjects and Methods

Animals

Heterozygous A_{2A} (+/−) KO mice in a C57Bl/6 background (back-crossed 8 generations; N8) were mated with heterozygous A_{2A} (+/−) KO mice that were also transgenic for wild-type (WT) *hw-αSYN* or the doubly mutant *hm²-αSYN* form of the human α-synuclein gene under the control of a 9kb rat tyrosine hydroxylase (TH) promoter.[9] The latter mice were generated by crossing N8 homozygous A_{2A} (−/−) KO mice to transgenic *hw-αSYN* and *hm²-αSYN* mice, which had been backcrossed with C57Bl/6J mice 3 to 4 times after receipt from E.K. Richfield. Nontransgenic (NT) controls generated from these crosses were also used. The 6 genotypes used in this experiment included: A_{2A}WT [NT (n = 6M, 6F)); *hw-αSYN* (n = 4M, 6F); *hm²-αSYN* (n = 4M, 5F)]; A_{2A}KO [NT (n = 7M, 6F); *hw-αSYN* (n = 4M, 4F); *hm²-αSYN* (n = 6M, 5F)]. Behavioral (see Supplemental Text and Figs. S1–S4) and neurochemical assessments were conducted on both sexes, with anatomical measures performed only on male samples.

Tissue Processing and Analysis

Mice were sacrificed by cervical dislocation at 20 to 24 months of age. The brain was removed and rostral and caudal portions separated by an axial cut made across the whole brain at the tail end of the striatum. Both striata were removed and frozen at −80°C until use. The remaining caudal brain portion was immediately fixed, placed in cryoprotectant, and stored at −80°C until use. The striatum was assayed for DA and 3,4-dihydroxyphenylacetic acid (DOPAC) by standard reverse phase high-performance liquid chromatography with electrochemical detection as routinely performed in our laboratory.[2] Fixed brains were cut on a Leica microtome into 30μm-thick sections and stored for immunolabeling studies in a cryoprotectant consisting of 30% sucrose and 30% ethylene glycol in 0.1M phosphate buffer. Sections were chromogenically stained for TH immunoreactivity (IR) followed by counterstaining with Nissl.[9] Double-label fluorescence immunohistochemistry (IHC) for both TH and hα-SYN was performed on 4 brain sections each

From the MassGeneral Institute for Neurodegenerative Disease, Department of Neurology, Massachusetts General Hospital and Harvard Medical School, Boston, MA.

Address correspondence to Dr Kachroo, MassGeneral Institute for Neurodegenerative Disease, MGH, 114 Street, Charlestown, MA 02129. E-mail: akachroo@partners.org

Additional Supporting Information can be found in the online version of this article.

Received May 23, 2011, and in revised form Aug 18, 2011. Accepted for publication Sep 2, 2011.

View this article online at wileyonlinelibrary.com. DOI: 10.1002/ana.22630

 © 2012 American Neurological Association

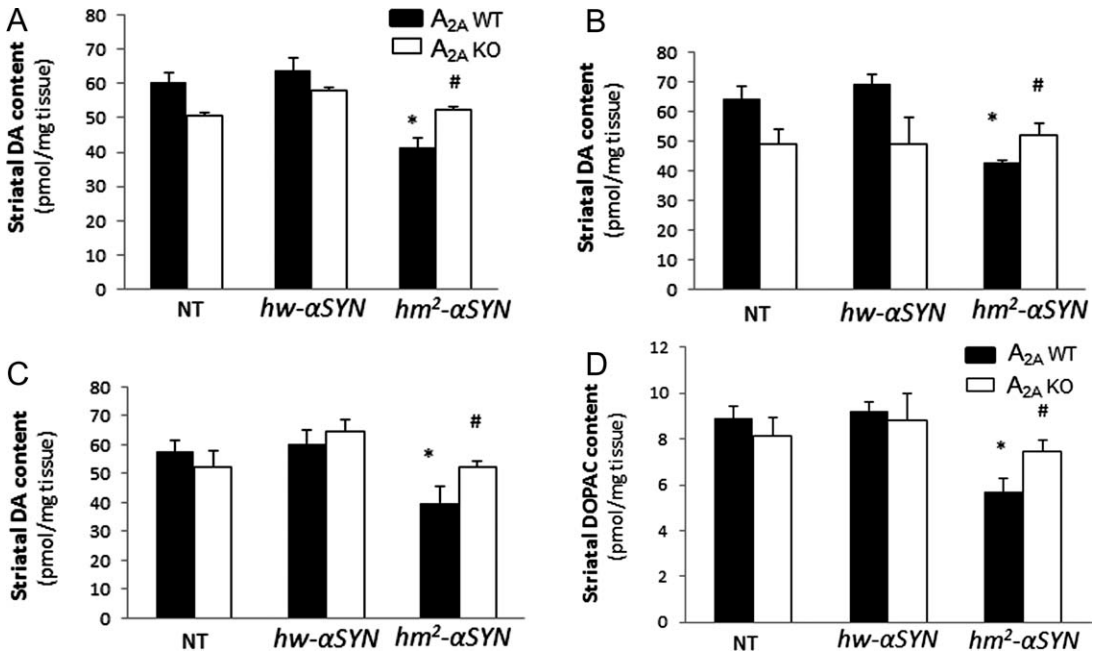

FIGURE 1: Mutant α-synuclein-induced striatal dopamine and DOPAC loss requires the A_{2A} receptor. (A) Striatal dopamine (DA) content was measured at 20 to 24 months of age in nontransgenic (NT) mice and those transgenic for the wild-type (*hw-αSYN*) and the double mutant (*hm*^{2}-*αSYN*) human synuclein gene. See Subjects and Methods section for numbers of mice/group. *$p < 0.001$ vs NT and *hw-αSYN*; $^{\#}p < 0.01$ vs A_{2A}WT [*hm*^{2}-*αSYN*]; individual 1-way ANOVAs with transgene as the between factor and subsequent post hoc analysis to determine differences between transgenic groups within an A_{2A} genotype; and unpaired *t* test for within transgene comparison between A_{2A} genotypes. (B) Striatal DA level for male mice. *$p < 0.01$ vs NT and *hw-αSYN*; $^{\#}p < 0.01$ vs A_{2A}WT [*hm*^{2}-*αSYN*]; individual 1-way ANOVAs with transgene as the between factor and subsequent post hoc analysis to determine differences between transgenic groups within an A_{2A} genotype; and unpaired *t* test for within transgene comparison between A_{2A} genotypes. (C) Striatal DA level for female mice. *$p < 0.05$ vs NT and *hw-αSYN*; $^{\#}p < 0.05$ vs A_{2A}WT [*hm*^{2}-*αSYN*]; individual 1-way ANOVAs with transgene as the between factor and subsequent post hoc analysis to determine differences between transgenic groups within an A_{2A} genotype; and unpaired *t* test for within transgene comparison between A_{2A} genotypes. (D) Striatal DOPAC content for male and female mice.*$p < 0.001$ vs NT and *hw-αSYN*; $^{\#}p < 0.05$ vs A_{2A}WT [*hm*^{2}-*αSYN*]; individual 1 way ANOVAs with transgene as the between factor and subsequent post hoc analysis to determine differences between transgenic groups within an A_{2A} genotype; and unpaired *t* test for within transgene comparison between A_{2A} genotypes.

from mice in the 2 *hm*^{2}-*αSYN* groups and data was analyzed using an optical density (OD) measure. To determine α-synuclein expression, the OD of the α-synuclein and TH immunoreactivities was measured in 100 randomly sampled TH+ neurons within the substantia nigra pars compacta (SNpc) using Fluoview software to determine the ratio of *h-αSYN*:TH+ ODs. Quantitative OD values for each neuron were generated at ×40 magnification for both TH and α-synuclein expression using green and red filters, respectively. Stereological assessment of neuronal loss in midbrain sections performed as previously described[5] was limited to the SNpc. All counts were performed by a single investigator blinded as to the groups.

Statistical Analysis

Data values reported for DA, DOPAC content, and stereological cell counts are expressed as mean ± standard error of the mean (SEM). Within-group and between-group comparisons were performed using *t* test and 1-way analysis of variance (ANOVA) followed by Bonferroni post hoc analysis, respectively.

Results

Mutant α-Synuclein-Induced Striatal DA Loss Requires the A_{2A} Receptor

In line with the previous finding of an age-dependent loss of striatal DA in *hm*^{2}-*αSYN* mice,[9] the striatal DA content of aged *hm*^{2}-*αSYN* mice was reduced by approximately 35% compared to transgenic *hw-αSYN* and NT controls (Fig 1A). By contrast, mutant α-synuclein appeared to have no effect on striatal DA level in mice lacking the A_{2A} receptor. Similarly, the level of DA metabolite DOPAC was reduced in striatum of *hm*^{2}-*αSYN* mice in the presence of adenosine A_{2A} receptors but not in their A_{2A} KO littermates (see Fig 1D). Separating the DA data out by sex showed a similar profile for male and female mice (see Fig 1B and C, respectively). Despite the DA deficiency observed in *hm*^{2}-*αSYN* mice no associated behavioral deficit was detected (see Supplementary Materials), possibly reflecting compensatory mechanisms.

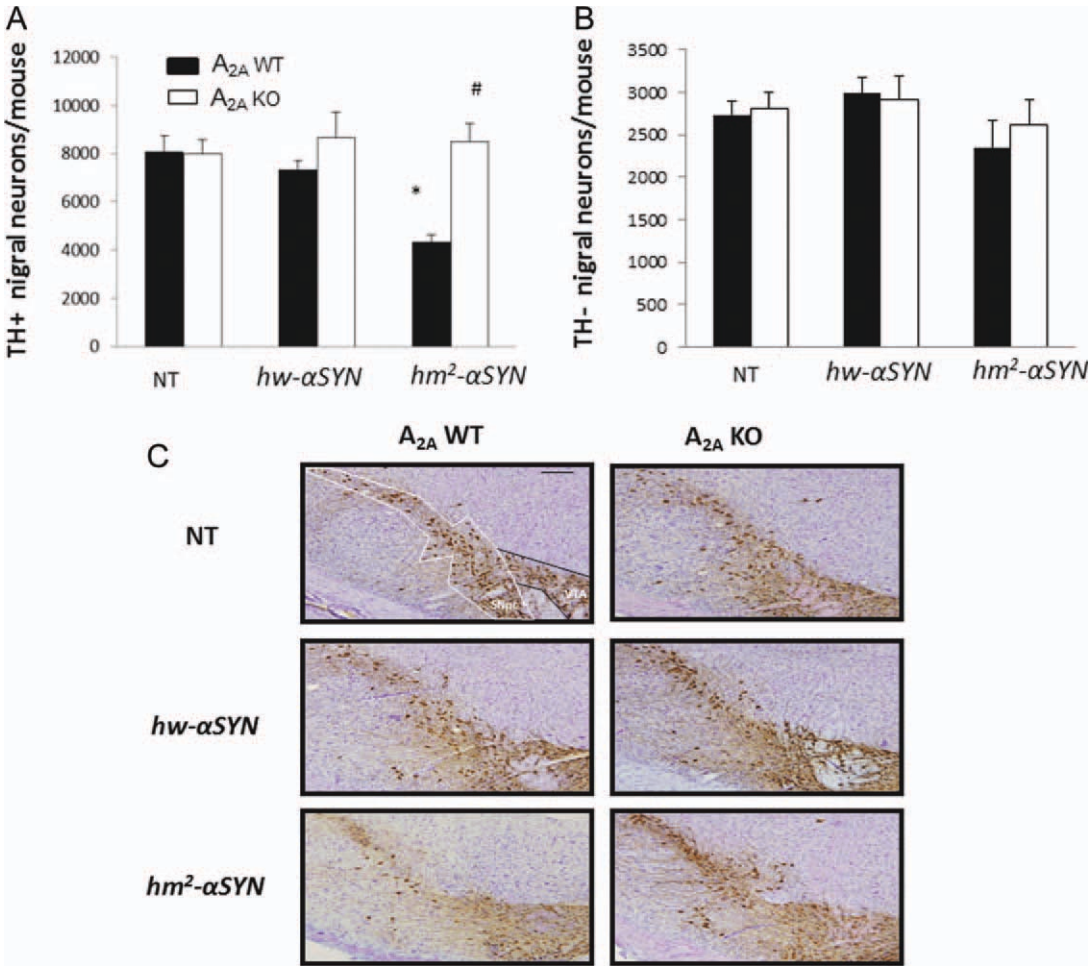

FIGURE 2: Dopaminergic neuron degeneration induced by transgenic mutant human α-synuclein is prevented in mice lacking the adenosine A_{2A} receptor. (A) Stereological cell counts of TH-immunoreactive (TH+) neurons from male mouse brains. See Subjects and Methods section for numbers of mice/group. *$p < 0.01$ vs NT and *hw-αSYN*; #$p < 0.01$ vs A_{2A}WT [*hm²-αSYN*]; individual 1-way ANOVAs with transgene as the between factor and subsequent post hoc analysis to determine differences between transgenic groups within an A_{2A} genotype; and unpaired *t* test for within transgene comparison between A_{2A} genotypes. (B) TH− nigral (Nissl) neurons were assessed in brain sections from male mice. $p > 0.05$; 1-way ANOVA with post hoc analysis and *t* test. (C) Representative photomicrographs showing chromogenically stained TH+ and TH− neurons of the SNpc. Bar = 60μm. [Color figure can be viewed in the online issue, which is available at www.annalsofneurology.org.]

Dopaminergic Neuron Degeneration Induced by Transgenic Mutant Human α-Synuclein Is Prevented in Mice Lacking the Adenosine A_{2A} Receptor

Given the similar profiles in neurochemical changes between the sexes as well as lesser variability of nigral neuron number among male mice, only male mice were used to assess α-synuclein-A_{2A} interaction at the level of neuronal cell counts. Consistent with the characteristic age-dependent loss of dopaminergic nigral neurons in *hm²-αSYN* mice,[9] the mutant α-synuclein mice (at an average age of 22 months) possessed 40% fewer TH+ nigral neurons than its WT *h-αSYN* and NT controls. By contrast, in the absence of A_{2A} receptors this attenuation was completely prevented (Fig 2A, C). Differences of TH+ nigral neurons between groups could not be attributed to altered TH expression since there were no differences in TH− nigral neuronal counts between groups (see Fig 2B, C).

Absence of Mutant α-Synuclein-Induced Neurodegeneration in A_{2A}KO Mice is Not Due to Reduced Transgene Expression

We explored whether altered *h-αSYN* expression might have contributed to the lack of a mutant α-synuclein effect on striatal DA or TH+ nigral neuronal cell counts in A_{2A} KO mice. The expression of *h-αSYN* protein product in dopaminergic nigral neurons was compared in *hm²-αSYN* male mice with or without A_{2A} receptors, using double-label IHC to normalize human α-synuclein-IR to TH-IR in the cell bodies of the SNpc. TH and h-αSYN immunoreactivities co-localized

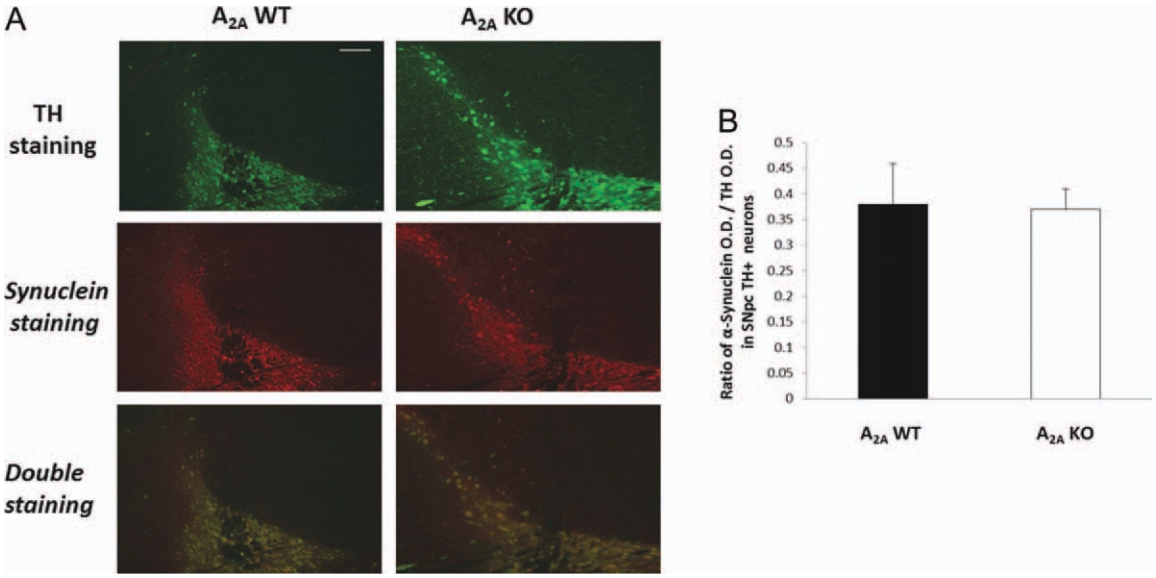

FIGURE 3: Absence of mutant α-synuclein-induced neurodegeneration in A_{2A}KO mice is not due to reduced expression of mutant α-synuclein. Brain sections from mice transgenic for the double mutant (*hm*^{2}-*αSYN*) human synuclein gene were used. Double label fluorescence IHC for expression of TH and α-synuclein was performed. (A) Fluorescent images (×10) generated from double label staining for TH *(green)*, α-synuclein *(red)*, and merged *(yellow)* are shown. (B) Ratio of α-synuclein OD/TH+ OD in SNpc TH+ neurons; $p > 0.05$; Student *t* test. Bar = 60μm. [Color figure can be viewed in the online issue, which is available at www.annalsofneurology.org.]

(Fig 3A) as previously reported.[9] The data showed no appreciable difference for the ratio of h-αSYN-IR:TH-IR optical densities in TH+ cells, between mice lacking or expressing the A_{2A} receptor (see Fig 3B).

Discussion

The present findings confirm the neurodegenerative phenotype in aging double mutant α-synuclein transgenic mice[9] and identify a requisite facilitative role of the adenosine A_{2A} receptor in this toxicity. Significant losses of striatal DA and nigral dopaminergic neurons were demonstrated in *hm*^{2}-*αSYN* mice, compared to both their transgenic (*hw-αSYN*) and nontransgenic controls, and were attenuated or prevented in mice lacking the adenosine A_{2A} receptor. Reversal of mutant α-synuclein toxicity by A_{2A} receptor depletion highlights the interplay between toxic and protective influences on dopaminergic neuron viability, raising the possibility that adenosine A_{2A} receptor antagonists, including caffeine, produce their well-documented neuroprotective effects in PD models by preventing synuclein-induced toxicity.

Although the A_{2A} KO phenotype has consistently recapitulated the neuroprotective effects of A_{2A} antagonists in multiple neurotoxin models of PD,[11,12] caution is warranted in extrapolating from the present genetic evidence for an adenosine A_{2A} receptor/α-synuclein link in mice. Despite advantages of absolute specificity and complete inactivation, knockout approaches to receptor function have their own limitations and do not always predict antagonist actions.[13] Accordingly, it remains to be determined whether chronic pharmacological blockade of A_{2A} receptors prevents α-synuclein pathology.

We considered whether attenuated *hm*^{2}-*αSYN* toxicity observed in A_{2A} KO mice could be attributed to a simple technical artifact of reduced transgene expression in the knockout. However, analysis of the ratio of human α-synuclein and TH immunoreactivities in dopaminergic neurons of the SNpc in *hm*^{2}-*αSYN* mice showed indistinguishable values between A_{2A} KO and WT littermates, suggesting that neuroprotection afforded in *hm*^{2}-*αSYN* mice by elimination of the A_{2A} receptor is not through attenuation of *h-αSYN* expression.

It remains unclear how genetic deletion or pharmacological blockade of the A_{2A} receptor attenuates the death of dopaminergic neurons in models of PD, although multiple mechanisms have been advanced, including the attenuation of excitotoxic and inflammatory effects of A_{2A} receptor activity.[12] Similar uncertainty exists over the mechanisms by which human *α-SYN* mutations or overexpression can produce neurodegeneration in PD and its models. However, consistent with evidence that α-synuclein toxicity may be mediated by proteasomal (ubiquitin system) dysfunction,[14] the ubiquitin proteasomal system (UPS) is impaired in aged transgenic mutant *hm*^{2}-*αSYN* mice like those studied here, compared to their transgenic WT *hw-αSYN* and nontransgenic controls.[15] Whether the prevention of cell loss observed in A_{2A} KO mice is due to attenuation of UPS dysfunction or downstream mediator of

α-synuclein toxicity remains to be clarified. Another plausible explanation involves a limitation of genetic deletion studies, such that the absence of the A_{2A} receptor throughout development may have resulted in an adult KO phenotype that in its own right might have influenced α-*SYN* toxicity. Although morphological and neurochemical assessments of the constitutive A_{2A} KO mice have not supported a developmental phenotype.[16] This question could be definitively addressed in future studies with the use of a conditional brain-specific A_{2A} KO-transgenic synuclein model.

With multiple specific adenosine A_{2A} antagonists as well as caffeine currently progressing through phase II and III clinical trials for the symptomatic treatment of PD,[17] this class of agent is well positioned for clinical testing of its neuroprotective potential. The present findings strengthen the rationale for disease modification trials of A_{2A} receptor antagonism. They complement epidemiological data on caffeine links to a reduced risk of PD, and substantially broaden the preclinical evidence for A_{2A} receptor-dependent neurodegeneration from acute toxin (eg, 1-methyl-4-phenyl-1,2,3,6-tetrahydropyridine [MPTP] and 6-hydroxydopamine [6-OHDA]) models[12] to an established chronic progressive (mutant human α*SYN*) model of PD. The results also strengthen the contemporary view that PD etiopathogenesis reflects an interplay between genetic (eg, mutant α-synuclein) and environmental (eg, adenosine A_{2A} receptor disruption) influences, and highlight the therapeutic potential of modifying the latter.

Acknowledgments

This research was supported by grants (to MAS) from the National Institutes of Health (NIEHS R01ES010804, and NINDS K24NS060991, R21NS058324); the American Federation for Aging Research/Paul Beeson Scholars Program; and the Department of Defense (W81XWH-04-1-0881).

We thank Dr. Eric K. Richfield, Kavita Prasad, Elizabeth Tarasewicz, and the Molecular Histology Center at the Environmental and Occupational Health Sciences Institute (EOHSI) (http://eohsi.rutgers.edu/mhc) for their expert advice, and processing of the tissue used for stereological assessments. We also thank Deborah Brown-Jermyn for technical assistance, and Drs. Eric Richfield and Howard Federoff for kindly providing the transgenic α-synuclein mouse lines from the University of Rochester.

Potential Conflicts of Interest

A.K. and M.A.S. have received the following grants: NIH R01ES010804, K24NS060991, R21NS058324, AFAR/Beeson Scholar program, DOD W81XWH-04-1-0881.

References

1. Ascherio A, Zhang SM, Hernan MA, et al. Prospective study of coffee consumption and risk of Parkinson's disease in men and women. Ann Neurol 2001;50:56–63.
2. Chen JF, Xu K, Petzer JP, et al. Neuroprotection by caffeine and A(2A) adenosine receptor inactivation in a model of Parkinson's disease. J Neurosci 2001;21:RC143 (1–6).
3. Xu K, Xu Y-H, Chen JF, Schwarzschild MA. Neuroprotection by caffeine: time course and the role of its metabolites in the MPTP model of Parkinson's disease. Neuroscience 2010;167: 475–481.
4. Aguiar LMV, Nobre HV Jr, Macedo DS, et al. Neuroprotective effects of caffeine in the model of 6-hydroxydopamine lesions in rats. Pharmacol Biochem Behav 2006;84:415–419.
5. Kachroo A, Irizarry MC, Schwarzschild MA. Caffeine protects against combined paraquat and maneb-induced dopaminergic neuron degeneration. Exp Neurol 2010;223:657–661.
6. Ikeda K, Kurokawa M, Aoyama S, et al. Neuroprotection by adenosine A2A receptor blockade in experimental models of Parkinson's disease. J Neurochem 2002;80:262–270.
7. Carta AR, Kachroo A, Schintu N, et al. Inactivation of neuronal forebrain A2A receptors protects dopaminergic neurons in a mouse model of Parkinson's disease. J Neurochem 2009;111: 1478–1489.
8. Popat RA, Van den Eeden SK, Tanner SM, et al. Coffee, ADORA2A and CYP1A2: the caffeine connection in Parkinson's disease. Eur J Neurol 2011;18:756–765.
9. Richfield EK, Thiruchelvam MJ, Cory-Slechta DA, et al. Behavioral and neurochemical effects of wild-type and mutated α-synuclein in transgenic mice. Exp Neurol 2002;175:35–48.
10. Chesselet MF. In vivo alpha-synuclein overexpression in rodents: a useful model of Parkinson's disease? Exp Neurol 2008;209:22–27.
11. Fredholm BB, Chen JF, Masino SA, et al. Actions of adenosine at its receptors in the CNS: insights from knockouts and drugs. Annu Rev Pharmacol Toxicol 2005;45:385–412.
12. Morelli M, Carta AR, Kachroo A, et al. Pathophysiological roles for purines: adenosine, caffeine and urate. Prog Brain Res 2010;183: 183–208.
13. Waddington JL, O'Tuathaigh C, O'sullivan G, et al. Phenotypic studies on dopamine receptor subtype and associated signal transduction mutants: insights and challenges from 10 years at the psychopharmacology-molecular biology interface. Psychopharmacology 2005;181:611–638.
14. Giorgi FS, Bandettini di Poggio A, Pellegrini A, et al. A short overview on the role of alpha-synuclein and proteasome in experimental models of Parkinson's disease. J Neural Transm Suppl 2006;70: 105–109.
15. Chen L, Thiruchelvam MJ, Madura K, et al. Proteasome dysfunction in aged human alpha-synuclein transgenic mice. Neurobiol Dis 2006;120–126.
16. Chen J-F, Huang Z, Ma J, et al. A_{2A} adenosine receptor deficiency attenuates brain injury induced by transient focal ischemia in mice. J Neurosci 1999;19:9192–9200.
17. Barkhoudarian MT, Schwarzschild MA. Preclinical jockeying on the translational track of adenosine A_{2A} receptors. Exp Neurol 2011; 228:160–164.

Neurology®

Caffeine in Parkinson disease : Better for cruise control than snooze patrol?

Michael A. Schwarzschild

Neurology; Published online before print August 1, 2012;
DOI 10.1212/WNL.0b013e318263580e

This information is current as of August 1, 2012

The online version of this article, along with updated information and services, is located on the World Wide Web at:
http://www.neurology.org/content/early/2012/08/01/WNL.0b013e318263580e

Neurology ® is the official journal of the American Academy of Neurology. Published continuously since 1951, it is now a weekly with 48 issues per year. Copyright © 2012 by AAN Enterprises, Inc. All rights reserved. Print ISSN: 0028-3878. Online ISSN: 1526-632X.

AMERICAN ACADEMY OF NEUROLOGY®

Published Ahead of Print on August 1, 2012 as 10.1212/WNL.0b013e318263580e Appendix B

EDITORIAL

Caffeine in Parkinson disease

Better for cruise control than snooze patrol?

Michael A. Schwarzschild, MD, PhD

Correspondence & reprint requests to Dr. Schwarzschild: MichaelS@helix.mgh.harvard.edu

Neurology® 2012;79:616–618

Caffeine, the world's most widely used psychomotor stimulant, potentiates the antiparkinsonian effects of levodopa in preclinical models, as noted nearly 40 years ago.[1] The findings prompted early placebo-controlled crossover studies of caffeine as an adjunct to levodopa or a dopamine agonist in Parkinson disease (PD).[2,3] No motor effect of caffeine was demonstrated other than exacerbation of dyskinesia. However, these small studies assessed caffeine at high doses (~1,100 mg/day, the equivalent of ~8 cups of brewed coffee/day), at which most subjects reported restlessness and insomnia. By contrast, another small study reported that caffeine at a much lower dose of 100 mg/day helped improve freezing of gait, though tolerance to caffeine seemed to limit benefit.[4]

In this issue of *Neurology*®, Postuma et al.[5] report the results of a randomized controlled trial of caffeine as a treatment of excessive daytime sleepiness in PD. Although efficacy for improving wakefulness assessed under the primary outcome did not reach statistical significance (yielding Class I evidence against such an indication in PD), a secondary outcome analysis provided evidence in support of an antiparkinsonian motor effect of caffeine. Sixty-one subjects with PD with documented daytime sleepiness and moderate motor symptoms, treated with ~600 mg per day of levodopa on average, were randomized 1:1 to placebo vs 100 mg caffeine twice a day for 3 weeks before advancing to 200 mg twice daily for 3 more weeks. After 6 weeks, those in the caffeine group showed improvement relative to controls on a standard clinical scale of parkinsonian dysfunction (close to 5 points on the total Unified Parkinson's Disease Rating Scale [UPDRS]), including its objective motor component and subscores for bradykinesia and rigidity, with similar findings at 3 weeks on the lower dose.

Several limitations of the study, as discussed by the authors, include the exploratory nature of the motor findings given the primary hypothesis of a nonmotor benefit; the possibility of incomplete blinding; and the brevity of treatment, leaving open the question of tolerance to caffeine. Nevertheless, these findings are noteworthy, the first to suggest antiparkinsonian effects of caffeine in a randomized clinical trial.

This Class II evidence that motor function in PD can be improved by caffeine is bolstered by mechanistic and clinical advances identifying adenosine A_{2A} receptor antagonism as the molecular basis of caffeine's psychomotor stimulant properties, and as a promising antiparkinsonian strategy. The discovery by the early 1980s that caffeine likely acts through antagonism of adenosine receptors[6] coupled with caffeine's antiparkinsonian effects in animal models[1] accelerated research into the neurobiology and neurotherapeutic potential of adenosine receptor blockade. Enthusiasm for targeting adenosine A_{2A} receptors in particular as a candidate antiparkinsonian strategy grew after the colocalization of A_{2A} receptors with dopamine D_2 receptors in striatopallidal output neurons, where their opposing cellular influences account for antiparkinsonian actions of both A_{2A} antagonists and D_2 agonists.[6,7] Moreover, the relatively restricted expression of CNS A_{2A} receptors to and within the striatum[7] (figure, A) suggests a low liability for neuropsychiatric side effects of A_{2A} antagonists, in contrast to existing nondopaminergic antiparkinsonian agents targeting much more widespread CNS receptors. Neuroimaging and behavioral data confirmed that caffeine indeed blocks striatal A_{2A} receptors (figure, B),[8] which appear required for its motor stimulant properties (figure, C).[9]

Caffeine's candidacy as an antiparkinsonian agent is strengthened further by progress made with several more specific A_{2A} antagonists (including istradefylline, preladenant, and tozadenant). Positive results have prompted ongoing phase II and III clinical trials of their antiparkinsonian potential. Epidemiologic and laboratory evidence that caffeine and specific A_{2A} antagonists may offer additional benefits of slowing the underlying neurodegenerative process or

See page 651

From the Department of Neurology, Massachusetts General Hospital, Boston.

Study funding: Supported by NIH grant K24NS060991 and DoD grant W81XWH-11-1-0150.

Go to Neurology.org for full disclosures. Disclosures deemed relevant by the author, if any, are provided at the end of this editorial.

Copyright © 2012 by AAN Enterprises, Inc.
Copyright © by AAN Enterprises, Inc. Unauthorized reproduction of this article is prohibited.

reducing the risk of dyskinesias,[7] while clinically untested, has helped justify a high level of investment in adenosine antagonism for PD.

Nevertheless, the findings of Postuma et al.[5] underscore the longstanding question of whether the greater selectivity for A_{2A} (over A_1 and other adenosine receptor subtypes) offered by adenosine antagonists in commercial development constitutes a clinically meaningful advantage over the relatively nonspecific adenosine antagonism of caffeine. Such benefits should be substantial to offset the unmatchable advantages of caffeine's long-term safety experience and cost. Moreover, as the authors note, their preliminary findings that caffeine improved total UPDRS score by 4–5 points, if substantiated, may be comparable to UPDRS improvements achieved to date with specific A_{2A} antagonists.

There are theoretical disadvantages of caffeine and its greater likelihood for "off-target " effects. For example, caffeine classically produces tolerance to its motor stimulant actions; by contrast, preclinical studies of a specific A_{2A} antagonist failed to demonstrate tolerance to motor stimulant and antiparkinsonian effects.[10] Ultimately, head-to-head comparisons may be required to distinguish the utility of A_{2A}-specific and mixed adenosine receptor antagonists for treating the motor symptoms or other features of PD. For the time being, the results of Postuma et al.[5] should encourage further investigation of a potential antiparkinsonian ("cruise control") benefit of caffeine without entirely discouraging pursuit of its putative alerting ("snooze patrol") action in PD. Although current data do not warrant a recommendation of caffeine as a therapeutic intervention in PD, they can reasonably be taken into consideration when discussing dietary caffeine use.

Figure Potential antiparkinsonian actions of caffeine through its blockade of adenosine A_{2A} receptors on striatal neurons

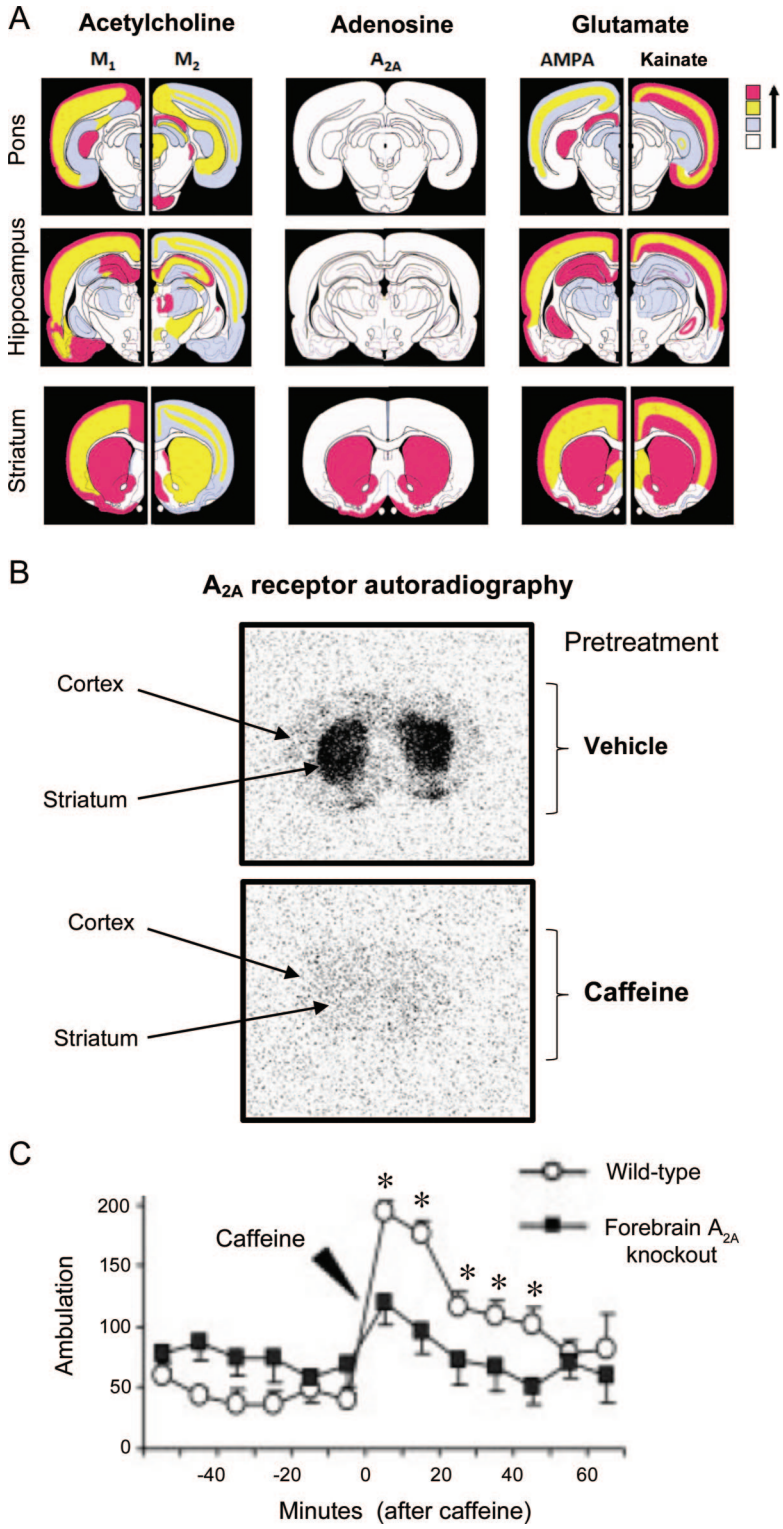

(A) Muscarinic acetylcholine receptors (left) and ionotropic glutamate receptors (right) are targeted by nondopaminergic antiparkinsonian drugs (e.g., trihexyphenidyl and amantadine, respectively). By contrast, the adenosine A_{2A} receptor (center) is discretely expressed in the CNS, primarily in the striatum.[7] (B) Caffeine blocks adenosine receptors including the A_{2A} receptor. A moderate dose of caffeine can markedly displace binding of endogenous adenosine or a radiolabeled A_{2A} receptor ligand.[8] (C) The psychomotor motor stimulant actions of caffeine require adenosine A_{2A} receptors, particularly those expressed on forebrain neurons as demonstrated by attenuated locomotor effects of caffeine in mice with a conditional knockout of neuronal A_{2A} receptors.[9] For details, see cited publications and references therein, from which panels are adapted with permission.

DISCLOSURE

M. Schwarzschild received research support from NIH grants K24NS060991, R01NS054978, R01NS061858, and R21NS058324, DoD grants W81XWH-04-1-0881 and W81XWH-11-1-0150, the Michael J. Fox Foundation, the RJG Foundation, and the American Parkinson's Disease Foundation. He serves on the Emory NIEHS-funded PD-CERC advisory board, and provides consultative service to Harvard University conducting Parkinson's disease case record reviews. **Go to Neurology.org for full disclosures.**

REFERENCES

1. Fuxe K, Ungerstedt U. Action of caffeine and theophyllamine on supersensitive dopamine receptors: considerable

Copyright © by AAN Enterprises, Inc. Unauthorized reproduction of this article is prohibited.

enhancement of receptor response to treatment with DOPA and dopamine receptor agonists. Med Biol 1974; 52:48–54.
2. Shoulson I, Chase T. Caffeine and the antiparkinsonian response to levodopa or piribedil. Neurology 1975;25: 722–724.
3. Kartzinel R, Shoulson I, Calne DB. Studies with bromocriptine: III: concomitant administration of caffeine to patients with idiopathic parkinsonism. Neurology 1976; 26:741–743.
4. Kitagawa M, Houzen H, Tashiro K. Effects of caffeine on the freezing of gait in Parkinson's disease. Mov Disord 2007;22:710–712.
5. Postuma RB, Lang AE, Munhoz RP, et al. Caffeine for treatment of Parkinson disease: a randomized controlled trial. Neurology 2012;79:651–658.
6. Fredholm BB, Bättig K, Holmén J, Nehlig A, Zvartau EE. Actions of caffeine in the brain with special reference to factors that contribute to its widespread use. Pharmacol Rev 1999;51:83–133.
7. Schwarzschild MA, Agnati L, Fuxe K, Chen JF, Morelli M. Targeting adenosine A_{2A} receptors in Parkinson's disease. Trends Neurosci 2006;29:647–654.
8. Moresco RM, Todde S, Belloli S, et al. In vivo imaging of adenosine A_{2A} receptors in rat and primate brain using [^{11}C]SCH442416. Eur J Nucl Med Mol Imaging 2005; 32:405–413.
9. Yu L, Shen HY, Coelho JE, et al. Adenosine A_{2A} receptor antagonists exert motor and neuroprotective effects by distinct cellular mechanisms. Ann Neurol 2008;63: 338–346.
10. Pinna A, Fenu S, Morelli M. Motor stimulant effects of the adenosine A_{2A} receptor antagonist SCH 58261 do not develop tolerance after repeated treatments in 6-hydroxydopamine-lesioned rats. Synapse 2001;39:233–238.

Copyright © by AAN Enterprises, Inc. Unauthorized reproduction of this article is prohibited.

Research article

Biomedical Chromatography

Received: 18 April 2012, Accepted: 26 April 2012 Published online in Wiley Online Library

(wileyonlinelibrary.com) DOI 10.1002/bmc.2760

Efficient determination of purine metabolites in brain tissue and serum by high-performance liquid chromatography with electrochemical and UV detection

Thomas C. Burdett[a†], Cody A. Desjardins[a†], Robert Logan[a], Nikolaus R. McFarland[b], Xiqun Chen[a]* and Michael A. Schwarzschild[a]

ABSTRACT: The purine metabolic pathway has been implicated in neurodegeneration and neuroprotection. High-performance liquid chromatography (HPLC) is widely used to determine purines and metabolites. However, methods for analysis of multiple purines in a single analysis have not been standardized, especially in brain tissue. We report the development and validation of a reversed-phase HPLC method combining electrochemical and UV detection after a short gradient run to measure seven purine metabolites (adenosine, guanosine, inosine, guanine, hypoxanthine, xanthine and urate) from the entire purine metabolic pathway. The limit of detection (LoD) for each analyte was determined. The LoD using UV absorption was 0.001 mg/dL for hypoxanthine (Hyp), inosine (Ino), guanosine (Guo) and adenosine (Ado), and those using coulometric electrodes were 0.001 mg/dL for guanine (Gua), 0.0001 mg/dL for urate (UA) and 0.0005 mg/dL for xanthine (Xan). The intra- and inter-day coefficient of variance was generally <8%. Using this method, we determined basal levels of these metabolites in mouse brain and serum, as well as in post-mortem human brain. Peak identities were confirmed by enzyme degradation. Spike recovery was performed to assess accuracy. All recoveries fell within 80–120%. Our HPLC method provides a sensitive, rapid, reproducible and low-cost method for determining multiple purine metabolites in a single analysis in serum and brain specimens. Copyright © 2012 John Wiley & Sons, Ltd.

Keywords: HPLC; electrochemical detection; UV–vis detection; biological specimens; purines

Introduction

A growing body of evidence supports an important role of the purine metabolic pathway (Fig. 1) in various neurological disorders including brain injury, Parkinson's disease (PD) and other neurodegenerative diseases (Burnstock, 2008). Adenosine (Ado) is well known to modulate neuronal and synaptic function through its A1 and A2 receptors (Stone, 2005; Schwarzschild *et al*., 2006). Inosine (Ino) has been shown to be neuroprotective either directly (Irwin *et al*., 2006) or indirectly through metabolic conversion to downstream metabolites (Gomez and Sitkovsky, 2003). Similarly, guanine (Gua)-based guanosine (Guo) is implicated as a modulator of neural function (Schmidt *et al*., 2007). Hypoxanthine (Hyp) and xanthine (Xan) have been linked to glutamate-mediated excitotoxicity (Stover *et al*., 1997) and oxidative stress (Quinlan *et al*., 1997), and a recent study implicated a potential role of Xan as a biomarker of PD (LeWitt *et al*., 2011). Remarkably, a convergence of laboratory and epidemiological data has recently identified urate (UA), the enzymatic end product of purine degradation in humans, as a molecular predictor of both risk and progression of PD and as a candidate neuroprotectant for the treatment of PD (Ascherio *et al*., 2009; Cipriani *et al*., 2010). Therefore, extensive detection and quantification of the purine degradation pathway metabolites in brain may provide insight into their relevance to different physiological and pathological conditions.

High-performance liquid chromatography (HPLC) has been the prevalent method of measuring nucleotides, nucleosides and major purine bases in different biological samples (Bakay *et al*., 1978; Nissinen, 1980; Ryba, 1981; Zakaria and Brown, 1981; Iriyama *et al*., 1984; Wynants and Van Belle, 1985; Smolenski *et al*., 1990; Liu *et al*., 1995; Takahashi *et al*., 2010; Struck *et al*., 2011). Although many of those HPLC-based protocols are capable of separating and quantifying multiple purines, they often demand a large injection volume and long retention time, and have low throughput and relatively low sensitivity. The ability to measure much of the purine degradation pathway in a

* Correspondence to: Xiqun Chen, The MassGeneral Institute for Neurodegenerative Disease, Department of Neurology, Massachusetts General Hospital, Harvard Medical School 114 16th, Charlestown, MA 02129, USA. E–mail: xchen17@partners.org

† These authors equally contributed to the paper and are considered co-first authors.

a The MassGeneral Institute for Neurodegenerative Disease, Department of Neurology, Massachusetts General Hospital, Harvard Medical School, 114 16th, Charlestown, MA 02129, USA

b University of Florida, Department of Neurology Center for Translational Research in Neurodegenerative Disease, PO Box 100159, Gainesville, FL 32610, USA

Abbreviations used: Ado, adenosine; DHBA, 3,4-dihydroxybenzylamine; Gua, guanine; Guo, guanosine; Hyp, hypoxanthine; Ino, inosine; MD, methyl-DOPA sesquihydrate; PD, Parkinson's disease; UA, urate; Xan, xanthine

 Copyright © 2012 John Wiley & Sons, Ltd.

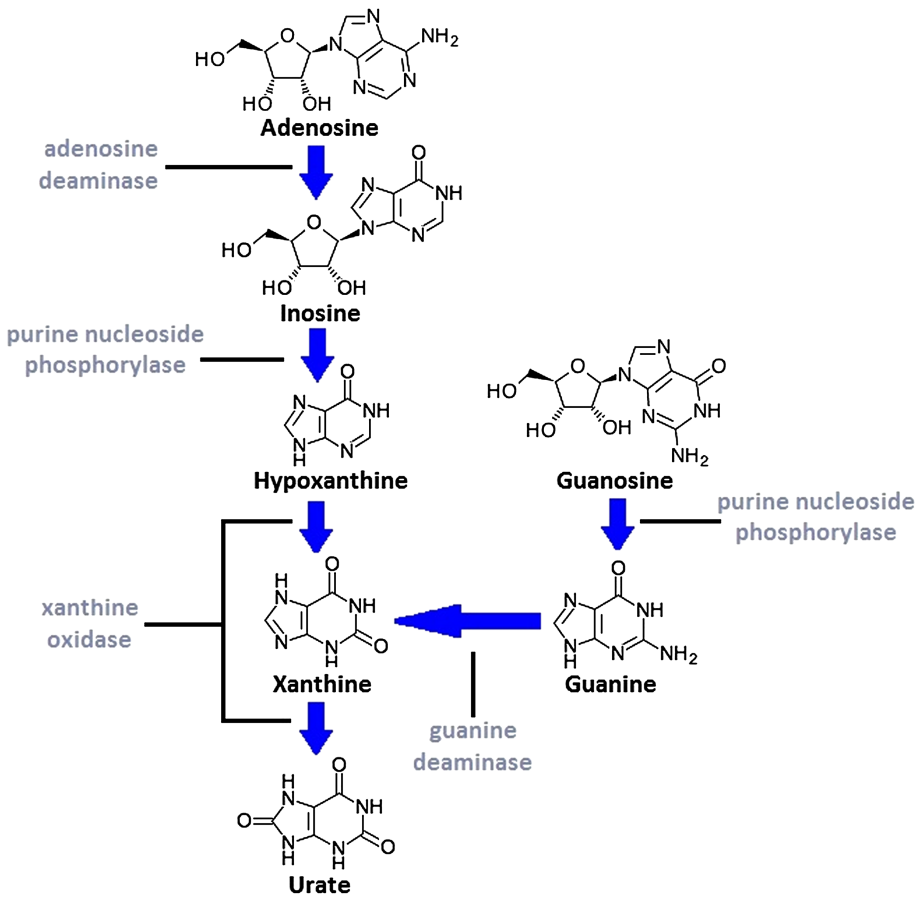

Figure 1. Purine degradation pathway. Adonosine is converted to inosine through the removal of the amine moiety by adenosine deaminase, and inosine is degraded to hypoxanthine through the removal of phospho-1-ribose by purine nucleoside phophorylase. Guanosine is converted to guanine via the action of purine nucleoside phosphorylase, and guanine is then degraded to xanthine through the action of guanine deaminase. In the presence of xanthine oxidase, hypoxanthine and xanthine are converted to urate. Urate constitutes the end product of purine catabolism in humans owing to lack of urate oxidase activity.

single analysis may prove to be a valuable tool in understanding its role in human diseases like PD, as well as in their animal models. A single-run analysis may lead to a better measurement of the purine pathway by eliminating the potential variation inherent in measuring analytes using separate analyses.

Towards this goal, we describe the development of a dual-pump gradient HPLC method using UV and electrochemical detection (ECD). This method achieves suitable separation and sensitivity in a short run time and is capable of measuring seven purine metabolites in tissue and serum with minimal sample preparation and high throughput.

Experimental protocol

Collection of mouse and human tissues

Mice 10 to 12 weeks old C57BL/6 (J) and weighing 29 ± 1.3 g were obtained from Jackson Laboratories (Bar Harbor, ME, USA). They were kept under standard conditions (temperature 21 ± 2°C, humidity 30–70%, 12 h light–dark cycle) and with water and standard pellet feed *ad libitum*. Mouse whole blood was collected via a lancet (Goldenrod Animal Lancet, Mineola, NY, USA) puncture of the submandibular vein. The mice were killed via cervical dislocation, and the brain was removed. The striatum of each hemisphere were collected separately and all tissue samples were frozen on dry ice. Postmortem human brain samples were obtained from the MassGeneral Aging and Disability Resource Center/Harvard NeuroDiscovery Center neuropathology core B repository in accordance with institutional, state and federal regulations, as well as the wishes of the families of donors. Fresh frozen tissue (stored at −80°C) samples were collected from 10 male control brains, defined as those without evidence of neurodegenerative disease (such as Parkinson, Huntington or Alzheimer's disease) and with postmortem interval <24 h (mean 19.8 ± 6.0) and age limited to >50 years (mean 82.0 ± 11.2). Tissue samples (~100–200 mg) were dissected on dry ice from striatum. All tissue was kept frozen at −80°C until processed for HPLC analysis.

Instrumentation

The reversed-phase HPLC system comprised two pumps, a model 584 and a model 582 isocratic pump, feeding a high-pressure gradient mixer. Samples were injected using a model 524 autosampler with a 100 μL sample loop and analysis was performed using a model 5600A CoulArray with a 528 UV–vis detector followed by two model 5011A coulometric cells. All equipment was obtained from ESA Biosciences (Chelmsford,

Copyright © 2012 John Wiley & Sons, Ltd.

MA, USA). Analyte separation was achieved using a batch-tested Varian Microsorb-MV reversed-phase C_{18} column (150 × 4.6 mm i.d., 5 μm, 100 A; Varian Inc., Palo Alto, CA, USA).

Chemicals and reagents

Acetonitrile (HPLC-grade), potassium phosphate monobasic (HPLC-grade) and EDTA (electrophoresis grade, ≥99%) were supplied by Fisher Chemical (Pittsburgh, PA, USA). Ado, Guo, Gua, Hyp, Ino, UA, Xan and 3,4-dihydroxybenzylamine (DHBA) standards (≥99%) were supplied by Sigma Aldrich (St Louis, MO, USA). Sodium 1-pentanesulfonate (≥99%) and methyl-DOPA sesquihydrate (MD, ≥99%) were obtained from Fluka Analytical (Sigma-Aldrich). Double-distilled water was obtained from a Milli-Q Water System (Millipore, Billerica, MA, USA). All water was subsequently passed through a C_{18} Maxi-Clean cartridge (Alltech, Deerfield, IL, USA) to remove any potential organic contaminants.

HPLC operating parameters

A dual mobile phase gradient was used to achieve appropriate separation of all analytes of interest. Mobile phase A contained 0.52 mM sodium 1-pentanesulfonate and 0.20 M KH_2PO_4 monobasic at pH 3.5 using 85% phosphoric acid (HPLC-Grade, Fisher Scientific, Pittsburgh, PA, USA). Mobile phase B had the same final concentrations as mobile phase A, except for the addition of 10% acetonitrile (v/v). The gradient composition is shown in Fig. 2. The flow rate was 1.0 mL/min, and the system was allowed to equilibrate at that flow rate for 15 min prior to the first sample injection. The sample injection volume was 12 μL.

The detectors were linked in series, with the Model 528 UV–vis light spectroscopy spectrophotometer upstream of both electrochemical cells. UV–vis detection was set to a wavelength of 254 nm. The first electrode was set to −0.10 V and acted as a conditioning cell. The analytical electrodes 1 and 2 were set at +0.15 and +0.45 V, respectively. Data were collected using CoulArray Data Station 3.0 software (ESA Biosciences) with auto-range gain enabled.

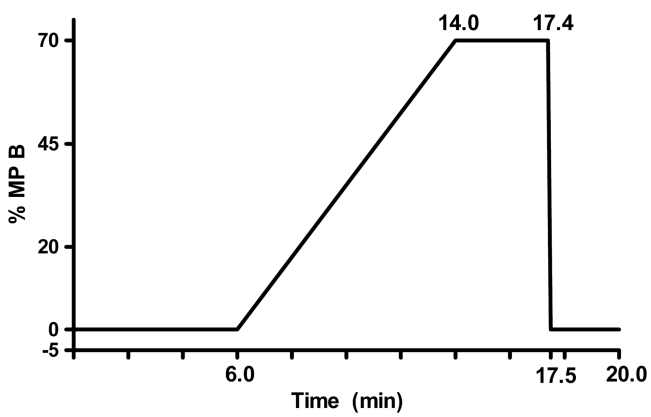

Figure 2. Mobile phase gradient paradigm. Mobile phase A: 0.2 M KH_2PO_4 monobasic, 0.52 mM sodium 1-pentanesulfonate, pH 3.5. Mobile phase B: 0.2 M KH_2PO_4 monobasic, 0.52 mM sodium 1-pentanesulfonate, 10% acetonitrile, pH 3.5. MP: Mobile phase.

Preparation of stock solutions and standards

Individual purine stock solutions were dissolved in double-distilled water that had been filtered through a C_{18} Maxi-Clean cartridge to a final concentration of 1.0 mg/mL except for UA, which was made at a stock concentration of 0.5 mg/mL owing to its solubility. Aliquots of the stocks were stored at −80°C until needed. A working mixed purine standard curve was created by serial dilutions of purine stocks in PE buffer containing 50 mM phosphoric acid, 0.1 mM EDTA, 50 μM MD and 1 μM DHBA (internal standards) from 1.0 mg/mL purine stocks. The working standard curve (except in limit of detection experiments) ranged from 1.0 to 0.001 mg/dL for all purines.

Preparation of mouse and human brain samples for purine analysis

Brain samples were weighed at −60°C and immediately homogenized on ice using a Teflon pestle in 20× volume (v:w) of PE buffer. Extracted samples were then centrifuged at 16,000***g*** for 15 min. The supernatant was then removed and filtered through a 0.22 μm Spin-X Cellulose Acetate filter tube (Corning, NY, USA) at 16,000***g*** for 5 min. Resulting filtrate was stored at −80°C until needed.

Preparation of mouse serum for purine analysis

Whole blood was collected and centrifuged at 16,000***g*** for 15 min. The serum was then transferred and stored at −80°C until needed. Serum deproteination was achieved by the addition of 30 μL of 0.4 M perchloric acid to 50 μL of serum and vortexing briefly. The solution was allowed to incubate on ice for 10 min prior to centrifugation at 1400***g*** for 15 min. The resulting supernatant was removed and added to 20 μL 0.2 M potassium phosphate (pH 4.75) with 1 μM DHBA (internal standard). The resulting solution was filtered through a 0.22 μm Spin-X Cellulose Acetate filter tube at 16,000***g***. The resulting filtrate was stored at −80°C until needed.

Enzyme degradation

To confirm peak identity, enzyme degradation was performed. Mixed purine standards and mouse brain samples were prepared in 0.2 M potassium phosphate monobasic (pH 7.75). Standards and samples were then incubated with the following individual enzymes: adenosine deaminase, purine nucleoside phosphorylase, xanthine oxidase and urate oxidase (all purchased from Sigma-Aldrich, St Louis, MO, USA). Reaction conditions were 25°C overnight for all enzymes, and concentration of each enzyme was predetermined to be sufficient to completely eliminate the target analyte over the overnight incubation period. The resulting mixtures were centrifuged for 15 min at 15,000 rpm, the supernatant was then filtered through a 0.22 μm Spin-X Cellulose Acetate filter tube (Corning, NY, USA) at 16,000***g*** for 5 min. The resulting filtrate was stored at −80°C until needed.

Spike recovery

Spike recovery experiments were performed to validate the accuracy of the method. Purine standards and mouse serum and brain samples were prepared. Baseline values of each analyte per sample were detected. Stock solutions were then

Copyright © 2012 John Wiley & Sons, Ltd.

made at 5 times the basal concentrations. Each experiment consisted of a sample control, spike control and spiked sample, all of which were individually made to 60 μL to allow for triplicate runs at 20 μL each. Sample plus mobile phase A (in the amount of the spike) constituted the sample control. The spike control had a specified volume of stock that resulted in 5 times the basal analyte levels plus mobile phase A. The spiked sample included the necessary spike amount of stock and sample. Recovery percentage was calculated by comparing the spiked sample analyte values to the analyte values of the sample control plus spike control levels.

Results and discussion

The main goals of this method were to obtain suitable separation and high sensitivity of seven purine metabolites with a single injection and short run time, allowing for high-throughput analysis of biological samples. This reversed-phase chromatographic method was built upon previous isocratic methods using ECD of UA and Xan (Iriyama *et al.*, 1984; Liu *et al.*, 1995) and underwent optimization of pH and an ion-pairing agent parameters to ensure adequate separation of the analytes of interest. We also took advantage of the differential selectivity of UV and electrochemical detectors for the major purines in biological samples to achieve better signal separation than previously observed.

Determination of electrode potentials and UV–vis wavelength

Hydrodynamic voltammograms were obtained for UA, Xan and Gua to determine the optimum oxidizing potentials for each analyte (Fig. 3). The oxidation of UA increased with greater voltages, reaching a plateau near +0.1 V. A slightly higher potential of +0.15 V (P_1) was chosen to ensure that UA was being fully oxidized, while avoiding oxidation of other similarly retained analytes that might have obscured the UA signal. Oxidation of Gua and Xan reached a plateau at +0.45 V (P_2), at which no co-eluting UA peak interfered with the Gua measurement (data not shown), suggesting that the upstream electrode set at 0.15 V potential had fully oxidized UA. Thus, +0.15 and +0.45 V were chosen as the analytical potentials because they provided full oxidation of the analytes, while avoiding co-oxidation of Gua and UA, which have very similar retention times. A pre-analytical electrode was set to −0.1 V (P_0) to oxidize any potential contaminants that are more easily oxidized than UA. The −0.1 V potential was chosen because more positive potentials partially oxidize UA (Fig. 3), which would weaken the measurable signal at the analytical +0.15 V electrode.

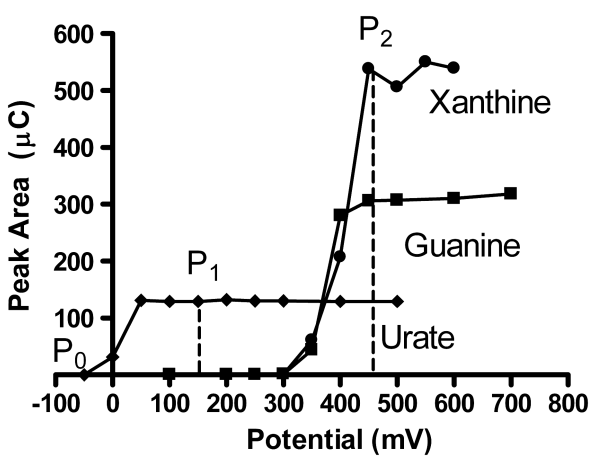

Figure 3. Hydrodynamic voltammogram curves for urate, guanine, and xanthine. Measurements were taken using a model 5011A coulometric cell. An analytical potential of +0.15 V (P_1) was selected for urate, and an analytical potential of +0.45 V (P_2) was selected for guanine and xanthine. A conditioning potential of −0.1 V (P_0) was chosen to minimize contaminant peaks.

Hyp, Ado, Ino and Guo were detected at a UV wavelength of 254 nm. UA, Xan and Gua were also detectable at this UV wavelength, but electrochemical detection provided a considerably lower limit of detection (LoD; Table 1). This advantage becomes apparent when measuring UA in brain tissue, in which UA concentrations are >5-fold lower than in serum (Cipriani *et al.*, 2010). UA and Gua also have very similar retention times, leading to co-elution and considerably overlapping peaks in UV detection that are easily avoided through electrochemical potential manipulation as described above.

Mobile phase and gradient development

Chromatographic baseline resolution of the analytes of interest was achieved through the manipulation of mobile phase composition and a gradient of organic solvent. The original mobile phase was adapted from Iriyama *et al.* (1984). Determination of the appropriate pH was performed through the measurement of retention times of all the analytes across a range of mobile phase pH values (Table 2). All other components of the mobile phase were kept constant through the pH calibration. pH dependencies of purine retention times were consistent with their respective values of pK_a in the pH range studied. For example, the greatest drop in the retention time of UA (pK_a at 5.4) occurred as pH was increased from 5 to 6, as expected given the increasing likelihood of the anionic urate form, which in contrast to neutral protonated form of urate is not retained on the hydrophobic interaction column. Conversely, Ado (pK_a 3.5) showed a markedly longer retention time as the pH was raised between 3 and 4, consistent with its loss of a proton to become neutral adenosine. Owing to poor separation between UA and Hyp below pH 3, and between Xan and Hyp at the higher pHs tested, a pH of 3.5 was selected for routine use.

After the optimal pH was determined, various concentrations of several ion-pairing agents were introduced into the mobile phase to manipulate retention time and individual peak shape. The retention times produced by the various ion-pairing agents and concentrations are shown in Table 2. It was determined that 0.5 mM 1-pentanesufonate produced the best peak symmetry and baseline separation of the variations.

In an attempt to keep analysis times short and throughput high, a gradient was introduced to elute Ado, Guo and Ino more quickly. Under the isocratic conditions these analytes eluted far later than any of the other analytes of interest. Their late elution led to excessive band spreading, contributing to a considerable loss of sensitivity. By using a gradient, these analytes were eluted sooner and with a sharper peak shape than was possible using an isocratic method (Fig. 4a). Optimization of the gradient percentage organic and ramp times was performed to produce the shortest run time possible with a clear chromatographic

Copyright © 2012 John Wiley & Sons, Ltd.

Table 1. Analytical parameters of merit for purine chromatographic peaks

Analytes	Retention time (min)	Method of detection	Limit of detection (mg/dL)	Standard range (mg/dL)	Slope-intercept	R^2
Guanine	4.52	EC (+0.45 V)	0.001	0.001–1.0	$y = 178.05x - 0.558$	0.9999
Urate	4.78	EC (+0.15 V)	0.0001	0.0001–5.0	$y = 131.76x + 0.5998$	1
Hypoxanthine	5.46	UV	0.001	0.001–5.0	$y = 10.928x - 0.0001$	1
Xanthine	6.90	EC (+0.45 V)	0.0005	0.0005–5.0	$y = 38.729x + 1.7033$	0.9977
Inosine	11.10	UV	0.001	0.001–5.0	$y = 7.8419x + 0.0708$	1
Guanosine	11.30	UV	0.001	0.005–1.0	$y = 5.3857x + 0.0048$	1
Adenosine	12.10	UV	0.001	0.001–5.0	$y = 9.9976x + 0.0725$	1
DHBA (IS)	3.38	EC (+0.15 V)	—	—	—	—
MD (IS)	8.76	EC (+0.15 V)	—	—	—	—

DHBA, 3,4-Dihydroxybenzylamine; IS, internal standard; MD, methyl-DOPA

Table 2. Retention times of purine metabolites vs pH and concentration of ion-pairing agent during method development

Chromatographic conditions	Retention time (min)					
pH[a]	Urate	Hypoxanthine	Xanthine	Inosine	Adenosine	MD
2.5	4.0	4.1	4.7	9.1	11.7	—
3.0	3.8	4.1	4.5	9.0	13.3	11.8
4.0	3.8	4.2	4.6	9.0	21.2	5.2
4.5	3.7	4.2	4.6	9.1	24.5	4.7
5.0	3.4	4.2	4.6	9.1	26.1	4.4
6.0	2.7	4.2	4.5	9.1	—	4.3
7.0	2.6	4.1	4.1	8.8	—	4.2
Ion-pairing agent[b]						
0.5 mM 1-Pentanesulfonate	4.3	4.6	5.3	11.8	14.4	—
1.5 mM 1-Pentanesulfonate	3.8	4.0	4.6	9.1	10.8	—
1.5 mM 1-Octanesulfonate	3.9	4.2	4.7	9.8	14.6	—

[a]Retention times with varying pH determined using 1.5 mM 1-pentanesulfonate.
[b]Retention times with varying ion-pairing agents/concentrations determined at pH 3.5.
MD, Methyl-DOPA

baseline resolution of the closely eluting Ado, Ino and Guo peaks, without affecting the resolution of earlier analytes.

Method validation

The validity of the method was assessed through determination of the limit of detection, calculation of the linearity and variation between separate standard curves, calculation of inter-/intra-day coefficient of variation (CV). Additionally peak identity and method accuracy were determined and are discussed together with biological sample results.

The LoD was defined as the lowest concentration of each analyte whose peak height exceeded 3 times the height of the average baseline noise. No analyte detected by UV was measurable below 0.001 mg/dL, while Xan and UA measured by electrochemical detection were measurable at 0.0005 and 0.0001 mg/dL, respectively (Table 1). Standard curves containing all the analytes of interest were then run in triplicate and the mean of these three curves was used to determine variation, the slope–intercept formula, and the R^2 for each analyte (Table 1). All standard curves had very little variation, with the greatest deviation coming from the Xan curve measured by ECD with an R^2 of 0.998.

The method detection limit (MDL) was also determined for each purine analyte. Eleven sequential runs of freshly prepared 0.005 mg/dL concentration standards were analyzed. The MDL for the Ado values was the highest of the analytes, at 0.0018 mg/dL, with a standard deviation of 0.0006 mg/dL. The MDL for the method is set at that value to ensure that all other analytes can be assayed with at least 99% confidence. Therefore, the limit of quantification (LOQ) of our method is 0.006 mg/dL of analyte, which is 10 times the Ado SD value.

Intra- and interday coefficient of variance percentages (CV) were derived from standard solutions prepared at concentrations of 1.0, 0.1 and 0.005 mg/dL analyte. The mean, standard deviation and CV were calculated (Table 3). The intraday CV experiment was performed by running three standard samples of each concentration at three different time points a day. The intraday variation CV for all analytes was below 10%. Interday CV was assessed by repeating the intraday experiment over the subsequent 2 days, utilizing the same standard solutions and time points as on the first. The first day of CV experiments (intraday

Copyright © 2012 John Wiley & Sons, Ltd.

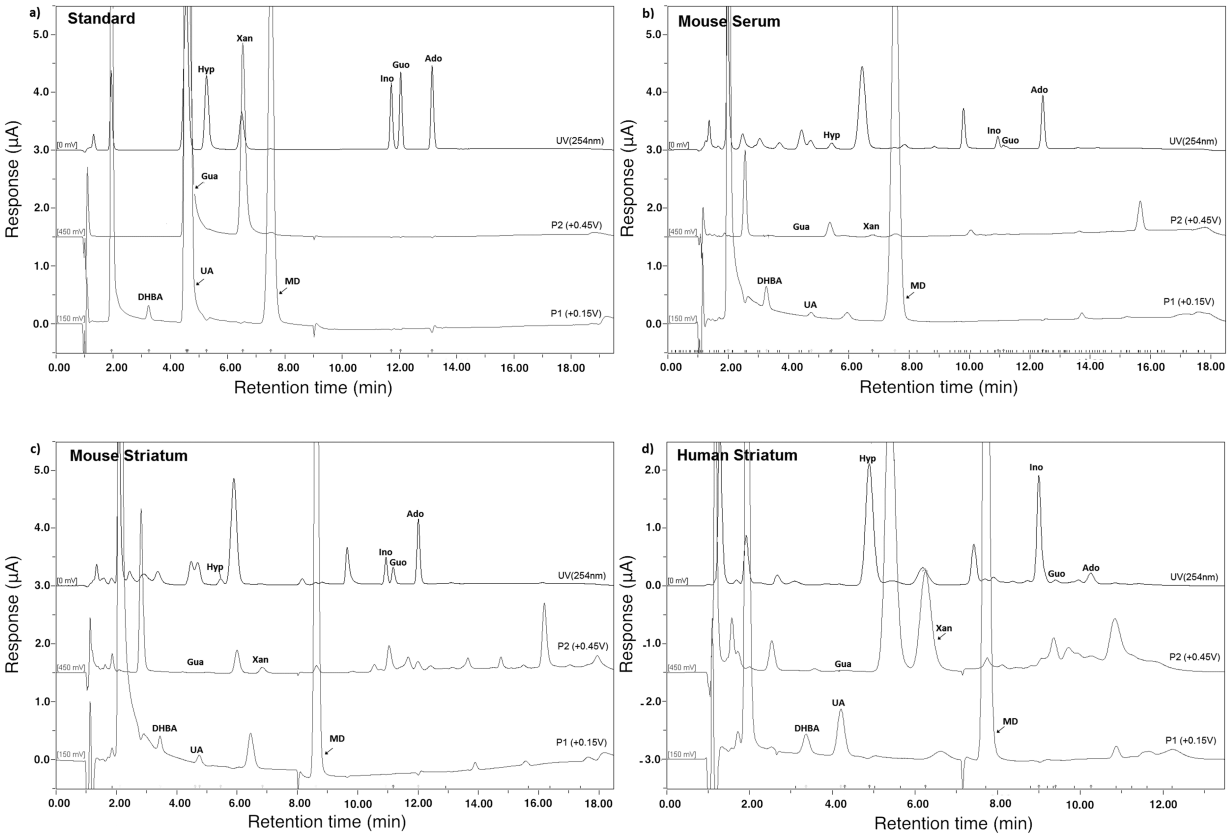

Figure 4. Chromatograms of 1 mg/dL standards mixture (a), mouse serum (b), mouse striatum (c) and human striatum (d). Detection of analytes was performed either by ECD at +0.15 V (P1), +0.45 V (P2), or UV–vis at 254 nm. Gua, Guanine; UA, urate; Hyp, hypoxanthine; Xan, xanthine; Ino: inosine; Guo: guanosine; Ado: adenosine. Internal Standards are 3,4-dihydroxybenzylamine (DHBA, 1 µM) and methyl-DOPA (MD, 50 µM).

assessment) was included in the interday CV calculations, totaling three days of data. Only Xan at 1.0 mg/dL had a CV that exceeded 10%. The increased variation in the Xan measurement is most likely due to variation in the baseline associated with the initiation of the gradient. The gradient begins at approximately the same time that Xan elutes, and causes a small artifact peak that introduces some variability into the Xan measurement that is not present in the measurements of all the other analytes (Table 3).

Measurement of purine metabolites in tissue and serum

The ultimate goal of this method was to obtain sufficient analyte separation and sensitivity to allow measurement of the purine metabolites of interest in mouse and human tissues, including brain and serum. After appropriate separation was achieved with standard mixtures, this method was applied to mouse serum and brain tissue (Fig. 4 b and c).

C57BL/6 mice were killed, and blood was collected. Serum was then analyzed after deproteination with perchloric acid. Mouse brains were extracted, their striatum were collected and purine analysis was performed. The concentrations were determined from the mean of 10 male mice. Except for guanine, all concentrations of metabolites of interest were considerably above their LoD (Table 1), allowing for accurate measurements of each analyte (Table 4). Routine application of this method later to measurement of purines in brain and serum in mice across different experiments has been consistently producing comparable basal level values, allowing direct comparison and data pooling.

This method was then applied to the analysis of post-mortem male human striatum ($n = 10$) processed in a similar manner to the mouse tissue (Table 4). We are aware that more work needs to be done to take postmortem interval into account when analyzing the final values. Nevertheless, the chromatogram of human tissue showed a satisfactory separation and sensitivity (Fig. 4d).

Two strategies were employed to further confirm peaks in biological samples and rule out peak contamination. First, we slightly altered the acetonitrile concentration in both mobile phases to change the analyte retention time in multiple runs of the same sample. Standards and sample analyte retention time changes matched, while analyte concentrations were held constant over different mobile phases (data not shown). Secondly, we performed enzyme degradation studies to eliminate analytes of interest. These studies once again confirmed analyte peaks and negligible underlying contamination. Incubation with urate oxidase, for example, eliminated 91% of urate peak value, and xanthine oxidase eliminated 98% of xanthine and 100% of hypoxanthine peak values.

To further validate the accuracy of our method, spike recovery was performed using mouse serum and brain samples. All recoveries fell within 80–120%. Mouse serum spike recoveries were 80.52% (UA), 103.83% (Xan), 96% (Hyp), 96.51% (Ino), 100.47% (Ado), 118.49% (Gua) and 89.8% (Guo). Mouse striatal spike recoveries were 95% (UA), 99% (Xan), 96% (Hyp), 86% (Ino), 93% (Ado), 84% (Gua) and 99% (Guo).

In conclusion, we have characterized an efficient method of separating seven purine metabolites using HPLC with dual-pump

Copyright © 2012 John Wiley & Sons, Ltd.

Table 3. Intra- and inter-day coefficient of variation

Analytes	Intra-day (the area under the peak)						Inter-day (the area under the peak)					
	0.005 mg/dL		0.1 mg/dL		1.0 mg/dL		0.005 mg/dL		0.1 mg/dL		1.0 mg/dL	
	$x \pm$ SD	CV (%)	$x \pm$ SD	CV (%)	$x \pm$ SD	CV (%)	$x \pm$ SD	CV (%)	$x \pm$ SD	CV (%)	$x \pm$ SD	CV (%)
Urate	0.48 ± 0.03	6.5	9.41 ± 0.26	2.7	81.51 ± 0.93	1.1	0.48 ± 0.03	6.5	9.41 ± 0.29	3.0	82.77 ± 3.87	4.7
Xanthine	1.08 ± 0.07	6.6	23.27 ± 0.65	2.8	159.01 ± 1.21	0.8	1.08 ± 0.07	6.6	23.32 ± 0.72	3.1	167.57 ± 25.73	15.4
Hypoxanthine	0.11 ± 0.01	7.4	2.25 ± 0.04	1.6	21.79 ± 0.11	0.5	0.11 ± 0.01	7.4	2.25 ± 0.04	1.7	21.83 ± 0.17	0.8
Inosine	0.07 ± 0	2.9	1.41 ± 0.01	0.8	13.14 ± 0.11	0.9	0.07 ± 0	2.9	1.41 ± 0.01	0.8	13.27 ± 0.41	3.1
Adonosine	0.09 ± 0	3.6	1.93 ± 0.02	1.0	19.36 ± 0.09	0.5	0.09 ± 0	3.6	1.93 ± 0.02	0.8	19.29 ± 0.25	1.3
Guanine	0.73 ± 0.07	9.7	20.13 ± 1.96	9.7	218.89 ± 2.02	0.9	0.73 ± 0.07	9.7	19.53 ± 0.39	2.0	218.44 ± 2.31	1.1
Guonosine	0.07 ± 0	5.3	1.57 ± 0.02	1.1	16.86 ± 0.14	0.8	0.07 ± 0	5.3	1.57 ± 0.01	0.8	16.76 ± 0.33	2.0

CV, Coefficient of variation.

Table 4. Basal levels of purine metabolites in mouse serum and striatum, and human striatum

Tissue	Urate	Xanthine	Hypoxanthine	Inosine	Adenosine	Guanine	Guanosine
Mouse serum (mg/dL)	1.03 ± 0.001	0.32 ± 0.003	0.13 ± 0.004	0.22 ± 0.001	0.03 ± 0.001	$0.003 \pm 4.2 \times 10^{-5}$	0.08 ± 0.002
Mouse striatum (ng/mg wet tissue)	0.46 ± 0.07	1.54 ± 0.19	2.25 ± 0.33	33.98 ± 4.90	190.4 ± 25.63	0.044 ± 0.006	69.62 ± 8.95
Human striatum (ng/mg wet tissue)	7.76 ± 0.89	26.80 ± 2.43	167.9 ± 5.64	89.83 ± 11.18	1.61 ± 0.28	—	—

Copyright © 2012 John Wiley & Sons, Ltd.

gradient and quantifying them using a combination of electrochemical and UV detection. This method has been validated to provide satisfactory sensitivity, specificity, accuracy and consistency for measurement in biological samples. The power of this method is its short run time and high sensitivity, both of which allow for high-quality and high-throughput analysis of biologically relevant tissue samples, with minimal variation between runs or days. The value of these technical refinements for neuroscience research is increasing with renewed interest in the neurobiology of purines in health and disease. Future efforts will include method development for measurement of allantoin, a nonezymatic oxidation product of UA and therefore an index of oxidative stress in humans (Marklund *et al*., 2000; Zitnanová *et al*., 2004) to advance our ability to assess the role of purine metabolic pathway in neurodegeneration and neuroprotection.

Acknowledgments

The authors would like to acknowledge Yuehang Xu for her excellent technical support. This work is supported by the RJG Foundation, Michael J. Fox Foundation, American Federation for Aging Research, NIH grants R21NS058324 and K24NS060991, and US Department of Defense W81XWH-11-1-0150.

References

Ascherio A, LeWitt PA, Xu K, Eberly S, Watts A, Matson WR, Marras C, Kieburtz K, Rudolph A, Bogdanov MB, Schwid SR, Tennis M, Tanner CM, Beal MF, Lang AE, Oakes D, Fahn S, Shoulson I. Schwarzschild MA and Parkinson Study Group DATATOP Investigators. Urate as a predictor of the rate of clinical decline in Parkinson disease. *Archives of Neurology* 2009; **66**(12): 1460–1468.

Bakay B, Nissinen E and Sweetman L. Analysis of radioactive and nonradioactive purine bases, nucleosides, and nucleotides by high-speed chromatography on a single column. *Analytical Biochemistry* 1978; **86**(1): 65–77.

Burnstock G. Purinergic signalling and disorders of the central nervous system. *Nature Reviews. Drug Discovery* 2008; **7**: 575–590.

Cipriani S, Chen X and Schwarzschild MA. Urate: a novel biomarker of Parkinson's disease risk, diagnosis and prognosis. *Biomarkers in Medicine* 2010; **4**(5): 701–712.

Gomez G and Sitkovsky MV. Differential requirement for A2a and A3 adenosine receptors for the protective effect of inosine in vivo. *Blood* 2003; **102**(13): 4472–4478.

Iriyama K, Yoshiura M, Iwamoto T and Ozaki Y. Simultaneous determination of uric and ascorbic acids in human serum by reversed-phase high-performance liquid chromatography with electrochemical detection. *Analytical Biochemistry* 1984; **141**(1): 238–243.

Irwin N, Li Y, O'Toole JE and Benowitz LI. Mst3b, a purine-sensitive Ste20-like protein kinase, regulates axon outgrowth. *Proceedings of the National Academy of Science USA* 2006; **103**(48): 18320–18325.

LeWitt P, Schultz L, Auinger P, Lu M and the Parkinson Study Group DATATOP Investigators. CSF xanthine, homovanillic acid, and their ratio as biomarkers of Parkinson's disease. *Brain Research* 2011; **1408**: 88–97.

Liu Z, Li T and Wang E. Simultaneous determination of guanine, uric acid, hypoxanthine and xanthine in human plasma by reversed-phase high-performance liquid chromatography with amperometric detection. *Analyst* 1995; **120**(8): 2181–2184.

Marklund N, Ostman B, Nalmo L, Persson L and Hillered L. Hypoxanthine, uric acid and allantoin as indicators of in vivo free radical reactions. Description of a HPLC method and human brain microdialysis data. *Acta Neurochirurgica (Wien)* 2000; **142**(10): 1135–41; discussion 1141–1142.

Nissinen E. Analysis of purine and pyrimidine bases, ribonucleosides, and ribonucleotides by high-pressure liquid chromatography. *Analytical Biochemistry* 1980; **106**(2): 497–505.

Quinlan GJ, Lamb NJ, Tilley R, Evans TW and Gutteridge JM. Plasma hypoxanthine levels in ARDS: implications for oxidative stress, morbidity, and mortality. *American Journal of Respiratory and Critical Care Medicine* 1997; **155**(2): 479–484.

Ryba M. Reversed-phase liquid column chromatography of pyrimidine and purine derivatives. *Journal of Chromatography* 1981; **219**: 245–254.

Schmidt AP, Lara DR and Souza DO. Proposal of a guanine-based purinergic system in the mammalian central nervous system. *Pharmacological Therapy* 2007; **116**(3): 401–416.

Schwarzschild MA, Agnati L, Fuxe K, Chen JF and Morelli M. Targeting adenosine A2A receptors in Parkinson's disease. *Trends in Neuroscience* 2006; **29**(11): 647–654.

Smolenski RT, Lachno DR, Ledingham SJ and Yacoub MH. Determination of sixteen nucleotides, nucleosides and bases using high-performance liquid chromatography and its application to the study of purine metabolism in hearts for transplantation. *Journal of Chromatography* 1990; **527**(2): 414–420.

Stone TW. Adenosine, neurodegeneration and neuroprotection. *Neurological Research* 2005; **27**(2): 161–168.

Stover JF, Lowitzsch K and Kempski OS. Cerebrospinal fluid hypoxanthine, xanthine and uric acid levels may reflect glutamate-mediated excitotoxicity in different neurological diseases. *Neuroscience Letters* 1997; **238**(1–2): 25–28.

Struck W, Waszczuk-Jankowska M, Kaliszan R and Markuszewski MJ. The state-of-the-art determination of urinary nucleosides using chromatographic techniques 'hyphenated' with advanced bioinformatic methods. *Analytical and Bioanalytical Chemistry* 2011; **401**(7): 2039–2050.

Takahashi T, Otsuguro K, Ohta T and Ito S. Adenosine and inosine release during hypoxia in the isolated spinal cord of neonatal rats. *British Journal of Pharmacology* 2010; **161**(8): 1806–1816.

Wynants J and Van Belle H. Single-run high-performance liquid chromatography of nucleotides, nucleosides, and major purine bases and its application to different tissue extracts. *Analytical Biochemistry* 1985; **144**(1): 258–266.

Zakaria M and Brown PR. High-performance liquid chromatography of nucleotides, nucleosides and bases. *Journal of Chromatography* 1981; **226**(2): 267–290

Zitnanová I, Korytár P, Aruoma OI, Sustrová M, Garaiová I, Muchová J, Kalnovicová T, Pueschel S and Duracková Z. Uric acid and allantoin levels in Down syndrome: antioxidant and oxidative stress mechanisms? *Clinica Chimica Acta* 2004; **341**(1–2): 139–146.

Copyright © 2012 John Wiley & Sons, Ltd.

Appendix D

Curr Neurol Neurosci Rep
DOI 10.1007/s11910-012-0282-7

MOVEMENT DISORDERS (SA FACTOR, SECTION EDITOR)

Urate in Parkinson's Disease: More Than a Biomarker?

Xiqun Chen · Guanhui Wu · Michael A. Schwarzschild

© Springer Science+Business Media, LLC 2012

Abstract Parkinson's disease (PD) is a progressive neurodegenerative disease with characteristic motor manifestations. Although appreciation of PD as a multisystem disorder has grown, loss of dopaminergic neurons in the substantia nigra remains a pathological and neurochemical hallmark, accounting for the substantial symptomatic benefits of dopamine replacement therapies. However, currently no treatment has been shown to prevent or forestall the progression of the disease in spite of tremendous efforts. Among multiple environmental and genetic factors that have been implicated in the pathogenesis of PD, oxidative stress is proposed to play a critical role. A recent confluence of clinical, epidemiological, and laboratory evidence identified urate, an antioxidant and end product of purine metabolism, as not only a molecular predictor for both reduced risk and favorable progression of PD but also a potential neuroprotectant for the treatment of PD. This review summarizes recent findings on urate in PD and their clinical implications.

Keywords Urate · Parkinson's disease · Oxidative stress · Clinical trial · Antioxidant · Neuroprotectant · Neurodegeneration · Neuroprotection · Biomarker · Disease modifier · Neurodegenerative diseases · Purine · Risk factor

X. Chen (✉) · G. Wu · M. A. Schwarzschild
Department of Neurology, Massachusetts General Hospital,
Harvard Medical School,
114 16th Street,
Charlestown, MA 02129, USA
e-mail: xchen17@partners.org

G. Wu
e-mail: gwu4@partners.org

M. A. Schwarzschild
e-mail: michaels@helix.mgh.harvard.edu

Introduction

The past two decades have witnessed exciting advances in our understanding of Parkinson's disease (PD), one of the most common neurodegenerative disorders. With the identification and investigation of PD gene mutations, the pathogenesis of PD is beginning to unfold. Among molecular mechanisms that have been proposed to play a key role leading to the degeneration of nigrostriatal dopaminergic pathway, oxidative stress may represent a central common pathway in the complex convergence of genetic and environmental etiologic factors. Dopaminergic neurons in the substantia nigra (SN) pars compacta have high levels of basal oxidative stress likely due to enzymatic and nonenzymatic oxidation of dopamine [1–3]. This process is considered enhanced in PD due to early compensatory changes in dopamine turnover resulting from the initiation of nigral cell degeneration [4]. Furthermore, calcium influx through L-type calcium channels during autonomous pacemaking specific to these neurons impairs mitochondrial function and enhances dopamine synthesis and therefore dopamine oxidation [5, 6]. Oxidative stress intertwines with almost all other mechanisms that have been implicated in PD including protein misfolding and aggregation, mitochondrial dysfunction, cell cycle reactivation, apoptosis, and excitotoxicity [7, 8]. In particular, several PD-linked genes such as *α-synuclein*, *DJ-1*, *PINK1*, and *Parkin* have been demonstrated to interact with oxidative stress to promote or attenuate reactive oxygen species (ROS) and reactive nitrogen species [6, 7], and these interactions may contribute to the progressive neurodegeneration underlying PD. Markers of oxidative stress and damage, including lipid peroxidation, DNA, and protein oxidation, were found to be present in dopaminergic neurons in the SN of postmortem brain of PD patients [9–11].

Published online: 12 May 2012

Despite the compelling evidence supporting a pathogenic role of oxidative stress [12], agents with antioxidant properties studied to date, including selegiline, vitamin E, rasagiline, and mostly recently coenzyme 10 (CoQ10), have disappointingly failed to show clear benefits as disease-modifying treatment of PD in human trials [13–17]. To learn from the failure of these clinical trials and improve prospects for future tests of candidate neuroprotectants, difficult questions need to be answered [18]. At the far end of the translational pipeline, clinical investigators are asking whether our trial designs rely on the right treatment group structures and outcome measures. Do they test the right doses? In the right subpopulations? For optimal durations? On the near end of the translational pipeline, questions have been raised over the adequacy of our laboratory models of PD neurodegeneration; do they reflect the disease itself? Finally and perhaps most proximal, are we selecting the best drug candidates to enter the pipeline? In this setting, selection from among the many scientifically rational candidate neuroprotectants can be greatly enhanced when convergent epidemiological data are available for PD risk or progression [19–21].

Urate and Antioxidant Defense (Peripheral vs Central Nervous System)

Urate, the anionic form of uric acid, is a potent antioxidant. The antioxidant properties of urate include scavenging singlet oxygen, hydroxyl radicals, hydroxyl peroxide, and peroxynitrite [22, 23]. Urate also interacts and stabilizes other antioxidant systems including superoxide dismutase (SOD), ascorbate, and tetrahydrobiopterin [24–26]. Furthermore, urate displays the ability to chelate iron and block iron-dependent oxidation reactions [27]. Due to a series of mutations in the urate oxidase (*UOx*) gene and loss of UOx activity during primate evolution, urate in humans circulates, as the end product of purine metabolism, at high concentrations near the limits of its solubility and it accounts for most of the antioxidant capacity in human plasma (Fig. 1) [28]. Thus, urate may serve as one of our major endogenous defenses against oxidative and nitrosative damage. It has long been hypothesized that *UOx* mutations and the resulting urate elevation may have conferred an evolutionary advantage upon ancestors of higher primates through enhanced antioxidant function, possibly protecting cells from oxidative damage and mutagenesis, although suggestions of reduced cancer risk and longer life span [22, 29] remain speculative. Efforts in humans to directly assess the effects of manipulating urate levels on markers of oxidative stress and damage have produced mixed results [30–32].

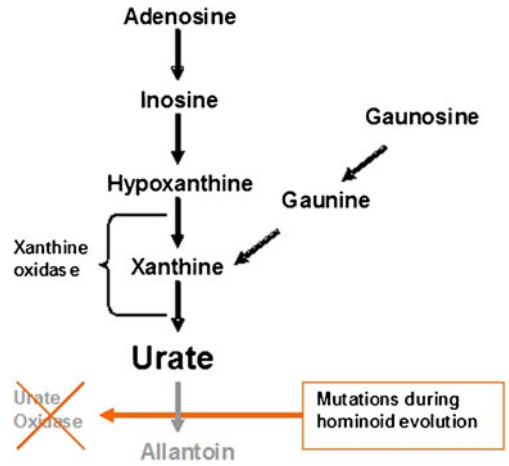

Fig. 1 Purine degradation pathway in humans. Urate is synthesized by xanthine oxidase from its purine precursors. Due to multiple mutations in the urate oxidase gene, urate circulates at high concentrations and it constitutes the end product of purine metabolism in humans

Nevertheless, a putative urate-based antioxidant defense has been proposed to be of particular importance in preventing oxidative damage in the more complex human brain [33]. Despite high blood urate, urate concentration in the central nervous system (CNS) is low, with cerebrospinal flood (CSF) urate consistently about 10 % of its peripheral concentration. This consistent gradient along with the close correlation between serum and CSF urate (despite the gradient) suggests that CNS (or at least CSF) urate concentration is dependent on blood urate and partial integrity of the blood–brain (or at least blood-CSF) barrier. Evidence that human brain has detectable activity of xanthine oxidase [34], the enzyme that catalyzes purine metabolism to urate, challenged the old hypothesis that urate is generated only peripherally in the liver and the small intestine. However, how local production contributes to CNS urate pool and how brain urate might be compartmentalized between neuron and glia, across cell membranes, and among different cellular organelles remains largely unknown. Nevertheless, recognition of the high oxygen consumption and high metabolic demands normally placed on CNS neurons and their particular susceptibility to oxidative damage led to the hypothesis that endogenous urate may serve as a protectant against neurodegenerative diseases [33]. Those with lower plasma urate levels and consequently even lower CNS urate may therefore be predisposed to neurodegenerative disorders such as PD where, as discussed above, oxidative stress is a major pathogenic mechanism [34].

Lower Urate in Patients with Parkinson's Disease

The first line of evidence supporting a link between urate and PD came from a postmortem study reporting reduced

levels of urate in SN from PD patients compared to age-matched controls [35]. Several case–control studies have since then consistently reported lower plasma or serum urate levels in idiopathic PD patients from Spain, Finland, Greece, the United States, and China, compared with their healthy controls [36–40]. Urine and CSF urate have also been studied but no clear differences were found, possibly due to limited sample size [37, 41, 42].

Urate, an Inverse Risk Factor for Parkinson's Disease

In addition to case–control studies, the initial pathological clue that urate is reduced in postmortem SN and striatum of PD patients [35] prompted a parallel series of epidemiological investigations in large prospectively followed populations. These studies consistently demonstrate that higher blood urate conveys a reduced risk for developing PD later in life [43–47]. A prospective study known as the Honolulu Heart Program first reported that among 7,968 men of Japanese or Okinawan ancestry, after adjusting for age and smoking, those with baseline urate concentrations higher than the median had a 40 % reduction in incidence of idiopathic PD during 30 years of follow-up [43]. In a larger prospectively followed cohort of 18,000 mostly Caucasian men, our neuroepidemiology group, led by Alberto Ascherio of the Harvard School of Public Health, found that those in the top quartile for plasma urate had a 55 % lower risk of PD than men in the bottom quartile. The decrease in risk was even greater in those with blood collected at least 4 years before diagnosis, suggesting that the lower urate in those with PD precedes symptom onset and is thus unlikely to be a consequence of changes in diet, behavior, or medical treatment early in the course of the disease [45]. Consistent with these findings, a recent community-based cross-sectional survey involving 69,000 subjects reported that participants with higher urate levels had lower odds of reporting PD with treatment compared to those with lower urate levels, indicating an association between higher urate levels and lower PD prevalence [47]. Another recent study in a community-based cohort demonstrated an association of low urate levels with higher PD risk but not high urate with lower PD risk, suggesting a more complex relationship between blood urate and PD risk in this particular population of older adults (≥65 years old) [48]. Other epidemiological studies also documented a relationship between urate-elevating diet [49] and gout [50, 51] and a lower risk of PD in prospectively followed men. In addition, variation in the urate transporter gene *SLC2A9*, which has been shown to be related to low serum urate levels, is associated with a lower age at onset of PD. These findings strengthen the link between urate and risk of developing PD [52•].

Interestingly, while robust and highly reproducible in men this inverse association between urate and PD risk is variably observed and weaker in women [46, 47, 53]. Whether the greater association in men reflects a true gender difference in the underlying biology is not clear. Alternatively, it may reflect the fact that men have substantially higher levels of urate than women and that the reduced risk is generally more robust for higher urate levels only above the median urate concentration. Of note, the gender difference in urate cannot explain the gender difference in PD risk (with men at greater risk than women) because the characteristically lower urate levels of women would have suggested that women should be at increased, not decreased, risk. The seeming paradox likely reflects the multiplicity of factors influencing PD risk, with potential factors other than urate (eg, estrogen) predominating in determining the reduced risk among women.

Urate, a Prognostic Biomarker of Favorable Progression in Parkinson's Disease

Remarkably, urate has also been linked to clinical progression of PD. Working with the Parkinson Study Group (PSG) and the Harvard School of Public Health, our group investigated two long-term, rigorously conducted clinical trials known as PRECEPT (Parkinson Research Examination of CEP-1347 Trial) and DATATOP (Deprenyl and Tocopherol Antioxidative Therapy of Parkinsonism), together comprising over 1,600 early cases of PD. We found that higher blood urate is strongly associated with a slower rate of clinical progression in both cohorts [54••, 55]. In the PRECEPT trial, serum urate was measured at a safety laboratory upon enrollment of 806 patients with early PD. The hazard ratio of reaching the primary study end point (ie, the development of disability warranting dopaminergic therapy) over nearly 2 years of follow-up declined with increasing serum urate. Similarly, the rate of Unified Parkinson's Disease Rating Scale (UPDRS) score worsening, a secondary end point in the PRECEPT study, was significantly higher in patients with lower urate levels [55]. The predictive association between higher urate at baseline and slower clinical progression in this cohort could be partially explained by the higher representation of subjects with a brain scan without evidence of dopaminergic deficit (SWEDD) among those with higher urate levels [56]. However, the inverse association between urate and clinical progression remained strong even after excluding all subjects with a baseline SWEDD from a secondary analysis (Unpublished data, by our and Dr. Alberto Ascherio's group with PSG investigators). Analysis of the independent 800-subject cohort of the DATATOP trial substantiated the inverse relationship between serum urate levels and subsequent disability progression early in PD as measured with the same primary outcome [54••].

Moreover, a similar robust inverse association was observed between baseline urate level and loss of striatal [123I] β-CIT uptake, a marker for the presynaptic dopamine terminal transporter [55]. Overall, the mean change among patients in the top quintile of serum urate was significantly lower than that of patients in the bottom quintile. Taking advantage of available stored CSF samples collected at baseline from 713 subjects of the DATATOP study, we measured CSF urate concentrations and found that like serum urate, lower CSF urate levels also predicted a slower rate of clinical disease progression in PD [54••]. The association of serum urate with the progression of PD has also been recently suggested in Chinese patients. Lower serum urate was found in patients with higher Hoehn and Yahr (H&Y) stages [40]. Furthermore, urate appears to be related to cognitive dysfunction, with higher urate predicting favorable neuropsychological performance in PD patients [57–59].

Urate and Links to Other Neurodegenerative Diseases

Consistent with the known antioxidant properties of urate and a common pathogenic mechanism of oxidative stress in neurodegeneration, increasing lines of evidence suggest relevance of urate to neurodegenerative diseases other than PD. A prospective population-based cohort study reported an inverse correlation between urate and cognitive function and risk of dementia later in life [60]. Reduced urate levels have also been implicated in Lewy body disease [61], Alzheimer's disease (AD) [62–64], Huntington's disease (HD) [65], and amyotrophic lateral sclerosis (ALS) [66, 67]. Furthermore, higher serum urate has been demonstrated to predict slower progression of HD [68], prolonged survival of ALS [69], and possibly lower rates of conversion to AD in untreated mild cognitive impairment [70]. These studies suggest that urate may play a general role across neurodegenerative disorders.

Neuroprotective Actions of Urate

Despite their statistical strength and reproducibility, these clinical and epidemiological findings do not settle the critical issue of whether urate is a primary pathogenic factor or a secondary disease marker. Although the question of causality is difficult to answer in humans without controlled clinical trials, evidence from experimental studies has to date provided valuable clues. For example, administration of urate is neuroprotective in both mechanical models of brain ischemia and thromboembolic models of autologous clot injection [71]. Urate not only reduced infarct volume in various models of ischemic brain injury, but also reduced ischemia-induced tyrosine nitration [72, 73]. In addition, inosine, a urate precursor, was also shown to have a beneficial effect in stroke models, perhaps by inducing axonal rewiring and improving behavioral performance as well as by reducing cerebral infarction volume [74, 75]. In an experimental allergic encephalomyelitis model of multiple sclerosis, urate and inosine were found to delay the onset and improve the clinical symptoms of disease in mice [76–78], possibly through inhibiting peroxynitrite-mediated oxidation [77]. Urate has also been shown to protect embryonic rat spinal cord neuron cultures against glutamate toxicity [79], and it protected against secondary damage including general tissue damage, nitrotyrosine formation, lipid peroxidation, activation of poly(ADP-ribose) polymerase, and improved functional recovery after spinal cord injury in vivo [80]. Treatment with urate increased total glutathione (GSH) production in hippocampal CA1 pyramidal neurons in the slice culture, and it protected these cells from oxidant insult. The same study further demonstrated in vivo increased GSH synthesis after injection of uric acid intraperitoneally in mice [81]. Results from human studies have demonstrated that systemic administration of uric acid was not only safe in healthy volunteers but also increased their serum antioxidant capacity [31]. Administration of urate, which falls quickly in patients with acute stroke, has been shown to lessen several biomarkers of oxidative stress and provide neuroprotection synergistically with thrombolytic therapies [32].

Regarding PD models, it is reported that 1-methyl-4-phenyl-1,2,3,6-tetrahydropyridine (MPTP) treatment induced an increase in urate levels in mice [82], and in rats, which was antagonized by allopurinol, a xanthine oxidase inhibitor [83]. Increased extracellular urate levels were also found after acute infusion of N-methyl-4-phenylpyridinium (MPP+), 6-hydroxydopamine (6-OHDA), or iron chloride through microdialysis in the SN of guinea pigs [84]. Increased urate may reflect a higher oxidative metabolism rate in CNS, or a compensatory protective mechanism after insult, because older animals failed to boost urate in brain after brain injury [85]. Data on urate in PD models are relatively scarce considering the centrality of oxidative mechanisms in PD models. Nevertheless, protective effects of urate have indeed been demonstrated in cellular and animal models of PD. In differentiated PC12 cells, urate was shown to block dopamine-induced apoptotic cell death and oxidant production [86]. Also in PC12 cells, treatment with urate protected against 6-OHDA toxicity. It significantly reduced 6-OHDA–induced oxidative stress, malondialdehyde formation, 8-hydroxy-deoxyguanosine (8-OHdG) generation, and lactate dehydrogenase release, and it induced SOD activity and increased GSH levels [87]. In human neuroblastoma SK-N-MC cells, urate prevented death of the cells induced by rotenone or iron plus homocysteine, an agent that sensitizes dopaminergic neurons to environmental toxins both in vitro and in vivo. It completely suppressed oxidative stress and largely prevented membrane

depolarization in those cells exposed to homocysteine plus rotenone or iron [88]. Primary cultures of the ventral mesencephalon dopaminergic neurons undergo spontaneous degeneration in vitro, and urate exerted robust, long-term protection of these cells. Urate protected the cells by reducing intracellular ROS production. This protective effect was reproduced by iron-chelating agent desferrioxamine, H_2O_2 scavenger enzyme catalase, and lipid peroxidation inhibitor of Trolox (Hoffman-LaRoche, Piscataway Township, NJ), suggesting that urate prevented neurodegenerative changes induced by Fenton-type reactions in midbrain primary cell cultures. Furthermore, urate-mediated neuroprotection in these primary cells was enhanced substantially by high K^+-induced depolarization through a mechanism involving L-type Ca^{2+} elevation and subsequently extracellular signal-regulated kinases 1/2 activation [89]. In a 6-OHDA rat model of PD, injection of urate significantly improved related behavioral responses and dopamine depletion. This systemic injection paradigm was shown to elevate urate in the striatum [90]. By employing complementary pharmacological and genetic approaches, our group has demonstrated in preliminary studies that urate protects dopaminergic neurons in cellular and in vivo models of PD [91–93].

Urate Elevation as a Therapeutic Strategy for Parkinson's Disease

The clinical and epidemiological findings that urate levels are inversely correlated with development and progression of PD, in conjunction with experimental evidence that urate is neuroprotective, provided a solid foundation to support testing of urate as a potential neuroprotective treatment of PD. In pursuit of a rapid clinical translation of these convergent findings, we have launched a national clinical trial to assess therapeutic candidacy of inosine, an orally bioavailable, brain-penetrant urate precursor. The phase II placebo-controlled double-blind dose-ranging randomized trial known as SURE-PD (Safety and Ability to Elevate Urate in Early Parkinson Disease) is being conducted in individuals with early PD at 16 clinical sites. Tolerability, defined as the extent to which an assigned treatment can be continued without dose reduction for more than 4 weeks due to adverse experience(s), and safety, defined as absence of serious adverse experiences that collectively warrant terminating an inosine treatment dose or the trial, are being assessed in analyses of short-term (12-week) and long-term (up to 2-year) treatment periods. Levels of urate in blood and CSF and oxidative damage biomarkers will also be determined as secondary outcome measures. Results from this trial will determine whether and how to proceed with a larger phase III trial of inosine as a urate-elevating strategy to modify disease progression in PD [94].

High Urate and Health Risks

In the above-mentioned Honolulu Heart Program, men in the top quartile of serum urate had a lower risk of developing PD than those with lower urate concentrations. By contrast, after adjusting for age, the total mortality rate in this quartile was about 30 % higher than men in the bottom quartile, although the risk was reduced after further adjustment for several risk factors for major chronic disease [43]. Of note, in people with PD higher urate has not been linked to increased mortality and in men with PD it actually appeared to be a predictor of reduced mortality [54••]. Nevertheless, elevated urate clearly is a pathogenic factor in diseases of urate or uric acid crystallization such as gout and uric acid urolithiasis, and is positively correlated with many other conditions such as hypertension, cardiovascular disease, and metabolic syndrome [95, 96]. Therefore, a responsible question is whether potential neuroprotective benefits of elevating urate for PD outweigh expected and theoretical medical risks for individual patients. In the SURE-PD trial, known risks for gouty arthritis and uric acid kidney stones and possible risks for blood pressure elevation and other medical conditions will be carefully assessed. It is also recommended that clinicians and PD patients not attempt to raise urate to treat PD before a better understanding of the role of urate in PD and the benefit-risk ratio of elevating urate is achieved.

Conclusions and Future Directions

A convergence of clinical and epidemiological data has identified urate as a molecular predictor of both (reduced) risk and (slowed) progression of idiopathic PD. Evolutionary and laboratory evidence further support a role of urate as an antioxidant and neuroprotectant in the pathogenesis of neurodegeneration in PD. Collectively these findings have facilitated rapid translation to a phase II clinical trial of the urate precursor inosine as a potential neuroprotective strategy for PD. They are also stimulating mechanistic investigation and insight into our understanding of urate and neurodegeneration, an area that remains largely uncharted. Given the complex nature of PD and its heterogeneous genetic and environmental influences, it is unlikely that urate on its own is a sufficiently specific biomarker of PD outcomes to warrant clinical application as a prognostic test. However, it would be reasonable to expect urate will contribute to a composite prognostic biomarker of disease risk or progress (akin to a multifactorial "cardiac index" as is commonly employed clinically to predict heart disease risk [97]) in combination with other emerging predictive factors. More immediate is the application of serum urate's prognostic biomarker properties to the improvement of clinical

trial design and analysis [98]. For example, a clinical trial of another candidate neuroprotectant may require substantially fewer PD subjects to achieve statistical significance for a true disease-modifying benefit if calculated progression rates were adjusted for baseline serum urate in the study analysis. Urate is emerging as a novel biomarker for PD risk, diagnosis, and prognosis [99]. Whether higher urate concentration will be found to be more than a biomarker of favorable outcomes for PD and other neurodegenerative diseases remains to be determined. Specifically, whether it offers disease-modifying strategy for the treatment of PD is being investigated and could be elucidated in the years to come.

Future studies will need to focus on some of the as-yet unaddressed important issues regarding urate and PD. First, our knowledge about basic purine biology, particularly how urate homeostasis is regulated and how urate may work as an endogenous antioxidant and neuroprotectant in CNS is limited. Second, evidence that urate is linked to PD came from studies among men or both genders. Studies to date reported either absence of or uncertainty over a relationship between urate and PD risk and progression in women [46, 47, 53, 54••]. Whether urate is associated with PD in women is less clear. Third, the association between urate and PD has thus far been characterized primarily in blood. Exploring urate in other body fluids (especially CSF and urine) and correlations between these compartments will not only improve our understanding of urate regulation in the CNS versus the periphery, but will also refine the clinical application of urate as a biomarker for PD.

Furthermore, unlike the proverbial path from preclinical discovery to clinical development of a neuroprotective agent, the urate story has unfolded mostly through human studies. Given the fundamental genetic and metabolic differences in urate biology between humans and lower mammalian animals, caution should be taken when interpreting and translating results from animal studies. However, complementing laboratory studies will still be necessary and valuable for characterization of the neuroprotective actions of urate and the underlying mechanisms in toxin and genetic models of PD. Finally, despite compelling evidence for causality, possible alternative explanations for the urate-PD association such as a purine pathway metabolite upstream of urate or another urate determinant serving as a pathogenic factor for which urate is merely a marker, deserve further investigation.

Acknowledgment This paper is supported by the National Institutes of Health/National Institute of Neurological Disorders and Stroke grant K24NS060991 and the US Department of Defense grant W81XWH-11-1-0150.

Disclosure Conflicts of interest: X. Chen: is employed by Massachusetts General Hospital; G. Wu: is employed by Suzhou Municipal Hospital; M.A. Schwarzschild: has been a consultant for Harvard University; is employed by Massachusetts General Hospital; has received payment for lectures including service on speakers bureaus from Emory University; has received=travel/accommodations/meeting expenses unrelated to activities listed from Emory University, Columbia University.

References

Papers of particular interest, published recently, have been highlighted as:
• Of importance
•• Of major importance

1. Graham DG. Oxidative pathways for catecholamines in the genesis of neuromelanin and cytotoxic quinines. Mol Pharmacol. 1978;14:633–43.
2. Tse DC, McCreery RL, Adams RN. Potential oxidative pathways of brain catecholamines. J Med Chem. 1976;19:37–40.
3. Adams RN, Murrill E, McCreery R, et al. 6-hydroxy-dopamine, a new oxidation mechanism. Eur J Pharmacol. 1972;17:287–92.
4. Youdim MB, Ben Shachar D, Riederer P. Is Parkinson's disease a progressive siderosis of substantia nigra resulting in iron and melanin induced neurogeneration? Acta Neurol Scand Suppl. 1989;126:47–54.
5. Surmeier DJ, Guzman JN, Sanchez-Padilla J, et al. The origins of oxidant stress in Parkinson's disease and therapeutic strategies. Antioxid Redox Signal. 2011;14(7):1289–301.
6. Guzman JN, Sanchez-Padilla J, Wokosin D, Kondapalli J, et al. Oxidant stress evoked by pacemaking in dopaminergic neurons is attenuated by DJ-1. Nature. 2010;468(7324):696–700.
7. Mosharov EV, Larsen KE, Kanter E, et al. Interplay between cytosolic dopamine, calcium, and alpha-synuclein causes selective death of substantia nigra neurons. Neuron. 2009;62(2):218–29.
8. Tsang AH, Chung KK. Oxidative and nitrosative stress in Parkinson's disease. Biochim Biophys Acta. 2009;1792(7):643–50.
9. Alam ZI, Jenner A, Daniel SE, et al. Oxidative DNA damage in the parkinsonian brain: an apparent selective increase in 8-hydroxyguanine levels in substantia nigra. J Neurochem. 1997;69:1196–203.
10. Dexter DT, Holley AE, Flitter WD, et al. Increased levels of lipid hydroperoxides in the parkinsonian substantia nigra: an HPLC and ESR study. Mov Disord. 1994;9:92–7.
11. Dexter DT, Sian J, Rose S, et al. Indices of oxidative stress and mitochondrial function in individuals with incidental Lewy body disease. Ann Neurol. 1994;35:38–44.
12. Henchcliffe C, Beal MF. Mitochondrial biology and oxidative stress in Parkinson disease pathogenesis. Nat Clin Pract Neurol. 2008;4(11):600–9.
13. Hart RG, Pearce LA, Ravina BM, et al. Neuroprotection trials in Parkinson's disease: systematic review. Mov Disord. 2009;24(5):647–54.
14. Olanow CW, Kieburtz K, Schapira AH. Why have we failed to achieve neuroprotection in Parkinson's disease? Ann Neurol. 2008;64 Suppl 2:S101–10.
15. Olanow CW, Rascol O, Hauser R, et al. A double-blind, delayed-start trial of rasagiline in Parkinson's disease. N Engl J Med. 2009;361(13):1268–78.
16. Ahlskog JE, Uitti RJ. Rasagiline, Parkinson neuroprotection, and delayed-start trials: still no satisfaction? Neurology. 2010;74(14):1143–8.
17. National Institute of Neurological Disorders and Stroke: Statement on the Termination of QE3 Study. Available at http://www.ninds.nih.gov/disorders/clinical_trials/CoQ10-Trial-Update.htm.

18. Hung AY, Schwarzschild MA. Clinical trials for neuroprotection in Parkinson's disease: overcoming angst and futility? Curr Opin Neurol. 2007;20(4):477–83.
19. Ravina BM, Fagan SC, Hart RG, et al. Neuroprotective agents for clinical trials in Parkinson's disease: a systematic assessment. Neurology. 2003;60(8):1234–40.
20. Morelli M, Carta AR, Kachroo A, et al. Pathophysiological roles for purines: adenosine, caffeine and urate. Prog Brain Res. 2010;183:183–208.
21. Quik M, Huang LZ, Parameswaran N, et al. Multiple roles for nicotine in Parkinson's disease. Biochem Pharmacol. 2009;78 (7):677–85.
22. Ames BN, Cathcart R, Schwiers E, et al. Uric acid provides an antioxidant defense in humans against oxidant- and radical-caused aging and cancer: a hypothesis. Proc Natl Acad Sci U S A. 1981;78 (11):6858–62.
23. Davies KJ, Sevanian A, Muakkassah-Kelly SF, et al. Uric acid-iron ion complexes. A new aspect of the antioxidant functions of uric acid. Biochem J. 1986;235(3):747–54.
24. Hink HU, Santanam N, Dikalov S, et al. Peroxidase properties of extracellular superoxide dismutase: role of uric acid in modulating in vivo activity. Arterioscler Thromb Vasc Biol. 2002;22(9):1402–8.
25. Sevanian A, Davies KJ, Hochstein P. Conservation of vitamin C by uric acid in blood. J Free Radic Biol Med. 1985;1(2):117–24.
26. Kuzkaya N, Weissmann N, Harrison DG, et al. Interactions of peroxynitrite with uric acid in the presence of ascorbate and thiols: implications for uncoupling endothelial nitric oxide synthase. Biochem Pharmacol. 2005;70(3):343–54.
27. Whiteman M, Halliwell B. Protection against peroxynitrite-dependent tyrosine nitration and alpha 1-antiproteinase inactivation by ascorbic acid. A comparison with other biological antioxidants. Free Radic Res. 1996;25(3):275–83.
28. Yeum KJ, Russell RM, Krinsky NI, et al. Biomarkers of antioxidant capacity in the hydrophilic and lipophilic compartments of human plasma. Arch Biochem Biophys. 2004;430(1):97–103.
29. Proctor P. Similar functions of uric acid and ascorbate in man? Nature. 1970;228(5274):868.
30. Hershfield MS, Roberts 2nd LJ, Ganson NJ, et al. Treating gout with pegloticase, a PEGylated urate oxidase, provides insight into the importance of uric acid as an antioxidant in vivo. Proc Natl Acad Sci U S A. 2010;107(32):14351–6.
31. Waring WS, Webb DJ, Maxwell SR. Systemic uric acid administration increases serum antioxidant capacity in healthy volunteers. J Cardiovasc Pharmacol. 2001;38(3):365–71.
32. Amaro S, Chamorro Á. Translational stroke research of the combination of thrombolysis and antioxidant therapy. Stroke. 2011;42 (5):1495–9.
33. Scott GS, Hooper DC. The role of uric acid in protection against peroxynitrite-mediated pathology. Med Hypotheses. 2001;56:95–100.
34. O'Neill RD, Lowry JP. On the significance of brain extracellular uric acid detected with in-vivo monitoring techniques: a review. Behav Brain Res. 1995;71(1–2):33–49.
35. Church WH, Ward VL. Uric acid is reduced in the substantia nigra in Parkinson's disease: effect on dopamine oxidation. Brain Res Bull. 1994;33(4):419–25.
36. Larumbe Ilundain R, Ferrer Valls JV, Vines Rueda JJ, et al. Case–control study of markers of oxidative stress and metabolism of blood iron in Parkinson's disease. Rev Esp Salud Publica. 2001;75 (1):43–53.
37. Annanmaki T, Muuronen A, Murros K. Low plasma uric acid level in Parkinson's disease. Mov Disord. 2007;22(8):1133–7.
38. Andreadou E, Nikolaou C, Gournaras F, et al. Serum uric acid levels in patients with Parkinson's disease: their relationship to treatment and disease duration. Clin Neurol Neurosurg. 2009;111 (9):724–8.
39. Bogdanov M, Matson WR, Wang L, et al. Metabolomic profiling to develop blood biomarkers for Parkinson's disease. Brain. 2008;131(Pt. 2):389–96.
40. Sun C, Luo F, Wei L, et al. Association of serum uric acid levels with the progression of Parkinson's disease in Chinese patients. Chin Med J. 2012;125(4):583–7.
41. Tohgi H, Abe T, Takahashi S, et al. The urate and xanthine concentrations in the cerebrospinal fluid in patients with vascular dementia of the Binswanger type, Alzheimer type dementia, and Parkinson's disease. J Neural Transm Park Dis Demet Sect. 1993;6 (2):119–26.
42. Maetzler W, Stapf AK, Schulte C, Hauser AK, et al. Serum and cerebrospinal fluid uric acid levels in lewy body disorders: associations with disease occurrence and amyloid-β pathway. J Alzheimers Dis. 2011;27(1):119–26.
43. Davis JW, Grandinetti A, Waslien CI, et al. Observations on serum uric acid levels and the risk of idiopathic Parkinson's disease. Am J Epidemiol. 1996;144(5):480–4.
44. de Lau LM, Koudstaal PJ, Hofman A, et al. Serum uric acid levels and the risk of Parkinson disease. Ann Neurol. 2005;58(5):797–800.
45. Weisskopf MG, O'Reilly E, Chen H, et al. Plasma urate and risk of Parkinson's disease. Am J Epidemiol. 2007;166 (5):561–7.
46. Chen H, Mosley TH, Alonso A, et al. Plasma urate and Parkinson's disease in the Atherosclerosis Risk In Communities (ARIC) study. Am J Epidemiol. 2009;169(9):1064–9.
47. Winquist A, Steenland K, Shankar A. Higher serum uric acid associated with decreased Parkinson's disease prevalence in a large community-based survey. Mov Disord. 2010;25(7):932–6.
48. Jain S, Ton TG, Boudreau RM, et al. The risk of Parkinson disease associated with urate in a community-based cohort of older adults. Neuroepidemiology. 2011;36(4):223–9.
49. Gao X, Chen H, Choi HK, et al. Diet, urate, and Parkinson's disease risk in men. Am J Epidemiol. 2008;167(7):831–8.
50. Alonso A, Rodriguez LA, Logroscino G, et al. Gout and risk of Parkinson disease: a prospective study. Neurology. 2007;69 (17):1696–700.
51. De Vera M, Rahman MM, Rankin J, et al. Gout and the risk of Parkinson's disease: a cohort study. Arthritis Rheum. 2008;59 (11):1549–54.
52.• Facheris MF, Hicks AA, Minelli C, et al. Variation in the uric acid transporter gene SLC2A9 and its association with AAO of Parkinson's disease. J Mol Neurosci. 2011;43(3):246–50. *This article reports that variation in the urate transporter gene SLC2A9 that was previously shown to be related to low serum urate levels, may be associated with an earlier age at onset of PD. It is the first study linking epidemiological findings to a genetic polymorphism and it strengthens the link between urate and risk of developing PD.*
53. O'Reilly EJ, Gao X, Weisskopf MG, et al. Plasma urate and Parkinson's disease in women. Am J Epidemiol. 2010;172 (6):666–70.
54.•• Ascherio A, LeWitt PA, Xu K, et al. Urate predicts rate of clinical decline in Parkinson disease. Arch Neurol. 2009;66(12):1460–8. *This study established association between serum urate and clinical progression in PD. It is also the first study identifying CSF urate as a predictor of rate of clinical decline in PD. These findings promoted a phase II clinical trial testing urate elevation as a therapeutic strategy for disease modification.*
55. Schwarzschild MA, Schwid SR, Marek K, et al. Serum urate as a predictor of clinical and radiographic progression in Parkinson disease. Arch Neurol. 2008;65(6):716–23.
56. Schwarzschild MA, Marek K, Eberly S, et al. Serum urate and probability of dopaminergic deficit in early "Parkinson's disease". Mov Disord. 2011;26(10):1864–8.

57. Annanmaki T, Pessala-Driver A, Hokkanen L, et al. Uric acid associates with cognition in Parkinson's disease. Parkinsonism Relat Disord. 2008;14(7):576–8.
58. Wang XJ, Luo WF, Wang LJ, et al. Study on uric acid and the related factors associated with cognition in the patients with Parkinson's disease. Chin Med J. 2009;89(23):1633–5.
59. Annanmaki T, Pohja M, Parviainen T, et al. Uric acid and cognition in Parkinson's disease: a follow-up study. Parkinsonism Relat Disord. 2011;17(5):333–7.
60. Euser SM, Hofman A, Westendorp RGJ, et al. Serum uric acid and cognitive function and dementia. Brain. 2009;132:377–82.
61. Maetzler W, Stapf AK, Schulte C, et al. Serum and cerebrospinal fluid uric acid levels in lewy body disorders: associations with disease occurrence and amyloid-β pathway. J Alzheimers Dis. 2011;27(1):119–26.
62. Maesaka JK, Wolf-Klein G, Piccione JM, et al. Hypouricemia, abnormal renal tubular urate transport, and plasma natriuretic factor(s) in patients with Alzheimer's disease. J Am Geriatr Soc. 1993;41(5):501–6.
63. Rinaldi P, Polidori MC, Metastasio A, et al. Plasma antioxidants are similarly depleted in mild cognitive impairment and in Alzheimer's disease. Neurobiol Aging. 2003;24(7):915–9.
64. Polidori MC, Mattioli P, Aldred S, et al. Plasma antioxidant status, immunoglobulin g oxidation and lipid peroxidation in demented patients: relevance to Alzheimer disease and vascular dementia. Dement Geriatr Cogn Disord. 2004;18(3–4):265–70.
65. Beal MF, Matson WR, Storey E, et al. Kynurenic acid concentrations are reduced in Huntington's disease cerebral cortex. J Neurol Sci. 1992;108(1):80–7.
66. Zoccolella S, Simone IL, Capozzo R, et al. An exploratory study of serum urate levels in patients with amyotrophic lateral sclerosis. J Neurol. 2011;258:238–43.
67. Keizman D, Ish-Shalom M, Berliner S, et al. Low uric acid levels in serum of patients with ALS: further evidence for oxidative stress? J Neurol Sci. 2009;285:95–9.
68. Auinger P, Kieburtz K, McDermott MP. The relationship between uric acid levels and Huntington's disease progression. Mov Disord. 2010;25(2):224–8.
69. Paganoni S, Zhang M, Quiroz Zárate A, et al. Uric acid levels predict survival in men with amyotrophic lateral sclerosis. J Neurol. 2012 Feb 10.
70. Irizarry MC, Raman R, Schwarzschild MA, et al. Plasma urate and progression of mild cognitive impairment. Neurodegener Dis. 2009;6(1–2):23–8.
71. Logallo N, Naess H, Idicula TT, et al. Serum uri acid: neuroprotection in thrombolysis. The Bergen NORSTROKE study. BMC Neurol. 2011;11:114.
72. Yu ZF, Bruce-Keller AJ, Goodman Y, et al. Uric acid protects neurons against excitotoxic and metabolic insults in cell culture and against focal ischemic brain injury in vivo. J Neurosci Res. 1998;53(5):613–25.
73. Romanos E, Planas AM, Amaro S, et al. Uric acid reduces brain damage and improves the benefits of rt-PA in a rat model of thromboembolic stroke. J Cereb Blood Flow Metab. 2007;27(1):14–20.
74. Chen P, Goldberg DE, Kolb B, et al. Inosine induces axonal rewiring and improves behavorial outcome after stroke. Proc Natl Acad Sci USA. 2002;99(13):9031–6.
75. Shen H, Chen GJ, Harvey BK, et al. Inosine reduces ischemic brain injury in rats. Stroke. 2005;36:654–9.
76. Hooper CD, Bagasra O, Marini JC, et al. Prevention of experimental allergic encephalomyelitis by targeting nitric oxide and peroxynitrite: implications for the treatment of multiple sclerosis. Proc Natl Acad Sci. 1997;94:2528–33.
77. Hooper DC, Spitsin S, Kean RB, et al. Uric acid, a natural scavenger of peroxynitrite in experimental allergic encephalomyelitis and multiple sclerosis. Proc Natl Acad Sci. 1998;95:675–80.
78. Scott GS, Spitsin SV, Kean RB, et al. Therapeutic intervention in experimental allergic encephalomyelitis by administration of uric acid precursors. Proc Natl Acad Sci. 2002;99(25):16303–8.
79. Du Y, Chen CP, Tseng CY, et al. Astroglia-mediated effects of uric acid to protect spinal cord neurons from glutamate toxicity. Glia. 2007;55(5):463–72.
80. Scott GS, Cuzzocrea S, Genovese T, et al. Uric acid protects against secondary damage after spinal cord injury. Proc Natl Acad Sci. 2005;102(9):3483–8.
81. Aoyama K, Matsumura N, Watabe M, et al. Caffeine and uric acid mediate glutathione synthesis for neuroprotection. Neuroscience. 2011;181:206–15.
82. Serra PA, Sciola L, Delogu MR, et al. The neurotoxin 1-methyl-4-phenyl-1,2,3,6-tetrahydropyridine(MPTP) induces apoptosis in mouse nigrostriatal glia. Relevance to nigral neuronal death and striatal neurochemical changes. J Biol Chem. 2002;277(37):34451–61.
83. Desole MS, Esposito G, Fresu L, et al. Further investigation of allopurinol effects on MPTP-induced oxidative stress in the striatum and brain stem of the rat. Pharmacol Biochem Behav. 1996;54(2):377–83.
84. Church WH, Fong YT. Changes in uric acid during acute infusion of MPP+, 6-OHDA, and FeCl3. A microdialysis studying the substantia nigra of the guinea pig. Mol Chem Neurpathol. 1996;27(2):131–44.
85. Moor E, Shohami E, Kanevsky E, et al. Impairment of the ability of the injured aged brain in elevating urate and ascorbate. Exp Gerontol. 2006;41(3):303–11.
86. Jones DC, Gunasekar PG, Borowitz JL, et al. Dopamine induced apoptosis is mediated by oxidative stess and is enhanced by cyanide in differentiated PC12 cells. J Neurochem. 2000;74(6):2296–304.
87. Zhu TG, Wang XX, Luo WF, et al. Protective effects of urate against 6-OHDA-induced cell injury in PC12 cells through antioxidant action. Neurosci Lett. 2012;506(2):175–9.
88. Duan W, Ladenheim B, Cutler RG, et al. Dietary folate deficiency and elevated homoocysteine levels endanger dopaminergic neurons in models of Parkinson's disease. J Neurchem. 2002;80(1):101–10.
89. Guerreiro S, Ponceau A, Toulorge D, et al. Protection of midbrain dopaminergic neurons by the end-product of purine metabolism uric acid: potentiation by low-level depolarization. J Neurochem. 2009;109(4):1118–28.
90. Wang LJ, Luo WF, Wang HH, et al. Protective effects of uric acid on nigrostriatal system injury induced by 6-hydroxydopamine in rats. [Article in Chinese]. Zhonghua Yi Xue Za Zhi. 2010;90(19):1362–5.
91. Cipriani S, Desjardins CA, Burdett TC, et al. Protective effect of urate on a dopaminergic cell line is potentiated by astrocytes (abstract 858.29). Presented at the annual meeting of Society of Neuroscience. San Diego, CA, Nov 12–17, 2010.
92. Cipriani S, Desjardins CA, Burdett TC, et al. Urate protects midbrain dopaminergic neurons from MPP+−induced toxicity (52.05). Presented at the annual meeting of Society of Neuroscience. Washington, DC, Nov 11–16, 2011.
93. Chen X, Desjardins CA, Burdett T, et al. Effects of urate oxidase transgene or knockout on 6-ohda neurotoxicity. Presented at the annual meeting of Society of Neuroscience. Washington, DC, Nov 11–16, 2011.
94. The Parkinson Study Group: Safety of Urate Elevation in Parkinson's Disease (SURE-PD). Available at http://clinicaltrials.gov/ct2/show/NCT00833690. Accessed September 2010.

95. Álvarez-Lario B, Macarrón-Vicente J. Uric acid and evolution. Rheumatology (Oxford). 2010;49(11):2010–5.
96. Kutzing MK, Firestein BL. Altered uric acid levels and disease states. J Pharmacol Exp Ther. 2008;324(1):1–7.
97. Goldman L, Caldera DL, Nussbaum SR. Multifactorial index of cardiac risk in noncardiac surgical procedures. N Engl J Med. 1977;297:845–50.
98. Schlossmacher MG, Mollenhauer B. Biomarker research in Parkinson's disease: objective measures needed for patient stratification in future cause-directed trials. Biomark Med. 2010;4(5):647–50.
99. Cipriani S, Chen X, Schwarzschild MA. Urate: a novel biomarker of Parkinson's disease risk, diagnosis and prognosis. Biomark Med. 2010;4(5):701–12.

OPEN ACCESS Freely available online

PLoS one

Urate and Its Transgenic Depletion Modulate Neuronal Vulnerability in a Cellular Model of Parkinson's Disease

Sara Cipriani*, Cody A. Desjardins, Thomas C. Burdett, Yuehang Xu, Kui Xu, Michael A. Schwarzschild

Neurology Department, MassGeneral Institute for Neurodegenerative Disease, Massachusetts General Hospital, Boston, Massachusetts, United States of America

Abstract

Urate is a major antioxidant as well as the enzymatic end product of purine metabolism in humans. Higher levels correlate with a reduced risk of developing Parkinson's disease (PD) and with a slower rate of PD progression. In this study we investigated the effects of modulating intracellular urate concentration on 1-methyl-4-phenyl-pyridinium (MPP^+)-induced degeneration of dopaminergic neurons in cultures of mouse ventral mesencephalon prepared to contain low (neuron-enriched cultures) or high (neuron-glial cultures) percentage of astrocytes. Urate, added to the cultures 24 hours before and during treatment with MPP^+, attenuated the loss of dopaminergic neurons in neuron-enriched cultures and fully prevented their loss and atrophy in neuron-astrocyte cultures. *Exogenous* urate was found to increase intracellular urate content in cortical neuronal cultures. To assess the effect of reducing cellular urate content on MPP^+-induced toxicity, mesencephalic neurons were prepared from mice over-expressing urate oxidase (UOx). Transgenic *UOx* expression decreased *endogenous* urate content both in neurons and astrocytes. Dopaminergic neurons expressing UOx were more susceptible to MPP^+ in mesencephalic neuron-enriched cultures and to a greater extent in mesencephalic neuron-astrocyte cultures. Our findings correlate intracellular urate content in dopaminergic neurons with their toxin resistance in a cellular model of PD and suggest a facilitative role for astrocytes in the neuroprotective effect of urate.

Citation: Cipriani S, Desjardins CA, Burdett TC, Xu Y, Xu K, et al. (2012) Urate and Its Transgenic Depletion Modulate Neuronal Vulnerability in a Cellular Model of Parkinson's Disease. PLoS ONE 7(5): e37331. doi:10.1371/journal.pone.0037331

Editor: Michelle L. Block, Virginia Commonwealth University, United States of America

Received February 27, 2012; **Accepted** April 19, 2012; **Published** May 14, 2012

Copyright: © 2012 Cipriani et al. This is an open-access article distributed under the terms of the Creative Commons Attribution License, which permits unrestricted use, distribution, and reproduction in any medium, provided the original author and source are credited.

Funding: Funding came from the United States National Institutes of Health http://www.nih.gov/(R21NS058324 and K24NS060991), US Department of Defense http://www.defense.gov/(W81XWH-11-1-0150), and the American Parkinson Disease Association http://www.apdaparkinson.org/userND/index.asp. The funders had no role in study design, data collection and analysis, decision to publish, or preparation of the manuscript.

Competing Interests: The authors have declared that no competing interests exist.

* E-mail: scipriani@partners.org

Introduction

Urate (2,6,8-trioxy-purine; a.k.a. uric acid) is generated within cells from the breakdown of purines. In most mammals urate is converted to allantoin by uricase (urate oxidase; UOx) [1], an enzyme primarily expressed in the liver [2]. In humans and apes, uricase is not synthesized due to the sequential non-sense mutations of its gene (*UOx*) that occurred during hominoid evolution [3–5]. Thus, in humans urate is the end product of the purine catabolism and achieves concentrations approaching the limit of solubility, which are more than fifty times higher than those in other mammals [6]. Due its high levels and radical scavenging properties [7–9] urate is considered a major antioxidant circulating in humans. It may have played a facilitative role in human evolution as was initially proposed based on putative central nervous system benefits [10–12] and later based on its antioxidant properties – perhaps to have partially compensated for the lost of the capability of synthesizing ascorbate [7,13]. Urate's antioxidant proprieties have been extensively characterized *in vitro* where it was found to be a peroxynitrite scavenger [14] and to form stable complex with iron ions, reducing their oxidant potential [15].

Identification of these antioxidant proprieties of urate, together with evidence that oxidative damage plays a critical role in the neurodegeneration of PD, raises the possibility that urate may protect from the development of the disease. Prompted further by post-mortem evidence that the urate levels in midbrain and striatum of PD patients are reduced compared to those of control brains [16], epidemiological and clinical cohorts were investigated for a possible link between urate level and the risk of PD or the rate of its progression. Several studies found lower blood urate concentration in healthy individuals to be a reproducible risk factor for developing PD later in life [17–19]. Furthermore, among those already diagnosed with PD, lower serum levels were consistently associated with a more rapid clinical and radiographic progression of PD [20–22], suggesting urate may be a prognostic biomarker in PD. In addition, an inverse correlation between serum urate level and disease duration has been reported in PD and raises the possibility that urate may also be a marker of disease stage [23], though falling urate may simply reflect the weight loss that accompanies disease duration.

A causal basis for the link between urate and favorable outcomes in PD is supported by the neuroprotective properties of urate in models of PD. Presumably by reducing ROS levels, urate can prevent cellular damage and increase cell viability in *in vitro* models of toxicant-induced or spontaneous cell death [24–27]. Moreover, urate increased cell survival in MPP^+-treated cell cultures [28] and prevented dopaminergic neuron loss in a rodent model of PD [29].

MPP^+ (1-methyl-4-phenylpyridinium) is the toxic metabolite of MPTP (1-methyl-4-phenyl-1,2,3,6-tetrahydropyridine) [30], an agent shown to induce a parkinsonian condition in humans [31]. MPP^+ is generated in astrocytes and up-taken by dopamine transporter into dopaminergic neurons [32]. Within the cells,

MPP^+ can induce the irreversible inhibition of complex I activity, failure of ATP synthesis and cell death [33,34]. In this study we assessed whether modulating urate level in primary dopaminergic neurons affects their vulnerability to MPP^+ toxicity in the presence of a low or high percentage of astrocytes.

Results

Urate prevents dopaminergic neuron loss in MPP^+-treated cultures

To identify an MPP^+ concentration with selective toxicity for dopaminergic neurons, mesencephalic neuron-enriched cultures (Fig. 1*A–D*) were treated for 24 hours with increasing concentrations of MPP^+. Toxicant treatment reduced the number of dopaminergic neurons, which were identified by their immunoreactivity for tyrosine hydroxylase (TH), in a concentration-dependent manner ($P<0.0001$). There was no change in the total number of neurons, which were scored as microtubule-associated protein 2-immunoreactive (MAP-2-IR) cells (Fig. 2*A*), due to the selectively toxic effect of MPP^+ on dopaminergic neurons and their low number in ventral mesencephalon cultures (2–3% of MAP-2-IR cells; see also Materials and Methods). To assess the effect of urate on dopaminergic neuron viability, neuron-enriched cultures were pretreated with urate 24 hours before and during exposure to 3 μM MPP^+. In MPP^+-treated cultures urate increased TH-IR viability over a concentration range of 0.1–100 μM ($P<0.0001$). The maximum effect was achieved at 100 μM with a 51% increase in TH-IR cell number in comparison to cells treated with MPP^+ only ($P<0.01$). Half-maximally effective concentration (EC_{50}) was achieved at a concentration of 1 μM [95% confidence interval (95%CI): 0.096–5.9] (Fig. 2B, D–*G*). Urate on its own produced no significant effect on dopaminergic neuron viability (Fig. 2*C*).

Previous data [35] have shown that urate's protective effect against toxin-induced neuronal cell death can be dependent on the presence of astrocytes in cultures. In our study urate treatment in neuron-enriched cultures only partially attenuated MPP^+ toxicity on dopaminergic neurons. To assess whether astrocytes might potentiate the protective effect of urate in our cells, urate was tested in MPP^+-treated mixed neuron-astrocyte cultures (Fig. 3*A–D*). To obtain selective degeneration of dopaminergic neurons without toxic effect on non-TH-IR cells, cultures were treated with relatively low concentrations of MPP^+ for four days as previously described [36]. MPP^+ induced selective loss of TH-IR neurons in a concentration-dependent manner ($P=0.0005$) with no statistically significant effect on MAP-2-IR or glial fibrillary acid protein-immunoreactive (GFAP-IR) cells (Fig. 4*A*). To assess the effect of urate, neuron-astrocyte cultures were pretreated with urate 24 hours before and during exposure to 0.5 μM MPP^+. Urate increased the number of TH-IR neurons over a concentration range of 0.1–100 μM ($P<0.0001$). The maximum effect was seen at 100 μM with a 97% increase in the number of TH-IR neurons in comparison to cultures treated with MPP^+ only ($P<0.01$; Fig. 4*B, F–I*), corresponding to a complete blockade of MPP^+ toxicity. Urate on its own did not affect TH-IR cell number (Fig. 4*C*). No statistically significant difference was seen at the estimated EC_{50}'s for urate in neuron-enriched and neuron-astrocytes cultures (~1 μM in both; $F_{1,53}=0.01$, $P=0.9$).

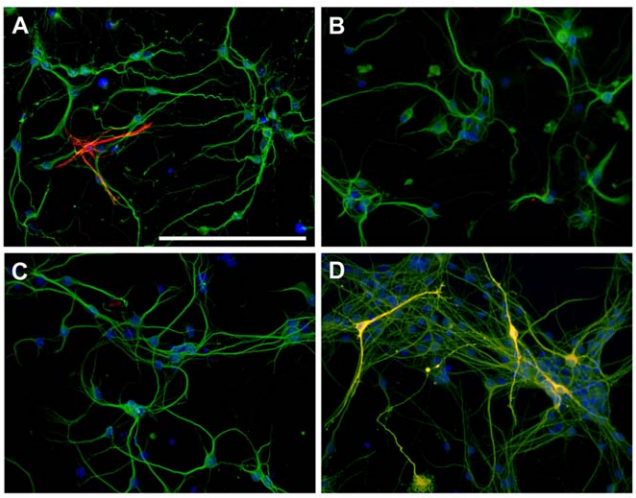

Figure 1. Cellular composition of neuron-enriched cultures. Composite fluorescence photomicrographs of neuron-enriched cultures that were immuno-stained with *A–D*) the neuronal marker MAP-2 (green) together with *A*) astrocyte marker GFAP (red) or *B*) the microglia marker CD11b (red, not detected) or *C*) the oligondendrocyte marker CNPase (red, not detected) or *D*) the dopaminergic neuron marker TH (yellow). Nuclei were counterstained with DAPI; scale bar length represents 100 μm.
doi:10.1371/journal.pone.0037331.g001

Urate prevents MPP^+-induced atrophic changes in dopaminergic neurons

To assess whether the protective effect of urate on neuronal viability correlates with an improvement in toxin-induced cellular atrophy, neurite length and soma size were analyzed in neuron-astrocyte cultures. In MPP^+-treated cultures TH-IR cells showed shorter neurites (−32%, $P<0.01$) and smaller soma area (−20%, $P<0.001$) in comparison to control cells (Fig. 4*D and E*, respectively). The concentration that fully protected against dopaminergic neuron loss, 100 μM urate, prevented the decrease in neurite length ($P<0.01$) and soma size ($P<0.001$) in TH-IR neurons (Fig. 4*D–E*).

Exogenous urate raises its intracellular level

To assess whether urate's protective effects are associated with an increase in its intracellular content, neuron-enriched cultures were treated with *exogenous* urate for 0, 6 and 24 hours. In order to obtain the large number of neurons required for intracellular analyte measurements, cultures were prepared from the mouse cortex for this assay. Urate content in neurons increased in a time-dependent manner with about 4 fold increase at 24 hours of treatment ($P=0.002$) (Fig. 5*A*), the time at which MPP^+ would be added to the cultures. *Exogenous* urate did not affect the concentration of any measured urate precursor (adenosine, inosine, hypoxanthine and xanthine) within neurons (unpublished data). Similar results were obtained in astrocyte-enriched cultures (unpublished data).

Transgenic *UOx* expression lowers intracellular urate

To assess whether intracellular urate content affects dopaminergic neuron resistance to MPP^+ we prepared ventral mesencephalon cultures from a mouse line expressing transgenic uricase (*UOx*) [37], the enzyme that converts urate to allantoin. Intracellular urate content was measured in cortical neurons and astrocytes prepared from non-transgenic *UOx* (non-Tg), hemizygous transgenic *UOx* (Tg) and homozygous (double) transgenic *UOx* (Tg/Tg) mice. In Tg/Tg neurons UOx expression was about 6 times higher than in Tg neurons as assessed by western blotting; in non-Tg neurons UOx was not detected (Fig. 6*A*). UOx expression reduced intracellular urate content by 50% ($P<0.01$) and 60% ($P<0.01$) in Tg and Tg/Tg neurons, respectively

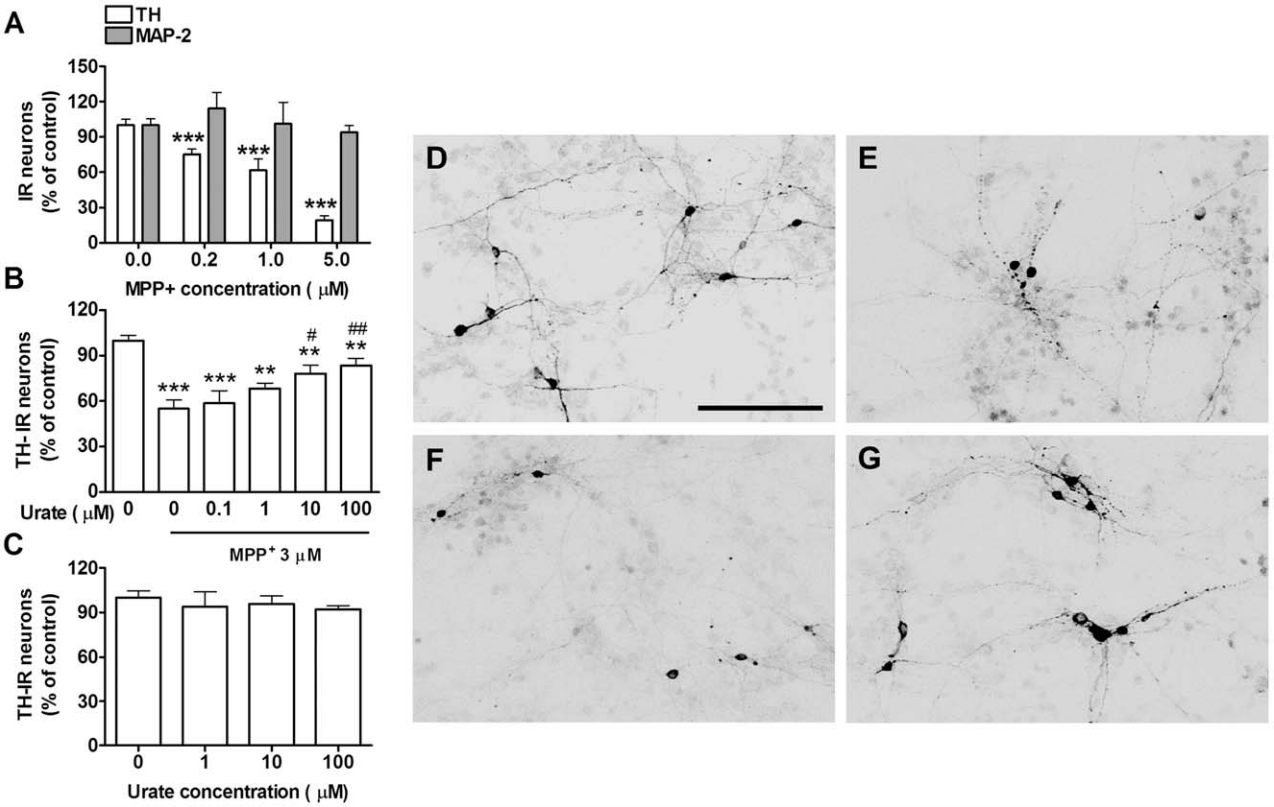

Figure 2. Urate's protective effect on dopaminergic neurons in neuron-enriched cultures. *A*) MPP^+ concentration-dependent effect on dopaminergic and total neuron viability expressed respectively as percentage of TH- and MAP-2-IR cell number in comparison to control cultures (n = 5). *B*) Urate concentration-dependent effect on TH-IR cell number in 3 μM MPP^+-treated cultures (n = 7). *C*) Lack of urate effect at any concentration on TH-IR neuron number in control (MPP^+-untreated) cultures (n = 5). Photomicrographs show TH-IR neurons in *D*) control cultures, *E*) MPP^+/0 urate-treated cultures, *F*) MPP^+/0.1 urate-treated cultures and *G*) MPP^+/100 μM urate-treated cultures. Scale bar = 50 μm. One-way ANOVA followed by Newman-Keuls test: $^{**}P<0.01$, $^{***}P<0.001$ *vs* 0 MPP^+ value; $^{\#}P<0.05$, $^{\#\#}P<0.01$ *vs* MPP^+/0 urate value.
doi:10.1371/journal.pone.0037331.g002

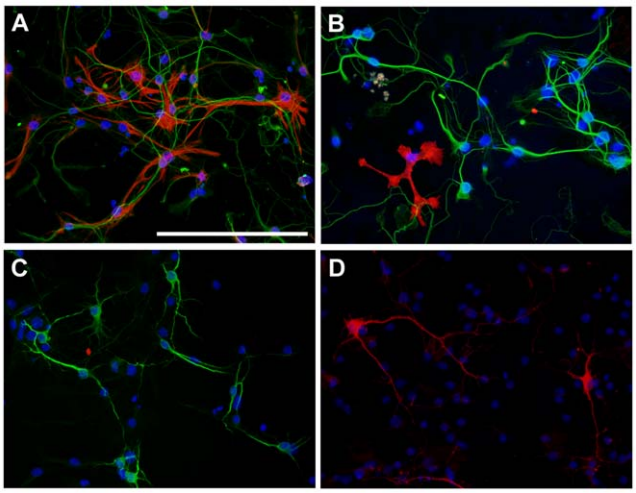

Figure 3. Cellular composition of neuron-astrocyte cultures. Composite fluorescence photomicrographs of neuron-astrocyte cultures that were immuno-stained with *A–C*) the neuronal marker MAP-2 (green) together with *A*) astrocyte marker GFAP (red) or *B*) the microglia marker CD11b (red) or *C*) the oligondendrocyte marker CNPase (red, not detected). *D*) Dopaminergic neurons were stained with the dopaminergic neuron marker TH (red). Nuclei were counterstained with DAPI; scale bar is 100 μm.
doi:10.1371/journal.pone.0037331.g003

(Fig. 6*B*). UOx activity was significantly increased in Tg/Tg ($p<0.001$) but not in Tg cell medium in comparison to non-Tg samples (Fig. 6*C*). In Tg/Tg astrocytes intracellular UOx expression was about 15 times higher than in Tg astrocytes; in non-Tg astrocytes UOx was not detected (Fig. 7*A*). UOx expression reduced intracellular urate content by 30% both in Tg and Tg/Tg ($P<0.01$) astrocytes (Fig. 7*B*). UOx activity was detected in the cell media of Tg and Tg/Tg astrocytes (Fig. 7*C*) where medium urate concentration was significantly reduced in comparison to that from non-Tg astrocytes ($P<0.001$) (Fig. 7*D*).

Transgenic UOx reduces neuronal resistance to MPP^+ toxicity

To determine whether the enzymatic reduction of intracellular urate exacerbates dopaminergic susceptibility to MPP^+, neuron-enriched ventral mesencephalon cultures from non-Tg, Tg and Tg/Tg mice were treated with increasing concentrations of toxin for 24 hours. Two-way ANOVA showed that both genotype ($F_{2,232} = 24.61$, $P<0.0001$) and MPP^+ concentration ($F_{2,232} = 312.64$, $P<0.0001$) affected the number of TH-IR neurons, and found significant interaction between these two factors ($F_{2,232} = 13.82$, $P<0.0001$). Dopaminergic viability was reduced in UOx expressing cultures in comparison to non-Tg cultures with a maximum effect at 1 μM MPP^+, which further reduced TH-IR neuron number by 10% and 18% in Tg and Tg/Tg cultures compared to non-Tg cultures, respectively (Fig. 8*A*).

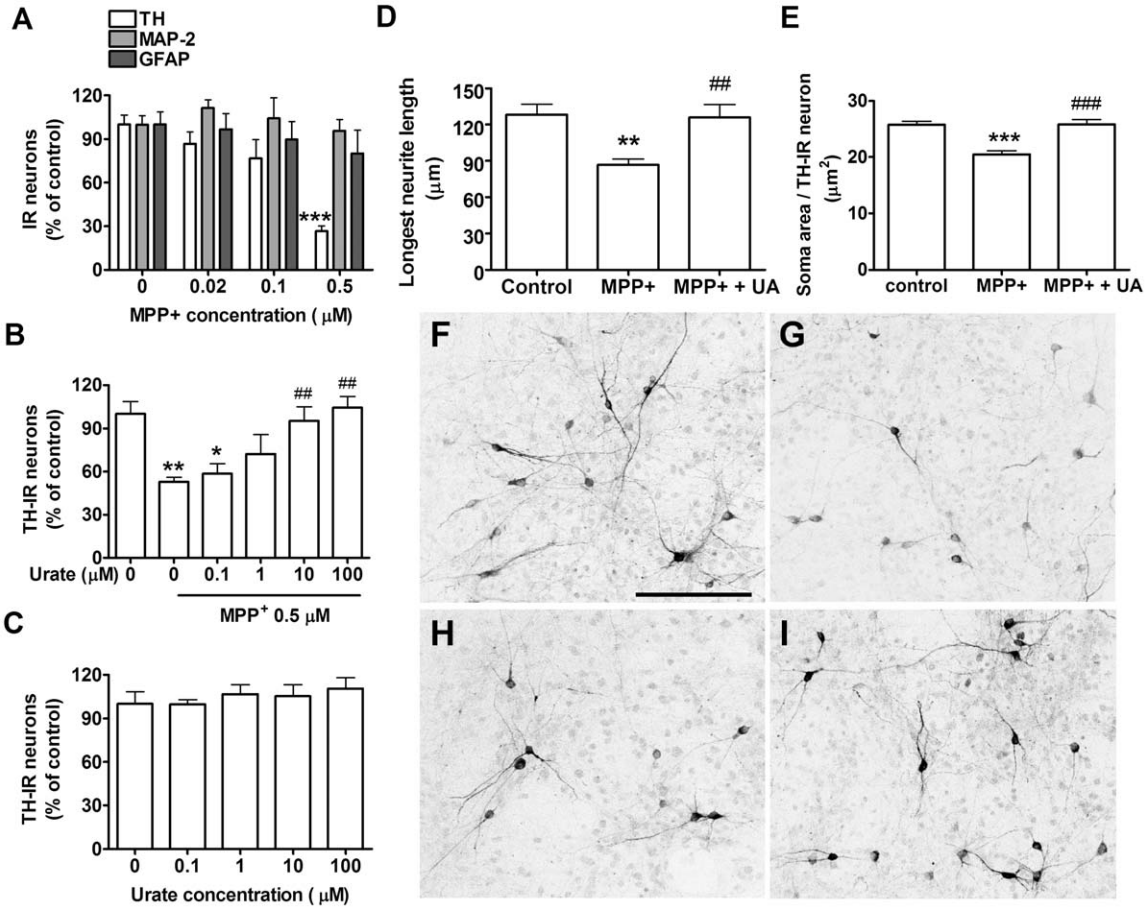

Figure 4. Urate's protective effect on dopaminergic neurons in mixed cultures. *A*) MPP^+ concentration-dependent effect on dopaminergic neuron, total neuron and astrocyte viability, expressed as percentage of TH-IR, MAP-2-IR and GFAP-IR cell number, respectively, in comparison to control cultures (n = 4). *B*) Urate concentration-dependent effect on TH-IR cell number in 0.5 μM MPP^+-treated cultures (n = 5). *C*) Lack of effect of urate at any concentration on TH-IR cell number (n = 5). Urate (100 μM) effects on reductions in *D*) longest neurite length and *E*) soma size in MPP^+ urate-treated TH-IR neurons. Photomicrographs show TH-IR neurons in *F*) control cultures, *G*) MPP^+/0 urate-treated cultures and *H*) MPP^+/0.1 urate-treated cultures and *I*) MPP^+/100 μM urate-treated cultures. Scale bar = 50 μm. One-way ANOVA followed by Newman-Keuls test: $^*P<0.05$, $^{**}p<0.01$, $^{***}P<0.001$ *vs* 0 MPP^+ value, $^{\#\#}P<0.01$ and $^{\#\#\#}P<0.001$ *vs* MPP^+/0 urate value.
doi:10.1371/journal.pone.0037331.g004

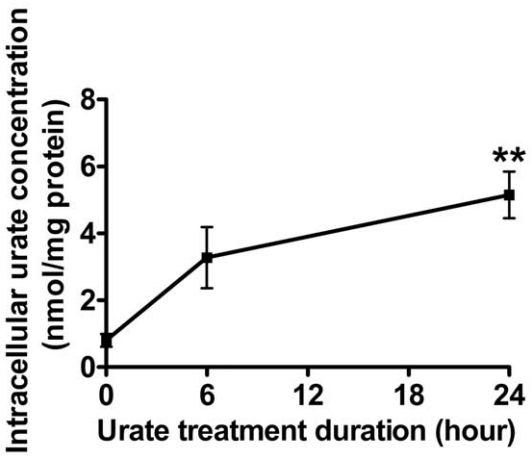

Figure 5. Urate accumulation in cortical neurons. *A*) Time-dependent effect of 100 μM *exogenous* urate on its intracellular content in primary cortical neurons. One-way ANOVA followed by Newman-Keuls test: $^{**}P<0.01$.
doi:10.1371/journal.pone.0037331.g005

The EC_{50} for MPP^+ was 5.2 μM (95%CI: 2.8–9.7 μM) in non-Tg cultures, 3.9 μM (95%CI: 2.4–6.4 μM) in Tg and 2.5 μM (95%CI: 0.9–6.8 μM) in Tg/Tg without statistically significant difference among genotypes ($F_{2,232} = 0.5612$, $P = 0.57$).

Two-way ANOVA of MPP^+-toxicity on MAP-2-IR cell number revealed significant effect of MPP^+ concentration ($F_{2,199} = 28.47$, $P<0.0001$), but neither a significant effect of genotype ($F_{2,199} = 1.64$, $P = 0.20$) nor a significant interaction between these two factors ($F_{2,199} = 1.20$, $P = 0.31$) (Fig. 8*B*).

To assess whether reducing basal urate levels in both, neurons and astrocytes, exacerbated the UOx effect on MPP^+-induced toxicity, we treated neuron-astrocyte cultures with MPP^+ for four days as mentioned above. Two-way ANOVA revealed significant effects of both genotype ($F_{2,284} = 10.09$, $P<0.0001$) and MPP^+ concentration ($F_{2,284} = 96.36$, $P<0.0001$) on the number of TH-IR neurons and a significant interaction between genotype and MPP^+ concentration ($F_{2,284} = 3.01$, $P = 0.007$) (Fig. 9*A*). Dopaminergic viability was reduced in UOx expressing cultures in comparison to non-Tg cultures with a maximum effect at 0.1 μM MPP^+, which further reduced TH-IR neuron number by 39% and 49% in Tg and Tg/Tg cultures compared to non-Tg cultures, respectively. The EC_{50} for MPP^+ was 0.11 μM (95%CI: 0.04–0.31 μM) in non-

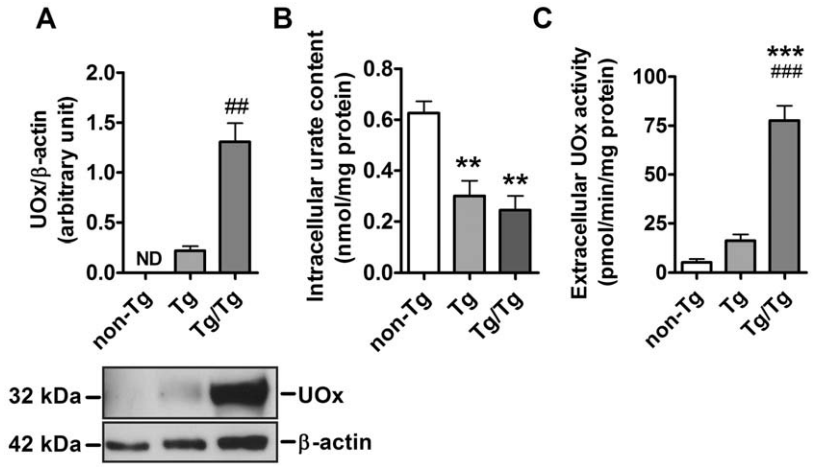

Figure 6. Characterization of non-Tg, Tg and Tg/Tg cortical neuron-enriched cultures. *A*) Western blot and graph showing UOx expression in wild-type (non-Tg) and UOx-expressing neurons (Tg and Tg/Tg) normalized to the β-actin level. Note that UOx was not detected in wild-type neurons (n = 3). *B*) Effect of UOx expression on intracellular urate content in neurons normalized to the protein level (n = 3). C) UOx activity in the media of non-Tg and UOx-expressing neurons (n = 6). Student's *t* test: $^{\#\#}P = 0.005$ *vs* Tg value; one-way ANOVA followed by Newman-Keuls test: $^{**}P<0.01$, $^{***}P<0.001$ *vs* non-Tg value and $^{\#\#\#}P<0.001$ *vs* Tg value.
doi:10.1371/journal.pone.0037331.g006

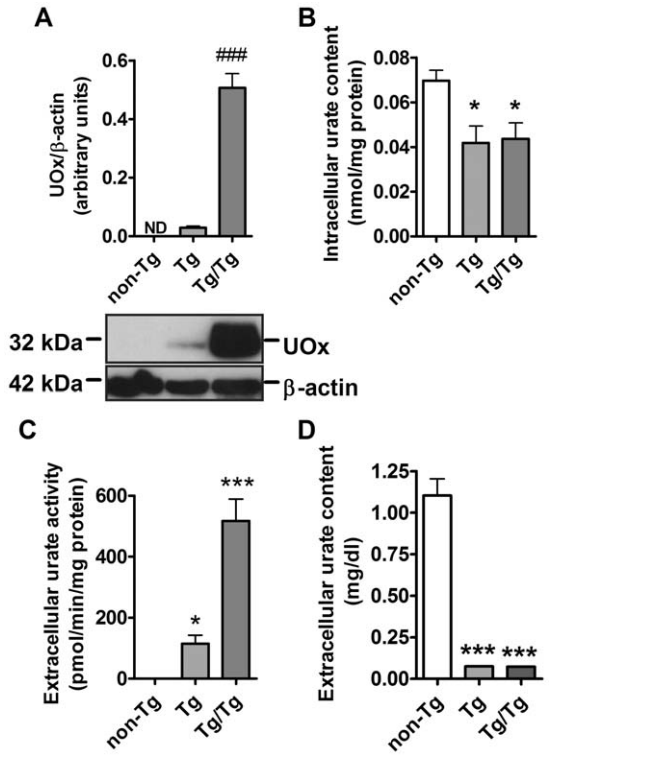

Figure 7. Characterization of non-Tg, Tg and Tg/Tg cortical astrocyte-enriched cultures. *A*) Western blot and graph showing UOx immunostaining in non-Tg and UOx-expressing astrocytes (Tg and Tg/Tg) normalized to the β-actin level. Note that UOx was not detected in non-Tg astrocytes (n = 7). *B*) Effect of UOx expression on the intracellular urate content normalized to the protein level (n = 5). *C*) UOx activity in the media of non-Tg and UOx-expressing astrocytes (n = 9). *D*) Effect of UOx expression on extracellular urate concentration in astroglial cultures (n = 6). Some error bars are not visible because of their small size. Student's *t* test: $^{\#\#\#}P<0.0001$ *vs* Tg value. One-way ANOVA followed by Newman-Keuls test: $^{*}P<0.05$, $^{***}P<0.001$ *vs* non-Tg value.
doi:10.1371/journal.pone.0037331.g007

Tg cultures, 0.05 μM (95%CI: 0.02–0.12 μM) in Tg and 0.02 μM (95%CI: 0.01–0.04 μM) in Tg/Tg with a statistically significant difference among genotypes ($F_{2,284} = 5.66$, $P = 0.0039$).

Analysis of MPP^+ effect on MAP-2-IR cell number revealed significant effect of MPP^+ concentration ($F_{2,236} = 5.89$, $P<0.0007$), but neither a genotype effect ($F_{2,236} = 0.27$, $P = 0.76$) nor significant interaction between these two factors ($F_{2,236} = 0.06$, $P = 1$) (Fig. 9B).

These data indicate that dopaminergic tolerance to MPP^+ was further reduced when basal urate content was reduced both in neurons and astrocytes.

Discussion

In our model we induced selective degeneration of dopaminergic neurons using the neurotoxin MPP^+ in mouse ventral mesencephalon cultures. Urate, a known powerful antioxidant [7–9], added to cultures 24 hours before and during toxicant treatment, attenuated MPP^+ toxicity in dopaminergic neurons. It increased the number of TH-IR cells both in neuron-enriched and neuron-astrocyte cultures containing respectively low and high percentage of astrocytes. In cultures with low percentage of astrocytes, urate only partially prevented dopaminergic neuron loss. On the other hand, in cultures prepared with a high percentage of astrocytes, urate completely prevented MPP^+-induced toxicity. Moreover, in these mixed neuron-astrocyte cultures, urate fully prevented atrophic morphological changes in neurite length and soma size induced by MPP^+. Both in neuron-enriched and neuron-astrocyte cultures, urate showed protective effects with an EC_{50} of about 1 μM, a concentration within the mouse physiological range where its CSF urate concentration is about 3 μM [38], ten-time lower than in humans [6].

Urate may have conferred protection against neuronal atrophy and death through its established antioxidant actions, as it has been shown to prevent ROS accumulation and oxidative damage in other neuronal populations [25,26,39] and to raise cysteine uptake and glutathione synthesis in mouse hippocampal slices [40]. Urate treatment might change the redox status of neurons, reducing their vulnerability to oxidative stress and preventing cellular degeneration. In fact, MPP^+ toxicity may depend on the

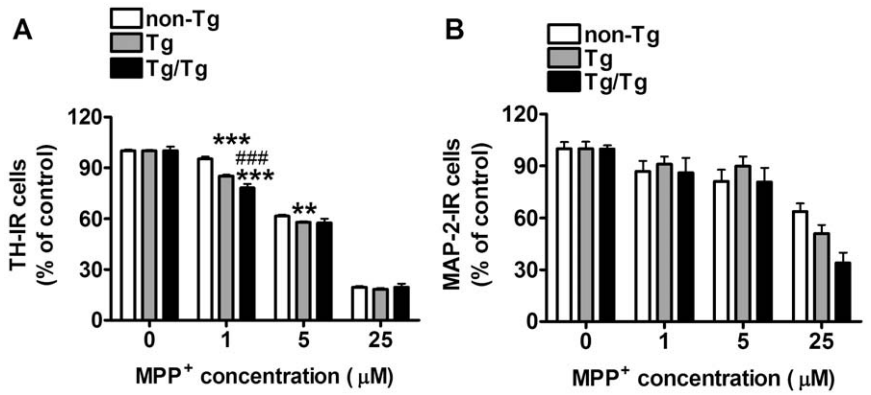

Figure 8. MPP$^+$ effect on non-Tg, Tg and Tg/Tg neuron-enriched cultures. *A*) MPP$^+$ effect on TH-IR cell number in non-Tg (n = 18), Tg (n = 35) and Tg/Tg (n = 8) neuronal cultures. *B*) MPP$^+$ effect on MAP-2-IR cell number in non-Tg (n = 18), Tg (n = 35) and Tg/Tg (n = 8) cultures. *C*) Two-way ANOVA followed by Bonferroni multiple comparison test: $^{**}P<0.01$, $^{***}P<0.001$ *vs* respective non-Tg value; $^{\#\#\#}P<0.01$ vs respective Tg value.
doi:10.1371/journal.pone.0037331.g008

antioxidant status of neurons. Previous studies have shown non-toxic levels of iron and glutathione synthesis inhibition to enhance degeneration of dopaminergic neurons treated with MPP$^+$ [41] and antioxidant enzymes to prevent MPP$^+$-induced toxicity [41–44].

Although its antioxidant properties have been extensively described, a question remains to be answered: How does *exogenous* urate prevents oxidant toxicity? Ascorbate, an important antioxidant in the CNS [45–47], is present at high levels in neurons where its concentration is thought to be raised and maintained by the sodium-dependent vitamin C transporter-2 (SVCT2) [48,49]. Urate may protect through a similar mechanism that relies on the elevation of intracellular antioxidant content as was demonstrated here with *exogenous* urate substantially increasing intracellular urate in cortical neuronal cultures. By contrast, although Guerreiro et al. [25] reported a similar protective effect of urate on dopaminergic neurons in primary cultures, they did not find an associated increase in intracellular urate, possibly due to a greater sensitivity of our electrochemistry-based analytical methods or other differences between our studies.

To directly address the hypothesis that endogenous urate contributes to dopaminergic neuron resistance to toxicants, MPP$^+$ toxicity was assessed in cultures expressing the UOx enzyme, which catalyzes urate degradation to allantoin. UOx is not normally synthesized in the mouse brain where, like in humans, urate is the enzymatic end product of the purine catabolism. Transgenic *UOx* expression reduced basal levels of urate both in cortical neurons and cortical astrocytes, even if this effect was not proportional to the increasing levels of UOx protein expression and enzyme activity observed with increasing transgene copy number. In neuron-enriched cultures, dopaminergic neurons expressing UOx were slightly more vulnerable to MPP$^+$ compared to wild-type neurons. In neuron-astrocyte cultures, transgenic *UOx* markedly exacerbated the toxicity and increased the potency of MPP$^+$ even though we did not see a greater decrease in intracellular urate concentration in astrocytes than in neurons. Because we were not able to measure urate content in ventral mesencephalic astrocytes and dopaminergic neurons due to their low number, we employed their cortical counterparts. Although urate transporter properties for each cell type are not expected to differ across brain regions, we cannot be sure that the changes in intracellular urate demonstrated in cortical cultures after both pharmacologic and genetic manipulations were achieved in ventral mesencephalic cells as well. Moreover, we cannot exclude that culturing neurons with astrocytes might affect the intracellular urate content in neurons. Nevertheless, our consistent observation of potentiated protection by astrocytes in cultures of dopaminergic

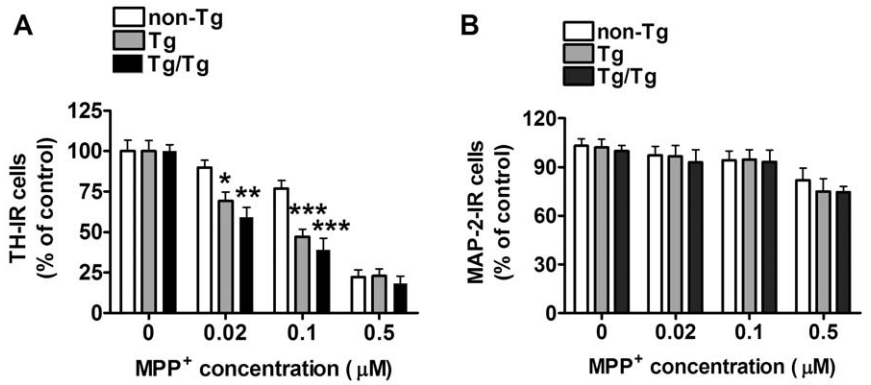

Figure 9. MPP$^+$ effect on non-Tg, Tg and Tg/Tg mixed neuron-astrocyte cultures. *A*) MPP$^+$ effect on TH-IR cell number in non-Tg (n = 18), Tg (n = 34) and Tg/Tg (n = 22) neuronal cultures. *B*) MPP$^+$ effect on MAP-2-IR cell number in non-Tg (n = 18), Tg (n = 34) and Tg/Tg (n = 22). Two-way ANOVA followed by Bonferroni multiple comparison test: $^{*}P<0.05$, $^{**}P<0.01$, $^{***}P<0.001$ *vs* respective non-Tg value.
doi:10.1371/journal.pone.0037331.g009

neurons strengthens the evidence for a facilitative role of astrocytes on the neuroprotective effect of urate [35].

The small protective effect of urate in neuron-enriched cultures containing few astrocytes and the far greater protection in neuron-astrocyte cultures may reflect the same astrocyte-dependent mechanism in both culture types. This interpretation is supported by the absolute astrocyte dependence previously observed for urate's protective effect in spinal cord cultures [35]. Although the content of astrocytes and other dividing glial cell populations was pharmacologically reduced in our preparation of neuron-enriched cultures, astroglia was not completely eliminated from these cultures. Indeed a small astrocyte-independent effect of urate acting directly on dopaminergic neurons cannot be excluded with the available data.

How physiological levels of urate in astrocytes might play an important role in dopaminergic neuron protection is not known. It has been suggested that urate may confer neuroprotection via astrocytes by stimulating their extracellular glutamate buffering capacity or their release of neurotrophic factors [35,50]. An intracellular antioxidant effect of urate on astrocytes might activate such glial functions. Indeed astrocytes were found to be susceptible to MPTP/MPP^+ treatment showing increased ROS level [51,52] and reduced glutamate buffering capacity [53,54]. Therefore, even though the toxicant concentration we employed was selected to be subthreshold for altering astroglial viability, reducing basal levels of urate in astrocytes might deplete their antioxidant reserves and indirectly enhance toxic MPP^+ effects on neurons. Although urate was found to protect neurons in association with the up-regulation of EAAT1 glutamate transporter expression in astrocytes [35], glutamate release was not detected in the striatum of MPP^+-perfused mice [55] and NMDA antagonism did not prevent MPP^+-induced dopaminergic cell death [56]. Further experiments will be needed to clarify the mechanism by which astrocytes play a facilitative role in the neuroprotective effect of urate and to confirm urate's protective effect in animal models of PD.

In conclusion, our data showed that intracellular urate may modulate dopaminergic neuron resistance to environmental toxins. This effect may be mediated by changes in astroglial urate content. A greater understanding of how urate protects neurons in models of PD may not only help elucidate its pathophysiology, it may also help accelerate or refine current urate-targeting strategies under investigation for their potential to slow or prevent PD (http://clinicaltrials.gov/ct2/show/NCT00833690).

Materials and Methods

Mice

UOx Tg mice [37] were obtained from Kenneth L. Rock at University of Massachusetts. Mice were backcrossed eight times on the C57BL/6 genetic background and phenotyped by measuring UOx activity in serum samples. Briefly, about two hundred µl of submandibular blood were collected from 1 month-old mice. Four µl of serum sample were added to 96 µl of 130 µM urate in 0.1 M borate (pH 8.5) and absorbance was read at 292 nm at the beginning of the assay and after 4–6 hours incubation at 37°C.

Ethics Statement

All experiments were performed in accordance with the National Institutes of Health Guide for the Care and Use of Laboratory Animals, with approval from the animal subjects review board of Massachusetts General Hospital (Permit Number: 2006N000120).

Neuron-enriched cultures

Ventral mesencephalon was dissected from embryonic day E15–17 mouse embryos. Tissue was carefully stripped of their meninges and digested with 0.6% trypsin for 15 min at 37°C. Trypsinization was stopped by adding an equal volume of culture preparation medium (DMEM/12, N2 supplement 5%, fetal bovine serum (FBS) 10%, penicillin 100 U/ml and streptomycin 100 µg/ml) to which 0.02% deoxyribonuclease I was added. The solution was homogenized by pipetting up and down, pelleted and re-suspended in culture medium (Neurobasal medium (NBM), B27 supplement 2%, L-gluatamine (2 mM), penicillin 100 U/ml and streptomycin 100 µg/ml). The solution was brought to a single cell suspension by passage through a 40-µm pore mesh. Cells were seeded at a density of 220,000 cells/cm^2 onto 96 well plates or chamber-slides coated with poly-L-lysine (100 µg/ml)/DMEM/F12) and cultured at 37°C in humidified 5% CO2-95% air. On the third day half medium was replaced with fresh NBM containing the antimetabolite cytosine arabinoside (Ara-C,10 µM) to inhibit glial growth and glucose 6 µM. Medium was fully changed after 24 hours and then a half volume was replaced every other day. After 6 days in vitro (DIV) cultures were pretreated with urate or vehicle, and 24 hours later MPP^+ or vehicle was added. Cultures were constitute of >95% neurons, of which 2–3% were dopaminergic neurons and <5% astrocytes; microglia and oligodendrocytes were not detected (See Figure 1).

For Tg neuronal cultures, individual cultures were prepared from the ventral mesencephalon of individual embryos generated by crossing two Tg mice (with a resulting distribution of 23% non-Tg, 44% Tg and 33% Tg/Tg). The rest of the brain was used for phenotyping by western blotting. Brain tissue extracts negative for UOx staining were considered non-Tg; tissue, positive for UOx staining were considered Tg when UOx/actin value was >0.1 and ≤0.6, and Tg/Tg when UOx/actin value was >1.5. Cultured cell phenotypes were confirmed by measuring UOx activity in the cell medium.

Neuron-astrocyte cultures

Tissue was processed as described above but no Ara-C was added to the cultures. At 4 DIV cells were treated with urate or vehicle, 24 hour later MPP^+ or vehicle was added. Cultures comprised 45–60% neurons, of which 2–3% were dopaminergic neurons, 40–50% astrocytes and <1 microglia, oligodendrocytes were not detected.

Immunocytochemistry: After treatments cultures were fixed with 4% paraformaldehyde for 1 hour at room temperature. Then, cells were loaded with a blocking solution (0.5% albumin, 0.3% Triton-X 100 in phosphate buffer saline) for 30 min at room temperature and then incubated with a mouse anti-TH (1:200, Millipore, Temecule, CA) and a rabbit anti-MAP-2 antibody (1:200, Millipore, Temecule, CA), or a rabbit anti-GFAP antibody, overnight at 4°C to label dopaminergic neurons neurons and astrocytes, respectively. Cultures were loaded with a cy3-conjugated anti-mouse antibody (1:500, Jackson InnunoResearch Laboratories, Inc.; West Grove, PA) and a FITC-conjugated anti-rabbit antibody (1:300, Jackson InnunoResearch Laboratories, Inc.; West Grove, PA) 2 hours at room temperature. Cultures were imaged using an Olympus BX50 microscope with a 20×/0.50 objective and Olympus DP70 camera. Images were processed with DP Controller software (Olympus) and merged with ImageJ (NIH). Cells cultured in plates were observed with a Bio-Rad Radiance 2100 confocal laser-scanning microscope with krypton-argon and blue diode lasers. Images were acquired through a Plan Fluor DIC ELWD 20×/0.45 Ph1 DM ∞/0–2 WD 7.4 objective on an inverted Nikon Eclipse TE300 fluorescent microscope with

408/454 nm excitation/emission (blue), 485/525 nm excitation-emission (green) and 590/617 nm excitation-emission (red).

Neurite length was measured by the Simple Neurite Tracer tool of ImageJ software. In each sample, neurite length was determined by the average of the longest neurite of 100 TH-IR neurons randomly selected in the well. Neurons having neurites ending outside the optic field were excluded from the analysis. Values were expressed in μm.

High-Performance Liquid Chromatography

Cells were scraped in a solution of 150 mM phosphoric acid, 0.2 mM EDTA, and 1 μM 3,4-dihydroxybenzylamine (DHBA; used as internal standard), clarified by centrifugation and filtered through a 0.2 μm Nylon microcentrifuge filter (Spin-X, Corning). Samples were chromatographed by a multi-channel electrochemical/UV HPLC system with effluent from the above column passing through a UV-VIS detector (ESA model 528) set at 254 nm and then over a series of electrodes set at −100 mV, +250 mV and +450 mV. Urate was measured on the +250 mV electrode with a limit of detection at 0.0001 mg/dl. In order to generate a gradient, two mobile phases were used. Mobile phase B increased linearly from 0% to 70% between 6th and 14th min of the run and immediately reduced to 0% at 17.4 min and allowed to re-equilibrate for the final 3.6 min. Mobile phase A consisted of 0.2 M potassium phosphate and 0.5 mM sodium 1-pentanesulfonate; mobile phase B consisted of the same plus 10% (vol/vol) acetonitrile. Both mobile phases were brought to pH 3.5 with 85% (wt/vol) phosphoric acid.

Western blot assay

Cells were scraped in RIPA buffer (Sigma Co., St. Luis, MO) and loaded (50 μg of proteins per well) into a 10% SDS-PAGE gel. Proteins were then transferred electrophoretically onto 0.2 μ nitrocellulose membranes (Biorad Laboratories) and probed with a rabbit polyclonal antibody anti-UOx (1:200; Santa Cruz, CA) overnight at 4°C. After washing in Tris Buffer Saline containing 0.1% Tween20, membranes were incubated with a horseradish peroxidase-conjugated anti-rabbit IgG (1:2000; Pierce, Biotechnology, Rockford, IL, USA) for 2 hours at room temperature. Proteins were visualized using chemiluminescence (Immobilon, Millipore). In order to normalize the values of UOx staining, β-actin was detected in the same western blot run. Membranes were incubated for 2 hours at room temperature with an anti-β-actin antibody (1:2000; Sigma, St Louis, MO) and then with a horseradish peroxidase-conjugated anti-rabbit IgG (1:5000; Pierce, Biotechnology, Rockford, IL) for 2 hours. Membranes were developed as above. Bands were acquired as JPG files and densitometric analysis of bands was performed by ImageJ software. UOx/β-actin values were expressed as arbitrary units.

UOx activity assay

Cell medium was added to 0.5 mg/ml urate and absorbance was red at 292 nm before and after 24 hours incubation at 37°C. Activity was calculated as percentage of absorbance decrease in comparison to starting values.

Protein detection: Proteins were quantified in 4 μl of each sample using Bio-Rad Protein Assay reagent (Bio-Rad, Hercules, CA, USA) and measured spectrophotometrically at 600 nm with Labsystems iEMS Analyzer microplate reader.

Acknowledgments

Transgenic *UOx* mice were kindly provided by Ken Rock and Hajime Kono of the University of Massachusetts. The authors would like to thank Dr. Antonio Valencia of the MassGeneral Institute for Neurodegenerative Disease, Boston, for the technical support with confocal microscopy.

Author Contributions

Conceived and designed the experiments: SC KX MAS. Performed the experiments: SC CAD TCB. Analyzed the data: SC. Contributed reagents/materials/analysis tools: CAD TCB YX. Wrote the paper: SC MAS.

References

1. Wu X, Wakamiya M, Vaishnav S, Geske R, Montgomery C Jr., et al. (1994) Hyperuricemia and urate nephropathy in urate oxidase-deficient mice. Proc Natl Acad Sci U S A 91(2): 742–746.
2. Truszkowski R, Goldmanowna C (1933) Uricase and its action: Distribution in various animals. Biochem J 27(3): 612–614.
3. Yeldandi AV, Yeldandi V, Kumar S, Murthy CV, Wang XD, et al. (1991) Molecular evolution of the urate oxidase-encoding gene in hominoid primates: Nonsense mutations. Gene 109(2): 281–284.
4. Wu XW, Muzny DM, Lee CC, Caskey CT (1992) Two independent mutational events in the loss of urate oxidase during hominoid evolution. J Mol Evol 34(1): 78–84.
5. Oda M, Satta Y, Takenaka O, Takahata N (2002) Loss of urate oxidase activity in hominoids and its evolutionary implications. Mol Biol Evol 19(5): 640–653.
6. Enomoto A, Kimura H, Chairoungdua A, Shigeta Y, Jutabha P, et al. (2002) Molecular identification of a renal urate anion exchanger that regulates blood urate levels. Nature 417(6887): 447–452.
7. Ames BN, Cathcart R, Schwiers E, Hochstein P (1981) Uric acid provides an antioxidant defense in humans against oxidant- and radical-caused aging and cancer: A hypothesis. Proc Natl Acad Sci U S A 78(11): 6858–6862.
8. Green CJ, Healing G, Simpkin S, Fuller BJ, Lunec J (1986) Reduced susceptibility to lipid peroxidation in cold ischemic rabbit kidneys after addition of desferrioxamine, mannitol, or uric acid to the flush solution. Cryobiology 23(4): 358–365.
9. Arduini A, Mancinelli G, Radatti GL, Hochstein P, Cadenas E (1992) Possible mechanism of inhibition of nitrite-induced oxidation of oxyhemoglobin by ergothioneine and uric acid. Arch Biochem Biophys 294(2): 398–402.
10. Haldane JB (1955) Origin of man. Nature 176(4473): 169–170.
11. Orowan E (1955) The origin of man. Nature 175(4459): 683–684.
12. Wu XW, Lee CC, Muzny DM, Caskey CT (1989) Urate oxidase: Primary structure and evolutionary implications. Proc Natl Acad Sci U S A 86(23): 9412–9416.
13. Proctor P (1970) Similar functions of uric acid and ascorbate in man? Nature 228(5274): 868.
14. Whiteman M, Ketsawatsakul U, Halliwell B (2002) A reassessment of the peroxynitrite scavenging activity of uric acid. Ann N Y Acad Sci 962: 242–259.
15. Davies KJ, Sevanian A, Muakkassah-Kelly SF, Hochstein P (1986) Uric acid-iron ion complexes. A new aspect of the antioxidant functions of uric acid. Biochem J 235(3): 747–754.
16. Church WH, Ward VL (1994) Uric acid is reduced in the substantia nigra in parkinson's disease: Effect on dopamine oxidation. Brain Res Bull 33(4): 419–425.
17. Weisskopf MG, O'Reilly E, Chen H, Schwarzschild MA, Ascherio A (2007) Plasma urate and risk of parkinson's disease. Am J Epidemiol 166(5): 561–567.
18. de Lau LM, Koudstaal PJ, Hofman A, Breteler MM (2005) Serum uric acid levels and the risk of parkinson disease. Ann Neurol 58(5): 797–800.
19. Davis JW, Grandinetti A, Waslien CI, Ross GW, White LR, et al. (1996) Observations on serum uric acid levels and the risk of idiopathic parkinson's disease. Am J Epidemiol 144(5): 480–484.
20. Schwarzschild MA, Schwid SR, Marek K, Watts A, Lang AE, et al. (2008) Serum urate as a predictor of clinical and radiographic progression in parkinson disease. Arch Neurol 65(6): 716–723.
21. Ascherio A, LeWitt PA, Xu K, Eberly S, Watts A, et al. (2009) Urate as a predictor of the rate of clinical decline in parkinson disease. Arch Neurol 66(12): 1460–1468.
22. Schwarzschild MA, Marek K, Eberly S, Oakes D, Shoulson I, et al. (2011) Serum urate and probability of dopaminergic deficit in early "parkinson's disease". Mov Disord 26(10): 1864–1868.
23. Andreadou E, Nikolaou C, Gournaras F, Rentzos M, Boufidou F, et al. (2009) Serum uric acid levels in patients with parkinson's disease: Their relationship to treatment and disease duration. Clin Neurol Neurosurg 111(9): 724–728.
24. Stinefelt B, Leonard SS, Blemings KP, Shi X, Klandorf H (2005) Free radical scavenging, DNA protection, and inhibition of lipid peroxidation mediated by uric acid. Ann Clin Lab Sci 35(1): 37–45.
25. Guerreiro S, Ponceau A, Toulorge D, Martin E, Alvarez-Fischer D, et al. (2009) Protection of midbrain dopaminergic neurons by the end-product of purine

metabolism uric acid: Potentiation by low-level depolarization. J Neurochem 109(4): 1118–1128.
26. Zhu TG, Wang XX, Luo WF, Zhang QL, Huang TT, et al. (2011) Protective effects of urate against 6-OHDA-induced cell injury in PC12 cells through antioxidant action. Neurosci Lett 506(2): 175–9.
27. Duan W, Ladenheim B, Cutler RG, Kruman II, Cadet JL, et al. (2002) Dietary folate deficiency and elevated homocysteine levels endanger dopaminergic neurons in models of parkinson's disease. J Neurochem 80(1): 101–110.
28. Haberman F, Tang SC, Arumugam TV, Hyun DH, Yu QS, et al. (2007) Soluble neuroprotective antioxidant uric acid analogs ameliorate ischemic brain injury in mice. Neuromolecular Med 9(4): 315–323.
29. Wang LJ, Luo WF, Wang HH, Ni GH, Ye Y, et al. (2010) Protective effects of uric acid on nigrostriatal system injury induced by 6-hydroxydopamine in rats. Zhonghua Yi Xue Za Zhi 90(19): 1362–1365.
30. Vila M, Przedborski S (2003) Targeting programmed cell death in neurodegenerative diseases. Nat Rev Neurosci 4(5): 365–375.
31. Langston JW, Ballard P, Tetrud JW, Irwin I (1983) Chronic parkinsonism in humans due to a product of meperidine-analog synthesis. Science 219(4587): 979–980.
32. Mayer RA, Kindt MV, Heikkila RE (1986) Prevention of the nigrostriatal toxicity of 1-methyl-4-phenyl-1,2,3,6-tetrahydropyridine by inhibitors of 3,4-dihydroxyphenylethylamine transport. J Neurochem 47(4): 1073–1079.
33. Cleeter MW, Cooper JM, Schapira AH (1992) Irreversible inhibition of mitochondrial complex I by 1-methyl-4-phenylpyridinium: Evidence for free radical involvement. J Neurochem 58(2): 786–789.
34. Mizuno Y, Suzuki K, Sone N, Saitoh T (1987) Inhibition of ATP synthesis by 1-methyl-4-phenylpyridinium ion (MPP+) in isolated mitochondria from mouse brains. Neurosci Lett 81(1–2): 204–208.
35. Du Y, Chen CP, Tseng CY, Eisenberg Y, Firestein BL (2007) Astroglia-mediated effects of uric acid to protect spinal cord neurons from glutamate toxicity. Glia 55(5): 463–472.
36. Wang T, Pei Z, Zhang W, Liu B, Langenbach R, et al. (2005) MPP+-induced COX-2 activation and subsequent dopaminergic neurodegeneration. FASEB J 19(9): 1134–1136.
37. Kono H, Chen CJ, Ontiveros F, Rock KL (2010) Uric acid promotes an acute inflammatory response to sterile cell death in mice. J Clin Invest 120(6): 1939–1949.
38. Schmidt AP, Bohmer AE, Antunes C, Schallenberger C, Porciuncula LO, et al. (2009) Anti-nociceptive properties of the xanthine oxidase inhibitor allopurinol in mice: Role of A1 adenosine receptors. Br J Pharmacol 156(1): 163–172.
39. Scott GS, Cuzzocrea S, Genovese T, Koprowski H, Hooper DC (2005) Uric acid protects against secondary damage after spinal cord injury. Proc Natl Acad Sci U S A 102(9): 3483–3488.
40. Aoyama K, Matsumura N, Watabe M, Wang F, Kikuchi-Utsumi K, et al. (2011) Caffeine and uric acid mediate glutathione synthesis for neuroprotection. Neuroscience 181: 206–215.
41. Gomez FJ, Aguirre P, Gonzalez-Billault C, Nunez MT (2011) Iron mediates neuritic tree collapse in mesencephalic neurons treated with 1-methyl-4-phenylpyridinium (MPP+). J Neural Transm 118(3): 421–431.
42. Park TH, Kwon OS, Park SY, Han ES, Lee CS (2003) N-methylated beta-carbolines protect PC12 cells from cytotoxic effect of MPP+ by attenuation of mitochondrial membrane permeability change. Neurosci Res 46(3): 349–358.
43. Kalivendi SV, Kotamraju S, Cunningham S, Shang T, Hillard CJ, et al. (2003) 1-methyl-4-phenylpyridinium (MPP+)-induced apoptosis and mitochondrial oxidant generation: Role of transferrin-receptor-dependent iron and hydrogen peroxide. Biochem J 371(Pt 1): 151–164.
44. Lee CS, Han JH, Jang YY, Song JH, Han ES (2002) Differential effect of catecholamines and MPP(+) on membrane permeability in brain mitochondria and cell viability in PC12 cells. Neurochem Int 40(4): 361–369.
45. Thorn NA, Nielsen FS, Jeppesen CK (1991) Characteristics of ascorbic acid uptake by isolated ox neurohypophyseal nerve terminals and the influence of glucocorticoid and tri-iodothyronine on uptake. Acta Physiol Scand 141(1): 97–106.
46. May JM, Li L, Hayslett K, Qu ZC (2006) Ascorbate transport and recycling by SH-SY5Y neuroblastoma cells: Response to glutamate toxicity. Neurochem Res 31(6): 785–794.
47. Huang J, May JM (2006) Ascorbic acid protects SH-SY5Y neuroblastoma cells from apoptosis and death induced by beta-amyloid. Brain Res 1097(1): 52–58.
48. Gess B, Sevimli S, Strecker JK, Young P, Schabitz WR (2011) Sodium-dependent vitamin C transporter 2 (SVCT2) expression and activity in brain capillary endothelial cells after transient ischemia in mice. PLoS One 6(2): e17139.
49. Scheers NM, Sandberg AS (2011) Iron regulates the uptake of ascorbic acid and the expression of sodium-dependent vitamin C transporter 1 (SVCT1) in human intestinal caco-2 cells. Br J Nutr 1–7.
50. Chen PS, Peng GS, Li G, Yang S, Wu X, et al. (2006) Valproate protects dopaminergic neurons in midbrain neuron/glia cultures by stimulating the release of neurotrophic factors from astrocytes. Mol Psychiatry 11(12): 1116–1125.
51. Wong SS, Li RH, Stadlin A (1999) Oxidative stress induced by MPTP and MPP(+): Selective vulnerability of cultured mouse astrocytes. Brain Res 836(1–2): 237–244.
52. Wu EY, Langston JW, Di Monte DA (1992) Toxicity of the 1-methyl-4-phenyl-2,3-dihydropyridinium and 1-methyl-4-phenylpyridinium species in primary cultures of mouse astrocytes. J Pharmacol Exp Ther 262(1): 225–230.
53. Volterra A, Trotti D, Floridi S, Racagni G (1994) Reactive oxygen species inhibit high-affinity glutamate uptake: Molecular mechanism and neuropathological implications. Ann N Y Acad Sci 738: 153–162.
54. Hazell AS, Itzhak Y, Liu H, Norenberg MD (1997) 1-methyl-4-phenyl-1,2,3,6-tetrahydropyridine (MPTP) decreases glutamate uptake in cultured astrocytes. J Neurochem 68(5): 2216–2219.
55. Uezono T, Matsubara K, Shimizu K, Mizukami H, Ogawa K, et al. (2001) Glutamate is not involved in the MPP+-induced dopamine overflow in the striatum of freely moving C57BL/6 mice. J Neural Transm 108(8–9): 899–908.
56. Michel PP, Agid Y (1992) The glutamate antagonist, MK-801, does not prevent dopaminergic cell death induced by the 1-methyl-4-phenylpyridinium ion (MPP+) in rat dissociated mesencephalic cultures. Brain Res 597(2): 233–240.

Journal of Neurochemistry JNC

JOURNAL OF NEUROCHEMISTRY | 2012 | 123 | 172–181 doi: 10.1111/j.1471-4159.2012.07820.x

Appendix F

ORIGINAL ARTICLE

Protection of dopaminergic cells by urate requires its accumulation in astrocytes

Sara Cipriani, Cody A. Desjardins, Thomas C. Burdett, Yuehang Xu, Kui Xu and Michael A. Schwarzschild

Molecular Neurobiology Laboratory, MassGeneral Institute for Neurodegenerative Disease, Massachusetts General Hospital, Boston, Massachusetts, USA

Abstract

Urate is the end product of purine metabolism and a major antioxidant circulating in humans. Recent data link higher levels of urate with a reduced risk of developing Parkinson's disease and with a slower rate of its progression. In this study, we investigated the role of astrocytes in urate-induced protection of dopaminergic cells in a cellular model of Parkinson's disease. In mixed cultures of dopaminergic cells and astrocytes oxidative stress-induced cell death and protein damage were reduced by urate. By contrast, urate was not protective in pure dopaminergic cell cultures. Physical contact between dopaminergic cells and astrocytes was not required for astrocyte-dependent rescue as shown by conditioned medium experiments. Urate accumulation in dopaminergic cells and astrocytes was blocked by pharmacological inhibitors of urate transporters expressed differentially in these cells. The ability of a urate transport blocker to prevent urate accumulation into astroglial (but not dopaminergic) cells predicted its ability to prevent dopaminergic cell death. Transgenic expression of uricase reduced urate accumulation in astrocytes and attenuated the protective influence of urate on dopaminergic cells. These data indicate that urate might act within astrocytes to trigger release of molecule(s) that are protective for dopaminergic cells.

Keywords: cell viability, HPLC, MES 23.5 cells, transgenic, transporter, uricase.

J. Neurochem. (2012) **123**, 172–181.

Currently, some 90% of Parkinson's disease (PD) cases are classified as sporadic, reflecting the uncertainty of their causes. A combination of genetic and environmental factors is thought to trigger pathogenic cascades that converge to increase oxidative stress or to reduce natural antioxidant defenses, leading to cellular impairment and the neurodegeneration characteristic of PD (Ross and Smith 2007). Dopaminergic neurons in the substantia nigra *pars compacta* are highly sensitive to oxidative stress and their selective degeneration is responsible for the progressive motor disability of PD.

Urate (2,6,8-trioxy-purine; a.k.a. uric acid) circulates in humans at concentrations that are near its limit of solubility and many fold higher than in most other mammals. In humans and apes, urate is the enzymatic end product of purine metabolism because of mutations of the uricase (a.k.a. urate oxidase) gene (*UOx*) that occurred during hominoid evolution (Oda *et al.* 2002). The resulting urate elevation has been hypothesized to have raised antioxidant levels in human ancestors and thereby lengthened their lifespans. Urate possesses antioxidant properties comparable to those of ascorbate (Ames *et al.* 1981) and forms stable coordination complexes with iron and other metal ions (Davies *et al.* 1986), accounting for its ability to reduce oxidative damage caused by reactive nitrogen and oxygen species (Whiteman *et al.* 2002).

Recently, epidemiological and clinical studies have found people with higher serum levels of urate to be less likely to develop PD (Weisskopf *et al.* 2007). Moreover, amongst PD patients those with higher urate in serum or CSF showed a slower rate of disease progression assessed clinically

Received May 1, 2012; revised manuscript received June 4, 2012; accepted June 5, 2012.

Address correspondence and reprint requests to Sara Cipriani, PhD, Molecular Neurobiology Laboratory, MassGeneral Institute for Neurodegenerative Disease, Massachusetts General Hospital, 114 16th street, Boston, MA 02129, USA. E-mail: pattona80@hotmail.com

Abbreviations used: Ara-C, cytosine arabinoside; DNPH, 2,4-dinitrophenylhydrazine; FBS, fetal bovine serum; GLUT9, glucose transporter 9; HCTZ, hydrochlorothiazide; OAT1, organic anion transporter 1; PZO, pyrazinoate; ROS, reactive oxygen species; Tg, transgenic; UOx, uricase; URAT1, urate transporter 1; WT, wild type.

ORIGINAL ARTICLE

© 2012 The Authors

(Schwarzschild *et al.* 2008; Ascherio *et al.* 2009), or radiographically as a reduced rate of dopaminergic nerve terminal marker loss (Schwarzschild *et al.* 2008). In PD models urate attenuated motor and dopaminergic deficits in rodents (Wang *et al.* 2010). *In vitro*, urate reduced oxidative stress as well as cell death induced by toxicants in dopaminergic cell lines (Duan *et al.* 2002; Haberman *et al.* 2007), and rescued dopaminergic neurons in a model of spontaneous cell death (Guerreiro *et al.* 2009). Similarly, we reported that urate prevented dopaminergic neuron death induced by MPP^+ in ventral mesencephalon cultures, and conversely that enzymatically lowering urate levels exacerbated this neurotoxicity (Cipriani *et al.* 2012). Although the mechanism of neuroprotection by urate remains largely unknown, urate rescue of spinal cord neurons from excitotoxicity has been found to depend upon an astroglial mechanism (Du *et al.* 2007), consistent with our recent evidence that the neuroprotection conferred on cultured dopaminergic neurons by raising intracellular urate can be enhanced by co-culturing with astroglia (Cipriani *et al.* 2012).

In the present study, we assess the role played by astrocytes in the protective effect of urate on dopaminergic cells in a cellular oxidative stress model of PD.

Materials and methods

Mice

Transgenic (Tg) *UOx* mice (Kono *et al.* 2010) were obtained from Kenneth L. Rock and the University of Massachusetts. Mice were backcrossed eight times on the C57BL/6 genetic background and phenotyped by measuring UOx activity in serum samples (Cipriani *et al.* 2012). All experiments were performed in accordance with the National Institutes of Health Guide for the Care and Use of Laboratory Animals with approval from the animal subjects review board of Massachusetts General Hospital.

MES 23.5 cell line

The rodent MES 23.5 dopaminergic cell line, which was derived from the fusion of a dopaminergic neuroblastoma and embryonic mesencephalon cells (Crawford *et al.* 1992), was obtained from Weidong Le at Baylor College of Medicine (Houston, TX, USA). Despite the inherent environmental (*in vitro*) and cellular (tumor cell) limitations in modeling dopaminergic neuron degeneration, the dopaminergic properties of MES 23.5 cells and their molecular responses to dopaminergic neuron toxins have been well characterized and support its relevance as a cellular model of the dopaminergic neuron degeneration in PD. The MES 23.5 cells were cultured on polyornithine-coated T75 flasks (Corning Co, Corning, NY, USA) in the Dulbecco modified Eagle medium (DMEM) (Invitrogen, Carlsbad, CA, USA/Gibco, Rockville, MD, USA), which contained Sato components (Sigma Immunochemicals), supplemented with 2% newborn calf serum (Invitrogen), 1% fibroblast growth factor (Invitrogen), penicillin 100 U mL^{-1} , and streptomycin 100 μg mL^{-1} (Sigma, St Louis, MO, USA) at 37°C in a 95% air–5% carbon dioxide humidified incubator. The culture medium was changed every 2 days, MES 23.5 cells were subcultured either in new T-75 flasks or plated onto polyornithine-coated plates. The MES 23.5 cells were used at passage 10–20, at which we confirmed the persistence of their dopaminergic phenotype (Crawford *et al.* 1992) by quantifying the dopamine content (23 ± 3 pmol mg^{-1} protein) using HPLC with electrochemical detection (Xu *et al.* 2010).

Astroglia-enriched cultures

Astroglial cultures were prepared from the brain of 1- or 2-day-old neonatal mice with modifications to previously reported procedures (Saura *et al.* 2005). Cerebral cortices were carefully stripped of their meninges and digested with 0.25% trypsin for 15 min at 37°C. Trypsinization was stopped by adding an equal volume of culture medium DMEM, fetal bovine serum 10%, penicillin 100 U mL^{-1}, and streptomycin 100 μg mL^{-1} to which 0.02% deoxyribonuclease I was added. The suspension was pelleted, re-suspended in culture medium, and triturated to a single cell suspension by repeated pipetting followed by passage through a 70 μM-pore mesh. Cells were seeded at a density of 1,800 cells per mm^2 on poly-L-lysine (100 μg mL^{-1})/DMEM/F12-coated flasks and cultured at 37°C in humidified 5% CO_2-95% air. Medium was fully changed on the fourth day and then every other day. Cultures reached confluency after 7–10 days *in vitro*.

To remove oligodendrocytes and microglial cells, flasks were agitated at 200 × g for 20 min in an orbital shaker. Following shaking medium was changed and flasks were again agitated at 100 × g for 18–20 h. Floating cells were washed away and cultures were treated with 10 μM cytosine arabinoside (Ara-C) for 3 days. Our astroglial cultures comprised > 95% astrocytes, < 2% microglial cells, and < 1% oligodendrocytes. No neuronal cells were detected (Figure S1a–c).

To prepare astroglia-enriched cultures from UOx wild-type (WT) and Tg pups individual cultures were prepared from cortices of each pup. The rest of the brain was used for phenotyping by western blotting. Brain tissue extracts were considered WT when they were negative to UOx staining and Tg when they showed a band at 32 kDa corresponding to UOx. Cultured cell phenotypes were confirmed by measuring UOx activity in the cell medium.

Co-cultures

Astroglia-enriched cultures were prepared as described above. After Ara-C treatment astrocytes were detached from flasks by mild trypsinization (0.1% for 1 min) and re-plated on pre-coated plates in DMEM plus 10% fetal bovine serum. Astrocytes were allowed to grow for 2 days before MES 23.5 cells were seeded on top of them at a concentration of 600 cells per mm^2. MES 23.5 cells were detached from astrocytes by pipetting before processing for dopamine and protein carbonyl assays.

Co-cultures were imaged by an Olympus BX50 microscope with a 20X/0.50 objective and Olympus DP70 camera. Images were processed with DP controller software (Olympus, Center Valley, PA, USA) and merged with ImageJ (NIH).

Conditioned medium experiments

Enriched astroglial cultures were treated with 100 μM urate, or vehicle. Twenty-four hours later conditioned media were collected and filtered through a 0.2 μM membrane to remove cellular debris and immediately used for following experiments. The MES 23.5 cells were treated with increasing proportions of

© 2012 The Authors

conditioned medium 24 h before and during H_2O_2 treatment. In UOx experiments the enzyme was added to astrocytes for 15 h before conditioned medium collection.

Drug treatment

Urate was dissolved in DMEM as 20× concentrated stocks. H_2O_2 was dissolved in phosphate-buffered saline (0.1 M, pH 7.4) as 100× concentrated stocks. Probenecid and hydrochlorothiazide (HCTZ) were dissolved in ethanol and pyrazinoate (PZO) in DMEM 50× concentrated stocks. Drugs were obtained from Sigma.

Cell viability

In MES 23.5 cultures, cell viability was measured by the 3-(4,5-dmethylthiazol-2-yl)-2,5-diphenyltetrazolium bromide assay (Sigma) (Hansen *et al.* 1989). MES 23.5 cells were seeded onto polyornithine-coated 96-well plates (600 cells per mm^2) and grown for at least 24 h until the cells became 70–80% confluent. The medium was changed to DMEM serum-free medium for 24 h before increasing concentrations (50–800 μM) of H_2O_2 were added to the culture medium. To assess protection by urate, increasing concentrations (0–100 μM) were loaded 24 h before and again during toxicant treatment. After three washes with DMEM, 100 μl of MTT solution (0.5 mg mL^{-1} in DMEM) was added for 3 h at 37°C. Then MES 23.5 cells were lysed with acidic isopropanol (0.01M HCl in absolute isopropanol) to extract formazan, which was measured spectrophotometrically at 490 nm with a Labsystems iEMS Analyzer microplate reader. The *n* for each treatment refers to the number of triplicate data points, which were usually obtained from separate 96-well plates.

In co-cultures, living MES 23.5 cells were quantified by immunocytochemistry. After treatments, astrocytes-MES 23.5 co-cultures were fixed with 4% paraformaldehyde for 1 h at 20°C. Then, cells were loaded with a blocking solution (0.5% albumin, 0.3% Triton-X in phosphate-buffered saline) for 30 min at 20°C and incubated with an Alexa 488-cojugated antibody specific for neuronal cells (1 : 200, overnight at 4°C; FluoroPan Neuronal Marker). The following day fluorescence was read at 535 nm by means of a microplate reader.

High-Performance Liquid Chromatography

Cells were scraped in a solution of 150 mM phosphoric acid, 0.2 mM EDTA, and 1 μM 3,4-dihydroxybenzylamine (DHBA; as internal standard) and chromatographed by a multi-channel electrochemical/UV HPLC system as previously described (Burdett *et al.* 2012).

Western blot assay

Cells were scraped in ice-cold extraction buffer (RIPA, Sigma), boiled for 5 min in an appropriate volume of 6 × loading buffer, loaded (50 μg of proteins per well) into a 12% sodium dodecyl sulfate–polyacrylamide gel electrophoresis (SDS-PAGE) gel and run at 120 mV. Proteins were then transferred electrophoretically onto 0.2 μ nitrocellulose membranes (Biorad, Hercules, CA, USA) and saturated for 1 h at 20°C with blocking buffer (5% non-fat dry milk in Tris buffered saline, 0.1% TWEEN-20). To detect urate transporter expression membranes were probed overnight with the following primary antibodies: rabbit glucose transporter 9 (GLUT9)-specific polyclonal antibody (1 : 2000; Abcam Inc, Cambridge, MA, USA), mouse organic anion transporter 1 (OAT1)-specific monoclonal antibody (1 : 200; Abbiotec, San Diego, CA, USA), goat urate transporter 1 (URAT1)-specific polyclonal antibody (1 : 200; Santa Cruz Biotechnology, Santa Cruz, CA, USA). Kidney extract was used as positive control. Proteins were visualized using chemiluminescence (Immobilon; Millipore Millipore Corporation, Billerica, MA, USA). To detect UOx expression, samples were prepared as described above and loaded into a 10% SDS-PAGE gel. Membranes were probed overnight with a rabbit UOx-specific polyclonal antibody (1 : 200; Santa Cruz, Inc). Liver extract was used as positive control.

To normalize the values of stained bands β-actin was detected on the same blot run. Membranes were stripped by strong agitation with 0.2 N NaOH (10 min at 20°C), blocked in blocking buffer for 1 h and probed for 2 h at 20°C with anti-β-actin antibody (1 : 2000; Sigma). Membranes were incubated with horseradish peroxidase-conjugated rabbit-specific (1 : 2000; Pierce Biotechnology), mouse-specific (1 : 2000; Pierce Biotechnology; Rockford, IL), or goat-specific antibody (1 : 2000; Biorad Laboratories) and developed as above. Bands were acquired as JPG files; densitometric analysis was performed by ImageJ software (NIH).

Nitrite (NO_2^-) release

The NO_2^- is an indicator of free radical generation and it is a major unstable product of nitric oxide and molecular oxygen reactions. After treatment, 100 μl of supernatant was added to 100 μl of Griess reagent (Sigma) and spectrophotometrically read at 540 nm with a microplate reader. Blanks were prepared by adding medium containing toxicants and/or protectants to Griess solution.

Protein carbonyl protein assay

Oxidized proteins were detected using the Oxyblot assay kit (Chemicon) according to the manufacturer's instructions. Briefly, protein carbonyl groups were derivatized with 2,4-dinitrophenylhydrazine, subjected to 10% SDS-PAGE and transferred electrophoretically onto 0.2 μ nitrocellulose membranes. Membranes were loaded with an antibody specific to the dinitrophenylhydrazone moieties of the proteins and developed using chemiluminescence.

Protein detection

Protein concentration was measured in 4 μl of each sample using Bio-Rad Protein Assay reagent (Biorad Laboratories) and reading the absorbance at 600 nm with a microplate reader.

Statistical analysis

Statistical analyses were performed by GraphPad Prism version 4.00 (GraphPad Software Inc., San Diego, CA, USA). Unpaired Student's *t*-test was used when only two group samples were compared. ANOVA analysis, followed by Newman Keuls or Bonferroni *post-hoc* test, was used when more than two group samples were compared. Values were expressed as mean ± SEM. Differences at the $p < 0.05$ were considered significant and indicated in figures by symbols explained in legends.

Results

Astrocyte-dependent protection of dopaminergic cells by urate

To reproduce an oxidative stress model of PD (Sherer *et al.* 2002; Anantharam *et al.* 2007) we incubated MES 23.5 cells

© 2012 The Authors

with increasing concentrations of H_2O_2. Treatment for 24 h with H_2O_2 decreased cell viability in a concentration-dependent manner (Fig. 1a) with about 60% of cell death at 200 μM, which was the H_2O_2 concentration chosen for following experiments.

To evaluate the effect of urate on H_2O_2-induced cell death urate was added to cultures 24 h before and during H_2O_2 application. Urate treatment tended to decrease H_2O_2-induced cell death over a concentration range of 0–100 μM (Fig. 1b) without a statistically significant effect.

Du and coworkers (Du *et al.* 2007) reported that urate's protective effect on primary spinal cord neurons was dependent on the presence of astrocytes in cultures. To assess whether urate protects dopaminergic cells cultured with astrocytes against oxidative stress, its effect was tested on MES 23.5-astrocytes co-cultures treated with H_2O_2. To minimize confounding effects by astroglial established inherent protection on dopaminergic cells (Yu and Zuo 1997), H_2O_2 toxicity was assessed in co-cultures established at astrocytes/MES 23.5 cells ratios of 0 : 1, 1 : 1, and 1 : 5. Astrocytes cultured with MES 23.5 cells at a ratio of 1 : 5 did not prevent H_2O_2-induced death in MES 23.5 cells (Fig. 1c); the same ratio was employed in following experiments. The H_2O_2 did not affect astrocyte viability up to the highest tested concentration of 200 μM (data not shown). Urate added to co-cultures 24 h before and during H_2O_2 application conferred significant, dose-dependent protection on H_2O_2-treated dopaminergic cells (Fig. 1d, e–g).

Urate decreased reactive oxygen species (ROS) production and protein oxidation

To determine if protection is associated with reduced oxidative stress and protein damage, we measured reactive oxygen species in cell media from H_2O_2-treated co-cultures of MES 23.5 cells and astrocytes. H_2O_2 raised the concentration of NO_2^- (nitrite) in the medium over time (Fig. 2a). Urate significantly decreased medium NO_2^- concentration in H_2O_2- treated cultures at 24 h of treatment (Fig. 2b). As an index of oxidative damage, protein carbonyl levels were measured in MES 23.5 cells (after removal from astrocytes) and found to be increased by H_2O_2 over time (Fig. 2c). Urate attenuated the increase in protein oxidation at 3 h of treatment with H_2O_2 (Fig. 2d).

Astrocytes mediate protection by urate without physically contacting dopaminergic cells

The MES 23.5 cells were treated with increasing percentages of medium collected from vehicle-treated (control) or

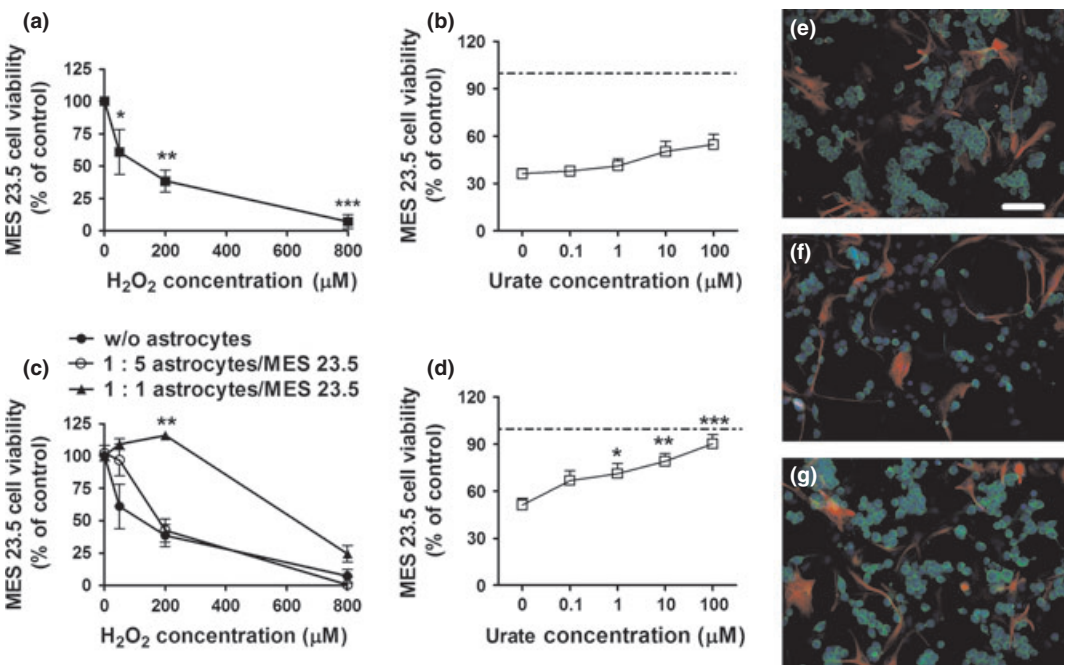

Fig. 1 Protection of MES 23.5 cells by urate is mediated by astrocytes. (a) Cell viability in MES 23.5 cultures after 24 h of H_2O_2 treatment at indicated concentrations. One-way ANOVA: $n = 3$, $^*p < 0.05$, $^{**}p < 0.001$, $^{***}p < 0.001$ versus 0 value. (b) Effect of urate ($n = 4$) treatment on 200 μM H_2O_2-induced cell death in MES 23.5 cultures. (c) Cell viability of MES 23.5 cells cultured for 24 h with increasing H_2O_2 concentrations and astrocyte densities. Ratio between astrocytes and MES 23.5 cells is shown in symbol key. Two-way ANOVA: $n = 3$; $^{**}p < 0.01$ versus 0 and 1 : 5. (d) Effect of urate treatment on 200 μM H_2O_2-induced cell death in co-cultures (1 : 5::astrocytes/MES 23.5). One-way ANOVA: $n = 13$; $^*p < 0.05$, $^{**}p < 0.01$, $^{***}p < 0.001$ versus respective 0 value. Photomicrograph of (e) untreated, (f) H_2O_2-treated, (g) H_2O_2 + 100 μM urate-treated and MES 23.5 cells (green) cultured on astrocytes (red), DAPI staining was used to label nuclei (blue). Scale bar is 50 μm. The dashed line indicates the control value (100%) against which the other values were measured.

© 2012 The Authors

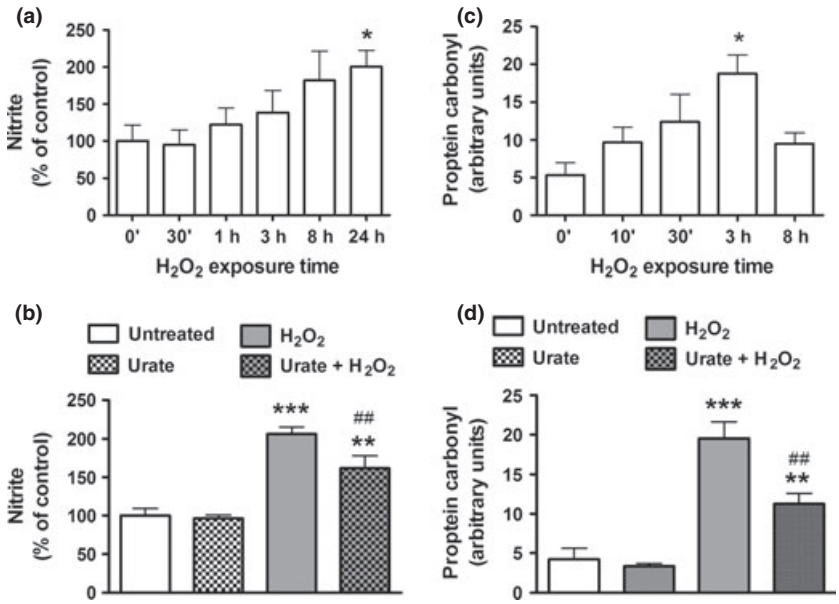

Fig. 2 Urate reduced reactive oxygen species and protein oxidation in MES 23.5 cells cultured with astrocytes. (a) NO_2^- release in co-culture medium after 200 μM H_2O_2 treatment for the indicated times. One-way ANOVA: $n = 15$; $^*p < 0.05$ versus 0′ value. (b) Effect of urate treatment on H_2O_2-induced NO_2^- release at 24 h of treatment. One-way ANOVA: $n = 16$; $^{**}P < 0.01$ and $^{***}P < 0.001$ versus control and urate values, $^{\#\#}p < 0.01$ versus H_2O_2 value. (c) Protein carbonyl content in MES 23.5 cells cultured with astrocytes after 200 μM H_2O_2 treatment for the indicated times. One-way ANOVA: $n = 5$; $^*p < 0.05$ versus 0 value. (d) Effect of urate treatment on H_2O_2-induced protein carbonylation at 3 h of treatment with H_2O_2. One-way ANOVA: $n = 7$; $^{**}p < 0.01$ and $^{***}p < 0.001$ versus control and urate values; $^{\#\#}p < 0.05$ versus H_2O_2 value.

urate-treated astrocytes. Medium from control astrocytes did not increase viability of H_2O_2-treated MES 23.5 cells at any concentration, whereas conditioned medium from astrocytes treated for 24 h with 100 μM urate significantly increased MES 23.5 viability in a concentration-dependent manner.

To address a possible direct effect of carry-over urate on MES 23.5 cells, we added UOx or vehicle to astroglial cultures after 24 h of treatment with 100 μM urate. UOx-catalyzed (> 99.9%) elimination of urate from the conditioned medium was confirmed by HPLC measurements of 0.020 ± 0.003 μM versus 98 ± 12 μM urate 15 h after addition of UOx versus vehicle, respectively ($p < 0.0001$). The protective effect of conditioned medium was only slightly attenuated by UOx, indicating that carry-over urate could not account for most of the protection conferred by urate-treated astrocyte-conditioned medium (Fig. 3b). The finding is consistent with our earlier observations that urate alone had no appreciable effect on dopaminergic cell viability.

Exogenous urate treatment increased intracellular urate content

Although intracellular antioxidant actions of urate might explain its observed attenuation of H_2O_2-induced oxidative

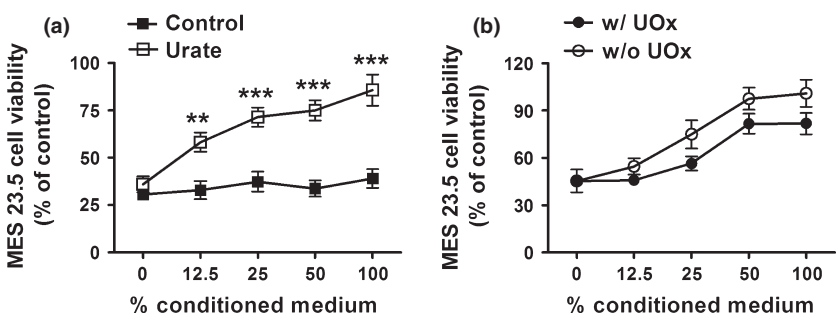

Fig. 3 (a) Effect of increasing percentages of conditioned medium from control or urate-treated astrocytes on MES 23.5 cell viability. Two-way ANOVA: $n = 15$; $^{**}p < 0.01$ and $^{***}p < 0.001$ versus respective control value. (b) Effect of uricase (UOx; 0.12 U/l) on conditioned medium from urate-treated astrocytes on MES 23.5 cell viability ($n = 4$). The UOx or vehicle was added to astroglial cultures after 24 h of urate treatment; conditioned media were collected after 15 more hours.

© 2012 The Authors

damage, Guerreiro *et al.* (Guerreiro *et al.* 2009) concluded that urate may act as an extracellular antioxidant to protect dopaminergic neurons. Similarly, the astrocyte-dependence of protection found in the present study leaves uncertain the site targeted by urate.

To determine whether urate entered MES 23.5 cells and astrocytes, intracellular urate was measured in dopaminergic and astroglial cells treated with vehicle or urate for 24 h. *Exogenous* urate raised intracellular urate content from 0.81 ± 0.30 to 5.09 ± 0.44 nmol/mg of protein ($p < 0.01$) and from 0.14 ± 0.06 to 0.38 ± 0.04 nmol/mg of protein ($p < 0.01$) in MES 23.5 cells and astrocytes, respectively (see Table S1 and S2), at the time when toxicant treatment would have been initiated. No statistically significant effect on its precursors was found either intracellularly (See Table S1 and S2) or extracellularly (data not shown).

To assess if urate was metabolized by UOx in MES 23.5 cells we treated the cell line with increasing concentrations of oxonate, a UOx selective inhibitor. Oxonate did not affect urate content in MES 23.5 cells at any given concentration (Figure S2a). This result was supported by western blotting analysis, which detected no staining for UOx in both MES 23.5 cells and astrocytes (Figure S2b).

Intracellular urate increase is required for dopaminergic protection

To determine whether urate accumulation into MES 23.5 cells and astrocytes is transporter-mediated, protein expression of urate transporters known to be key regulators of urate levels in rodents (Hosoyamada *et al.* 2004; Preitner *et al.* 2009) was investigated. Immunostaining for URAT1 and GLUT9 was positive in MES 23.5 cells and astrocytes, while immunostaining for OAT1 was negative in both cell types (Fig. 4a). To investigate whether any of these transporters played a role in increasing intracellular urate levels, cells were loaded with urate immediately after one of the following drugs: PZO, the active metabolite of pyrazinamide (a URAT1 inhibitor), probenecid (a URAT1 and GLUT9 inhibitor), and HCTZ (a URAT1 and OAT1 inhibitor).

The HPLC determinations showed that HCTZ significantly reduced urate accumulation in a concentration-dependent manner in MES 23.5 cells, whereas probenecid and PZO had no effect (Fig. 4b). By contrast, PZO, probenecid and HCTZ markedly reduced urate accumulation in astrocytes in a concentration-dependent manner (Fig. 4c).

To determine if intracellular urate accumulation was required for urate's protective effect, we conducted viability experiments pretreating mixed cultures with HCTZ, PZO, or probenecid together with urate 24 h before toxicant treatment. The PZO and HCTZ prevented dopaminergic protection induced by urate in a concentration-dependent manner; a similar effect was seen with 0.5 mM probenecid (Fig. 4d). PZO, HCTZ and probenecid did not affect susceptibility of MES 23.5 cells to H_2O_2 in urate-untreated cultures (data not shown).

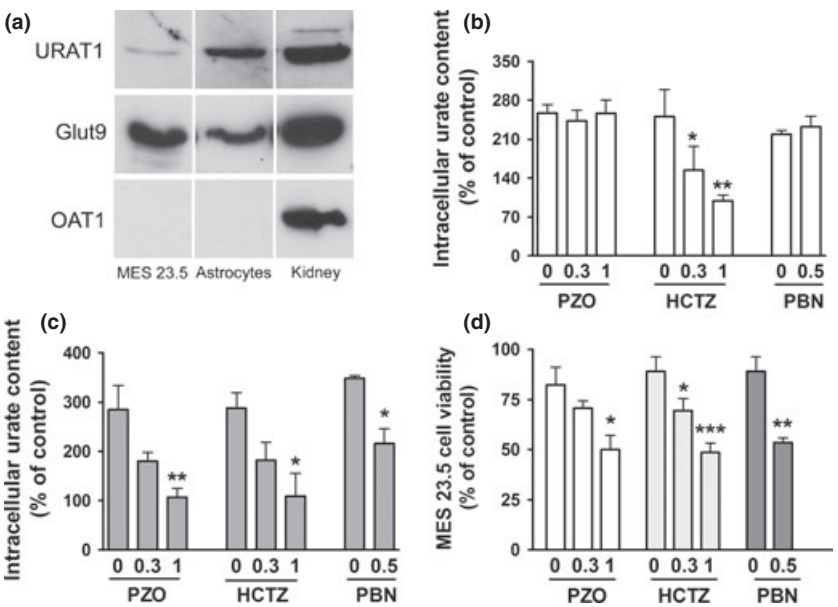

Fig. 4 Urate's protective effect depends on its accumulation in astrocytes. (a) Western blotting shows urate transporter 1 (URAT1), GLUT9 and organic anion transporter 1 (OAT1) urate transporter expression in extracts of MES 23.5 cells and astrocytes. Kidney extract was used as positive control. (b) Urate concentration in MES 23.5 cells and (c) astrocytes treated with urate transporter inhibitors: pyrazinoate (PZO), hydrochlorothiazide (HCTZ), or probenecid (PBN), at the indicated concentrations (mM) ($n = 4$–7). (d) Effects of urate transporter inhibitors: PZO, HCTZ and PBN, at the indicated concentrations (mM), on MES 23.5 cell viability in H_2O_2-treated co-cultures expressed as percentage of control ($n = 4$–6). One-way ANOVA: $^*p < 0.05$, $^{**}p < 0.01$, $^{***}p < 0.001$ versus 0 value.

© 2012 The Authors

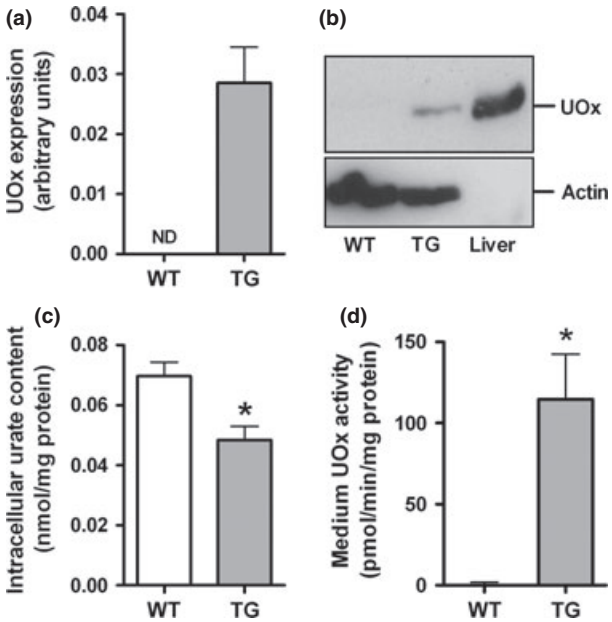

Fig. 5 UOx expression in transgenic (Tg) astrocytes reduced urate intracellular content. (a) Uricase (UOx) expression in Tg *UOx* astrocytes with no detection (ND) in wild-type (WT) astrocytes. (b) Western blot of UOx immunoreactivity in 50 μg of WT and Tg astrocytes; liver extract (10 μg) was used as positive control. Actin was used as loading control. (c) Basal intracellular urate content in WT and Tg astrocytes. Student's *t*-test: $n = 5$; $^*p = 0.02$. (d) Basal UOx activity in media from WT and Tg astrocytes. Student's *t*-test: $n = 10$, $^*p = 0.015$.

Transgenic urate degradation in astrocytes reduces protection by conditioned medium

To exclude possible secondary pharmacological effects of urate-lowering transport inhibitors, we also took a genetic approach to reduce urate content through enzymatic degradation within astrocytes. To that end, astrocytes were prepared from mice over-expressing *UOx* (*UOx* Tg) (Kono *et al.* 2010). Cultured Tg astrocytes expressed UOx protein, which was undetectable in WT astrocytes (Fig. 5a and b). The UOx expression reduced urate basal levels in Tg compared with WT astrocytes (Fig. 5c). Because the UOx transgene we employed (Kono *et al.* 2010) can lead to secretion of the enzyme (Fig. 5d), we assessed the extent to which extracellular urate was catabolized in Tg and WT astrocyte cultures after addition of medium containing 100 μM urate. We found that urate was not altered for at least 8 h in the medium, although by the end of the 24 h treatment period a small but significant (21%) reduction was appreciated (Fig. 6a). The intracellular urate content in Tg astrocytes was reduced compared with WT astrocytes after 8 h of exposure to urate (Fig. 6b). Thus transgenic *UOx* expression in astrocytes produced marked and rapid reduction primarily of intracellular urate. To assess whether reduced urate accumulation affected the protective effect of conditioned medium on MES 23.5 cells, medium was collected from urate-treated WT and Tg astrocytes and immediately used to pretreat MES 23.5 cells. Cell viability of MES 23.5 cells pretreated with medium collected from urate-treated Tg astrocytes was reduced in comparison to cell viability of MES 23.5 cells pretreated with medium collected from urate-treated WT astrocytes, suggesting a critical role for intracellular urate in the release of a soluble astrocyte-derived protective factor (Fig. 6c).

Discussion

In cultures, urate markedly enhanced survival of dopaminergic neurons in a model of spontaneous cell death (Guerreiro *et al.* 2009) and reduced oxidative stress as well as cell death induced by toxicants (Duan *et al.* 2002; Haberman *et al.* 2007; Zhu *et al.* 2011; Cipriani *et al.* 2012). Urate's protective effects have been also found *in vivo*, where urate prevented dopaminergic cell death in a rodent model of PD (Wang *et al.* 2010).

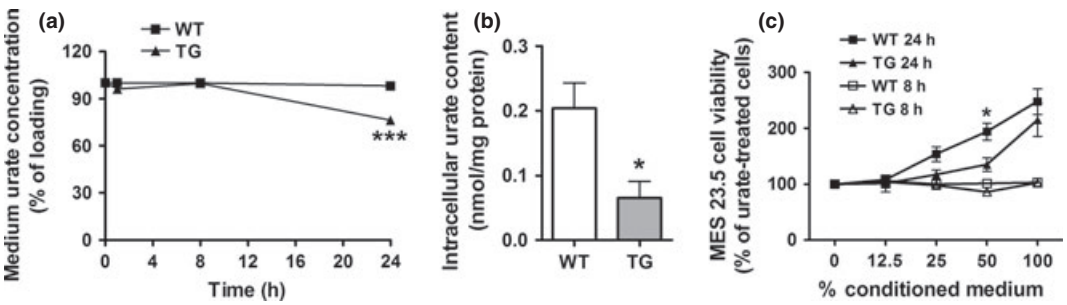

Fig. 6 UOx expression in transgenic astrocytes reduced astrocyte-mediated protection of H_2O_2-treated MES 23.5 cells. (a) Medium urate concentration in 100 μM urate-treated wild-type (WT) and transgenic (Tg) astroglial cultures over the time ($n = 3$; $^{***}P < 0.001$ vs. respective WT value). Error bars were smaller than symbols for all data points. (b) Intracellular urate content in WT and Tg astrocytes after 8 h of treatment with 100 μM urate; Student's *t*-test ($n = 4$, $^*p = 0.02$). (c) Effect of conditioned medium collected from urate-treated WT and Tg astrocytes on viability of 200 μM H_2O_2-treated cells ($n = 4$; $^*p < 0.05$ vs. respective Tg value).

© 2012 The Authors

Although considerable evidence indicates that urate is a powerful antioxidant few studies have been investigated alternative mechanisms of its protective effect. Du and coworkers (Du *et al.* 2007) reported that the protective effect of urate on primary spinal cord neurons was dependent on the presence of astrocytes in cultures. They showed that urate induced up-regulation of the EAAT-1 glutamate transporter in astrocytes, suggesting that urate may enhance the ability of astrocytes to reduce extracellular glutamate levels around nearby neurons. Moreover, our previous studies showed that the effect of modulating intracellular urate content on the susceptibility of dopaminergic neurons to MPP^+ treatment was amplified in cultures containing a high percentage of astrocytes in comparison to cultures were glial growth was inhibited (Cipriani *et al.* 2012). Of note, the data reported in the present study argue against an important direct antioxidant action of urate in protecting stressed dopaminergic cells, or at least that this putative antioxidant action of urate is not sufficient to account for its benefits in this model.

In the present study, the protective role of urate on dopaminergic cells was demonstrated not only in co-cultures but also in conditioned medium experiments. The inability of UOx to prevent completely urate's effect confirmed that protection of dopaminergic cells is not induced by carry-over urate on its own, but more likely by the release of soluble protective factor(s) by astrocytes in response to urate. This finding also excludes a direct interaction between H_2O_2 and urate as an explanation for how urate attenuates H_2O_2 toxicity. Similarly, the previously reported ability of urate to increase EAAT-1 expression on astrocytes and thereby reduce local glutamate buffering (Du *et al.* 2007) could not directly explain urate's protective effect in the present study, in which the astrocyte-dependence does not require proximity between astrocytes and dopaminergic cells. Of note, the capacity of astrocytes to mediate neuroprotection by urate is not likely to be restricted to the cortical astrocytes- which we employed in this study based on their abundance relative to those in stratum or mesencephalon- being consistent with enhanced neuroprotection achieved with spinal cord and ventral mesencephalon astrocytes as well (Du *et al.* 2007; Cipriani *et al.* 2012).

Although the identity of a putative protective factor released by urate-stimulated astrocytes remains to be determined, there is ample precedent for the inducible release of neuroprotectants from astrocytes. For example, protective effects of pramipexole on a human dopaminergic cell line were found to be mediated by astroglial release of the brain-derived neurotrophic factor (Imamura *et al.* 2008). Similarly, grape seed extract was found to protect primary neurons against H_2O_2-induced cell death inducing IL-6 release from astrocytes (Fujishita *et al.* 2009; Li *et al.* 2009).

In the present study, we investigated whether the protective effect of urate could be mediated by elevation of its intracellular content in dopaminergic cells and astrocytes. In agreement with our previous findings (Cipriani *et al.* 2012), we found that *exogenous* urate elevated intracellular urate content in dopaminergic cells and astrocytes. Thus urate may have a protective effect on dopaminergic cells not only by modulating the redox status of cellular membranes, as previously suggested by (Guerreiro *et al.* 2009), but also by acting on intracellular targets. Increasing intracellular content by *exogenous* urate might better explain the effect induced in astroglial cultures where it was found to up-regulate protein expression (Du *et al.* 2007).

An intracellular conversion of urate to allantoin, a possible active metabolite of urate, was largely excluded by the absence of UOx expression in dopaminergic cells and astrocytes and by the lack of oxonate effect in dopaminergic cells. These data are in agreement with previous studies that reported low UOx activity in the brain (Truszkowski and Goldmanowna 1933; Robins *et al.* 1953). Moreover, if allantoin were the active, protective metabolite of urate then one would have expected transgenic *UOx* expression to have enhanced the protective effect of urate (by increasing it conversion to allantoin), rather than attenuating it as observed.

To investigate whether cellular urate accumulation was dependent on membrane carriers, transporter inhibitors were employed. The increase in intracellular urate content of MES 23.5 cells and astrocytes treated with urate was markedly reduced by these transport inhibitors, indicating that urate accumulation in cells was likely because of the uptake of *exogenous* urate rather than a modulation of the purine pathway. This hypothesis was also supported by the finding that *exogenous* urate did not significantly affect, intracellularly or extracellularly, the content of any other purine measured. In mixed cultures, all three of the urate transporter inhibitors tested – HCTZ, probenecid, and PZO – prevented urate's protective effect. The correlation of these protective effects with the blockade of urate accumulation in astrocytes but not in MES 23.5 cells, strengthens the evidence that urate increase in astrocytes is a critical first step in its protective effect on cultured dopaminergic cells. This hypothesis is supported by the finding that transgenic expression of UOx in astrocytes attenuated urate's protective effect on dopaminergic cells. Of interest, the loss of UOx enzyme during hominoid evolution (Oda *et al.* 2002) has increased urate levels in the human body and it has been proposed to have raised antioxidant levels in human ancestors and thereby lengthened their lifespans. Verisimilarly, loss of UOx expression may have enhanced cellular antioxidant defenses by not only increasing circulating levels of urate in the human body but also presumably its intracellular content.

Urate transporters are highly expressed in the kidney where they control urate secretion and reabsorption. Urate transporters have also been found in the human and rodent

© 2012 The Authors

brain at the level of choroid plexus and blood-brain barrier (Alebouyeh *et al.* 2003; Mori *et al.* 2003) and localized in neuronal and endothelial cells (Ohtsuki *et al.* 2004; Bahn *et al.* 2005). The presence of urate transporters suggests a possible role for these carriers in regulating urate homeostasis in the brain, although their function there is unknown. Interestingly, an allelic variation in the *GLUT9* gene, associated with lower serum uric acid levels, was reported to correlate with a lower age at onset in PD (Facheris *et al.* 2011).

Translational significance

A compelling convergence of epidemiological, clinical, and initial cellular studies has suggested a potential neuroprotective effect of higher urate levels on dopaminergic neurons (Cipriani *et al.* 2010; Shoulson 2010) and expedited development of a phase II randomized clinical trial of inosine to elevate urate in PD (http://clinicaltrials.gov/ct2/show/NCT00833690). In parallel, efforts to gain mechanistic insight into protection by urate might be of considerable therapeutic as well as biological value as they could impact both the rationale and the pace of advancing to phase III clinical investigation. The present findings, in a cellular oxidative stress model of PD, provide evidence of a novel urate mechanism, possibly independent of its established antioxidant properties and support its candidacy as a neuroprotective agent for PD. They also suggest a more intricate mechanism of action that involves an astroglial intermediate, consistent with a growing appreciation of the critical pathophysiological role for astrocytes in the cellular microenvironment of degenerating neurons in PD (Rappold and Tieu 2010).

In addition, our findings that urate transporters can modify purine uptake and dopaminergic cell death extend the range of translational strategies for targeting urate levels in PD. Although initial human trials aiming to raise CNS urate elevation in PD are conservatively focused on a precursor (inosine) approach, a drawback is the increased risk of gout and uric acid urolithiasis that accompanies the associated systemic rise in urate levels. Our demonstration that urate transport inhibitors commonly employed in clinical practice (e.g., probenecid and HCTZ, which lower and raise serum urate, respectively) can block urate uptake and dopaminergic cell death *in vitro* suggests that transport-targeted therapeutics may provide an alternative or adjunct to urate precursors. Thus they may avoid peripheral complications of hyperuricemia. Because the directionality of urate transport at the tissue (e.g., blood-brain barrier) as well as the cellular levels are not easily addressed in culture models, *in vivo* preclinical studies of urate transport pharmacology in the CNS and in whole animal models of PD will be an important next step.

In conclusion, we found that protection of dopaminergic cells by urate depends on its accumulation in astroglial cells that in turn release soluble protective factors. The data bolster the rationale for targeting urate elevation as a therapeutic strategy for PD and indicate that urate transporters on astrocytes might also be a pharmacological target to modulate urate levels in PD brain.

Acknowledgements

This work was supported by the American Parkinson Disease Association, US National Institutes of Health grants R21NS058324, K24NS060991 and the US Department of Defense grant W81XWH-11-1-0150. MES 23.5 cells, transgenic *UOx* mice and technical advice were kindly provided by Weidong Le, Ken Rock, and Hajime Kono. We would like to thank Dr. Mount from Brigham and Women's Hospital, Boston, for his thoughtful comments regarding urate transporter experiments. The authors declare no competing financial interests.

Supporting information

Additional supporting information may be found in the online version of this article:

Figure S1. Cellular composition of astroglia-enriched cultures.

Figure S2. Undectable uricase expression in MES 23.5 cells and astrocytes.

Table S1. Intracellular urate accumulation in vehicle (control) and urate-treated MES 23.5 cells.

Table S2. Intracellular urate accumulation in vehicle (control) and urate-treated astrocytes.

As a service to our authors and readers, this journal provides supporting information supplied by the authors. Such materials are peer-reviewed and may be re-organized for online delivery, but are not copy-edited or typeset. Technical support issues arising from supporting information (other than missing files) should be addressed to the authors.

References

Alebouyeh M., Takeda M., Onozato M. L. *et al.* (2003) Expression of human organic anion transporters in the choroid plexus and their interactions with neurotransmitter metabolites. *J. Pharmacol. Sci.* **93**, 430–436.

Ames B. N., Cathcart R., Schwiers E. and Hochstein P. (1981) Uric acid provides an antioxidant defense in humans against oxidant- and radical-caused aging and cancer: a hypothesis. *Proc. Natl. Acad. Sci. USA* **78**, 6858–6862.

Anantharam V., Lehrmann E., Kanthasamy A., Yang Y., Banerjee P., Becker K. G., Freed W. J. and Kanthasamy A. G. (2007) Microarray analysis of oxidative stress regulated genes in mesencephalic dopaminergic neuronal cells: relevance to oxidative damage in Parkinson's disease. *Neurochem. Int.* **50**, 834–847.

Ascherio A., LeWitt P. A., Xu K. *et al.* (2009) Urate as a predictor of the rate of clinical decline in Parkinson disease. *Arch. Neurol.* **66**, 1460–1468.

Bahn A., Ljubojevic M., Lorenz H., Schultz C., Ghebremedhin E., Ugele B., Sabolic I., Burckhardt G. and Hagos Y. (2005) Murine renal organic anion transporters mOAT1 and mOAT3 facilitate the transport of neuroactive tryptophan metabolites. *Am. J. Physiol. Cell Physiol.* **289**, C1075–1084.

© 2012 The Authors

Burdett T. C., Desjardins C. A., Logan R., McFarland N. R., Chen X. and Schwarzschild A. M. (2012) Efficient determination of purine metabolites in brain tissue and serum by high-performance liquid chromatography with electrochemical and UV detection. *Biomed. Chromatogr.* Accepted.

Cipriani S., Chen X. and Schwarzschild M. A. (2010) Urate: a novel biomarker of Parkinson's disease risk, diagnosis and prognosis. *Biomark. Med.* **4**, 701–712.

Cipriani S., Desjardins A. C., Burdett C. T., Xu Y., Xu K. and Schwarzschild A. M. (2012) Urate and its transgenic depletion modulate neuronal vulnerability in a cellular model of Parkinson's disease. *PLoS One*, **7**, e37331.

Crawford Jr G. D., Le W. D., Smith R. G., Xie W. J., Stefani E. and Appel S. H. (1992) A novel N18TG2 x mesencephalon cell hybrid expresses properties that suggest a dopaminergic cell line of substantia nigra origin. *J. Neurosci.* **12**, 3392–3398.

Davies K. J., Sevanian A., Muakkassah-Kelly S. F. and Hochstein P. (1986) Uric acid-iron ion complexes A new aspect of the antioxidant functions of uric acid. *Biochem. J.* **235**, 747–754.

Du Y., Chen C. P., Tseng C. Y., Eisenberg Y. and Firestein B. L. (2007) Astroglia-mediated effects of uric acid to protect spinal cord neurons from glutamate toxicity. *Glia* **55**, 463–472.

Duan W., Ladenheim B., Cutler R. G., Kruman I. I., Cadet J. L. and Mattson M. P. (2002) Dietary folate deficiency and elevated homocysteine levels endanger dopaminergic neurons in models of Parkinson's disease. *J. Neurochem.* **80**, 101–110.

Facheris M. F., Hicks A. A., Minelli C. *et al.* (2011) Variation in the uric acid transporter gene SLC2A9 and its association with AAO of Parkinson's disease. *J. Mol. Neurosci.* **43**, 246–250.

Fujishita K., Ozawa T., Shibata K., Tanabe S., Sato Y., Hisamoto M., Okuda T. and Koizumi S. (2009) Grape seed extract acting on astrocytes reveals neuronal protection against oxidative stress via interleukin-6-mediated mechanisms. *Cell. Mol. Neurobiol.* **29**, 1121–1129.

Guerreiro S., Ponceau A., Toulorge D., Martin E., Alvarez-Fischer D., Hirsch E. C. and Michel P. P. (2009) Protection of midbrain dopaminergic neurons by the end-product of purine metabolism uric acid: potentiation by low-level depolarization. *J. Neurochem.* **109**, 1118–1128.

Haberman F., Tang S. C., Arumugam T. V., Hyun D. H., Yu Q. S., Cutler R. G., Guo Z., Holloway H. W., Greig N. H. and Mattson M. P. (2007) Soluble neuroprotective antioxidant uric acid analogs ameliorate ischemic brain injury in mice. *Neuromolecular Med.* **9**, 315–323.

Hansen M. B., Nielsen S. E. and Berg K. (1989) Re-examination and further development of a precise and rapid dye method for measuring cell growth/cell kill. *J. Immunol. Methods* **119**, 203–210.

Hosoyamada M., Ichida K., Enomoto A., Hosoya T. and Endou H. (2004) Function and localization of urate transporter 1 in mouse kidney. *J. Am. Soc. Nephrol.* **15**, 261–268.

Imamura K., Takeshima T., Nakaso K., Ito S. and Nakashima K. (2008) Pramipexole has astrocyte-mediated neuroprotective effects against lactacystin toxicity. *Neurosci. Lett.* **440**, 97–102.

Kono H., Chen C. J., Ontiveros F. and Rock K. L. (2010) Uric acid promotes an acute inflammatory response to sterile cell death in mice. *J. Clin. Invest.* **120**, 1939–1949.

Li X. Z., Bai L. M., Yang Y. P., Luo W. F., Hu W. D., Chen J. P., Mao C. J. and Liu C. F. (2009) Effects of IL-6 secreted from astrocytes on the survival of dopaminergic neurons in lipopolysaccharide-induced inflammation. *Neurosci. Res.* **65**, 252–258.

Mori S., Takanaga H., Ohtsuki S., Deguchi T., Kang Y. S., Hosoya K. and Terasaki T. (2003) Rat organic anion transporter 3 (rOAT3) is responsible for brain-to-blood efflux of homovanillic acid at the abluminal membrane of brain capillary endothelial cells. *J. Cereb. Blood Flow Metab.* **23**, 432–440.

Oda M., Satta Y., Takenaka O. and Takahata N. (2002) Loss of urate oxidase activity in hominoids and its evolutionary implications. *Mol. Biol. Evol.* **19**, 640–653.

Ohtsuki S., Kikkawa T., Mori S., Hori S., Takanaga H., Otagiri M. and Terasaki T. (2004) Mouse reduced in osteosclerosis transporter functions as an organic anion transporter 3 and is localized at abluminal membrane of blood-brain barrier. *J. Pharmacol. Exp. Ther.* **309**, 1273–1281.

Preitner F., Bonny O., Laverriere A., Rotman S., Firsov D., Da Costa A., Metref S. and Thorens B. (2009) Glut9 is a major regulator of urate homeostasis and its genetic inactivation induces hyperuricosuria and urate nephropathy. *Proc. Natl. Acad. Sci. USA* **106**, 15501–15506.

Rappold P. M. and Tieu K. (2010) Astrocytes and therapeutics for Parkinson's disease. *Neurotherapeutics* **7**, 413–423.

Robins E., Smith D. E. and McCaman R. E. (1953) Microdetermination of purine nucleoside phosphorylase activity in brain and its distribution within the monkey cerebellum. *J. Biol. Chem.* **204**, 927–937.

Ross C. A. and Smith W. W. (2007) Gene-environment interactions in Parkinson's disease. *Parkinsonism Relat. Disord.* **13**(Suppl 3), S309–15.

Saura J., Angulo E., Ejarque A. *et al.* (2005) Adenosine A2A receptor stimulation potentiates nitric oxide release by activated microglia. *J. Neurochem.* **95**, 919–929.

Schwarzschild M. A., Schwid S. R., Marek K. *et al.* (2008) Serum urate as a predictor of clinical and radiographic progression in Parkinson disease. *Arch. Neurol.* **65**, 716–723.

Sherer T. B., Betarbet R., Stout A. K., Lund S., Baptista M., Panov A. V., Cookson M. R. and Greenamyre J. T. (2002) An in vitro model of Parkinson's disease: linking mitochondrial impairment to altered alpha-synuclein metabolism and oxidative damage. *J. Neurosci.* **22**, 7006–7015.

Shoulson I. (2010) Therapeutic directions for Parkinson's disease. *Mov. Disord.* **25**(Suppl 1), S152–4.

Truszkowski R. and Goldmanowna C. (1933) Uricase and its action: distribution in various animals. *Biochem. J.* **27**, 612–614.

Wang L. J., Luo W. F., Wang H. H., Ni G. H., Ye Y., Li D. and Liu C. F. (2010) Protective effects of uric acid on nigrostriatal system injury induced by 6-hydroxydopamine in rats. *Zhonghua Yi Xue Za Zhi* **90**, 1362–1365.

Weisskopf M. G., O'Reilly E., Chen H., Schwarzschild M. A. and Ascherio A. (2007) Plasma urate and risk of Parkinson's disease. *Am. J. Epidemiol.* **166**, 561–567.

Whiteman M., Ketsawatsakul U. and Halliwell B. (2002) A reassessment of the peroxynitrite scavenging activity of uric acid. *Ann. N. Y. Acad. Sci.* **962**, 242–259.

Xu K., Xu Y. H., Chen J. F. and Schwarzschild M. A. (2010) Neuroprotection by caffeine: time course and role of its metabolites in the MPTP model of Parkinson's disease. *Neuroscience* **167**, 475–481.

Yu P. H. and Zuo D. M. (1997) Enhanced tolerance of neuroblastoma cells towards the neurotoxin 6-hydroxydopamine following specific cell-cell interaction with primary astrocytes. *Neuroscience* **78**, 903–912.

Zhu T. G., Wang X. X., Luo W. F., Zhang Q. L., Huang T. T., Xu X. S. and Liu C. F. (2011) Protective effects of urate against 6-OHDA-induced cell injury in PC12 cells through antioxidant action. *Neurosci. Lett.* **506**, 175–179.

© 2012 The Authors

Disrupted and transgenic *urate oxidase* alter urate and dopaminergic neurodegeneration

Xiqun Chen[1], Thomas C. Burdett, Cody A. Desjardins, Robert Logan, Sara Cipriani, Yuehang Xu, and Michael A. Schwarzschild

Department of Neurology, Massachusetts General Hospital, Harvard Medical School, Boston, MA 02129

Edited by Tomas G. M. Hökfelt, Karolinska Institutet, Stockholm, Sweden, and approved November 19, 2012 (received for review October 4, 2012)

Urate is the end product of purine metabolism in humans, owing to the evolutionary disruption of the gene encoding urate oxidase (UOx). Elevated urate can cause gout and urolithiasis and is associated with cardiovascular and other diseases. However, urate also possesses antioxidant and neuroprotective properties. Recent convergence of epidemiological and clinical data has identified urate as a predictor of both reduced risk and favorable progression of Parkinson's disease (PD). In rodents, functional UOx catalyzes urate oxidation to allantoin. We found that *UOx* KO mice with a constitutive mutation of the gene have increased concentrations of brain urate. By contrast, *UOx* transgenic (Tg) mice overexpressing the enzyme have reduced brain urate concentrations. Effects of the complementary *UOx* manipulations were assessed in a mouse intrastriatal 6-hydroxydopamine (6-OHDA) model of hemiparkinsonism. *UOx* KO mice exhibit attenuated toxic effects of 6-OHDA on nigral dopaminergic cell counts, striatal dopamine content, and rotational behavior. Conversely, Tg overexpression of *UOx* exacerbates these morphological, neurochemical, and functional lesions of the dopaminergic nigrostriatal pathway. Together our data support a neuroprotective role of endogenous urate in dopaminergic neurons and strengthen the rationale for developing urate-elevating strategies as potential disease-modifying therapy for PD.

Urate, the anionic component of uric acid, predominates at physiological pH. As an apparent consequence of mutations in the *urate oxidase* (*UOx*) gene during primate evolution, urate constitutes the enzymatic end product of purine metabolism in humans (1). There remains controversy over how the loss of UOx activity and the resultant high urate concentrations in hominoids may have been beneficial and whether it still is. On one hand, urate is considered a pathogenic factor in gout, urolithiasis, and nephropathy, and hyperuricemia is associated with other medical conditions, such as hypertension, cardiovascular disease, and metabolic syndrome (2). On the other hand, the loss of UOx activity through multiple independent mutations in hominoids presumably conferred evolutionary advantages. Urate possesses potent antioxidant properties. High urate levels may have provided an antioxidant defense against aging and cancer, thereby contributing to a prolonged hominoid life span (3). In addition, increased urate may mediate blood pressure homeostasis in low-salt environments. Furthermore, higher urate has been suggested to enhance human intelligence or motivational behaviors or promote neuronal integrity and function (4).

Recently a series of population and clinical epidemiology studies have lent support to a potential neuroprotective effect of urate (5, 6). These studies demonstrated a robust inverse link between urate levels and both the risk and clinical progression of Parkinson's disease (PD), one of the most common neurodegenerative diseases. Given the putative role of oxidative stress in the pathogenesis of PD (7), these studies have identified urate as not only a unique biomarker for PD risk and progression but also a potential new target for treatment of PD (5, 6). A clinical trial of a urate precursor in PD has been launched as part of an effort to explore urate elevation as a possible disease-modifying strategy for PD (8).

To better understand the biological basis for a role of urate in PD and better gauge the therapeutic potential of urate in the treatment of neurodegenerative disease, we investigated the effects of urate manipulation in a well-established mouse 6-hydroxydopamine (6-OHDA) model of PD. Urate concentrations were altered by modifying the *UOx* gene, which in rodents encodes a functional enzyme catalyzing the degradation of urate to allantoin. Comprehensive pathological, neurochemical, and behavioral outcome measures were evaluated to determine nigrostriatal dopaminergic pathway deficits after unilateral intrastriatal 6-OHDA infusion in *UOx* KO and transgenic (Tg) mice, in which respective elevations and reductions were achieved in brain concentrations of urate.

Results

Altered Urate but Not Its Precursors in *UOx* KO and Tg Mouse Brain. Western blotting was performed to confirm deletion and overexpression of UOx in peripheral tissues and brain of adult mice from *UOx* KO and Tg lines. As expected, there was no detectable UOx in liver, heart, or brain in *UOx* KO mice. In contrast, UOx was expressed in all organs examined in *UOx* Tg mice. Littermate WT animals did not have detectable UOx in brain and heart, consistent with a previous report that UOx is a liver-specific enzyme (Fig. 1*A*) (9).

Urate and its purine precursors—adenosine, inosine, hypoxanthine, and xanthine—in serum and brain tissue (striatum) were quantified by HPLC coupled with UV and electrochemical detection. In *UOx* KO mice, serum urate reached 5.2 mg/dL, more than 10-fold greater than in their WT littermates ($P < 0.01$, *t* test) (Fig. 1*B*). Despite the absence of UOx in the brain of naïve mice and presumably minimal local central nervous system (CNS) effects of *UOx* disruption, the increase of urate in the periphery was accompanied by a significant increase in urate in brain. Striatal urate in *UOx* KO animals was four times higher than in WT littermate controls ($P < 0.01$, *t* test) (Fig. 1*C*). Disruption of *UOx* did not result in changes in purine precursors of urate in brain. Similarly, striatal levels of the urate metabolite allantoin in *UOx* KO mice, which was quantified by LC-MS, was not different from WT mice, in agreement with undetectable UOx activity in WT brain (9) and therefore minimal local enzymatic contribution to CNS levels of allantoin (Fig. 1*D*).

In *UOx* Tg animals, HPLC analysis revealed a more than fivefold reduction in serum urate when compared with WT non-Tg littermates ($P < 0.01$, *t* test) (Fig. 1*E*). Striatal urate was also significantly lower in the Tg mice ($P < 0.05$, *t* test) but to a lesser extent than in serum despite broad expression of UOx transgene driven by a β-actin promoter (10) (Fig. 1*F*). The similar gradient and yet tight correlation in urate concentrations between blood and brain in both *UOx* KO and Tg mice may reflect a role of blood–brain barrier in regulating brain concentrations of urate (6). No significant differences in adenosine, inosine, hypoxanthine, or xanthine were observed between *UOx* Tg mice and their WT non-Tg littermates. However, striatal allantoin was elevated in *UOx* Tg mice, consistent with locally increased UOx activity in these mice (Fig. 1*G*).

Author contributions: X.C. and M.A.S. designed research; X.C., T.C.B., C.A.D., R.L., S.C., and Y.X. performed research; X.C. analyzed data; and X.C. and M.A.S. wrote the paper.

The authors declare no conflict of interest.

This article is a PNAS Direct Submission.

[1]To whom correspondence should be addressed. E-mail: xchen17@partners.org.

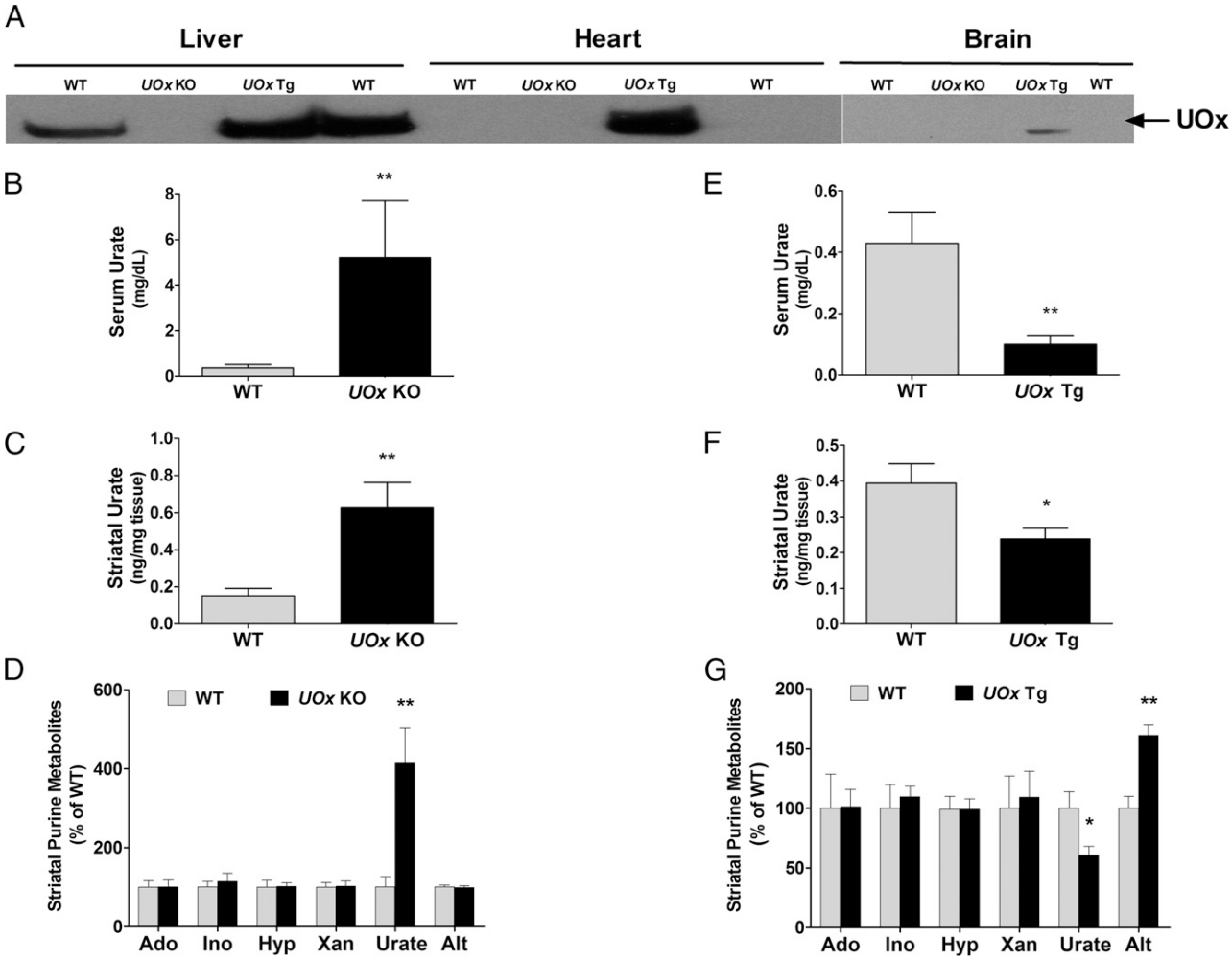

Fig. 1. Altered urate in serum and brain in *UOx* KO and Tg mice. (*A*) Western blot of UOx showing the absence of UOx in liver, heart, and brain in a *UOx* KO mouse (10 mo old). UOx is expressed in liver, heart, and brain in a *UOx* Tg mouse (12 mo old), and it is not detectable in heart and brain in WT mice. HPLC analysis indicates elevated urate levels in blood (*B*) and brain (*C*) in *UOx* KO mice. (*D*) Changes in urate levels are not accompanied by changes in concentrations of urate precursors adenosine (Ado), inosine (Ino), hypoxanthine (Hyp), xanthine (Xan), or urate metabolite allantoin (Alt) in brain in *UOx* KO mice. Conversely, *UOx* Tg mice have lower urate levels in blood (*E*) and brain (*F*). Overexpression of *UOx* also leads to an increase in striatal Alt in the Tg mice (*G*). There are no significant differences in striatal Ado, Ino, Hyp, or Xan between *UOx* Tg mice and the non-Tg WT littermate controls (*G*). Data are expressed as mean ± SEM. $n = 6$, WT and *UOx* KO (8–10 mo old); $n = 9$, WT and *UOx* Tg (4–5 mo old). $^{*}P < 0.05$ vs. WT; $^{**}P < 0.01$ vs. WT.

Impaired Renal Function in UOx KO Mice but Not *UOx* Tg Mice. Given that altered urate levels are often associated with renal dysfunction and that urate nephropathy has been reported in *UOx* KO mice (11), we monitored kidney and body weights and urea levels, an indicator of kidney function, in both the KO and Tg mice. As shown in Fig. 2*A*, adult (4 mo old) *UOx* KO had 30% lower kidney to body weight ratio, compared with WT littermates ($P < 0.01$, *t* test). Body weight in *UOx* KO mice was slightly lower but not statistically different from that in WT littermates during the entire experimental course. Brain urea levels in the KO animals were more than twice as high as in WT littermates ($P < 0.01$, *t* test) (Fig. 2*B*). *UOx* Tg mice had normal gross renal morphology, as well as kidney to body weight ratio, compared with WT littermates (Fig. 2*C*). Brain urea was not changed in these mice (Fig. 2*D*).

***UOx* Disruption or Overexpression Changes Levels of Protein Carbonyls.** Urate is known to have antioxidant properties; altered urate levels resulting from *UOx* gene manipulation may therefore change susceptibility to oxidative stress. To evaluate oxidative stress status, levels of protein carbonyls, a general marker of oxidative damage, were assessed by Western blotting of immunoreactivity to derivitized protein carbonyl groups (Oxyblot) with tissues from adult *UOx* KO and Tg mice. Band densities were normalized with Ponceau staining of the blots. The results did not demonstrate decreased levels of protein carbonyls, as one might expect, but instead a trend toward increased levels of protein carbonyls in liver of the KO animals (Fig. 3*A*) and significantly higher levels in brain ($P < 0.01$, *t* test) (Fig. 3*B*) compared with those in WT littermates. Overexpression of *UOx* also increased protein carbonyl content in both liver and brain, as shown in Fig. 3 *C* and *D*; relative band densities in liver and brain tissues from *UOx* Tg mice were higher than in WT non-Tg littermates ($P < 0.05$, both liver and brain, *t* test).

***UOx* KO Mice Are Resistant to 6-OHDA Neurotoxicity.** To evaluate the effects of *UOx* disruption and urate elevation in a standard mouse model of PD, young adult *UOx* KO mice (average age, 3 mo) and their WT littermates received unilateral intrastriatal infusion of 6-OHDA, a dopaminergic toxin. Spontaneous and amphetamine-induced rotational behaviors were recorded 3 and 4 wk after lesioning, as behavioral indices of ipsilateral dopaminergic deficit. Animals were killed at 5 wk after lesion (Fig. 4*A*). *UOx* KO mice showed markedly reduced spontaneous net ipsilateral rotations ($P < 0.05$, *t* test) and a trend toward reduced amphetamine-induced rotations ipsilateral to the lesion (Fig. 4*B*). Neurochemical

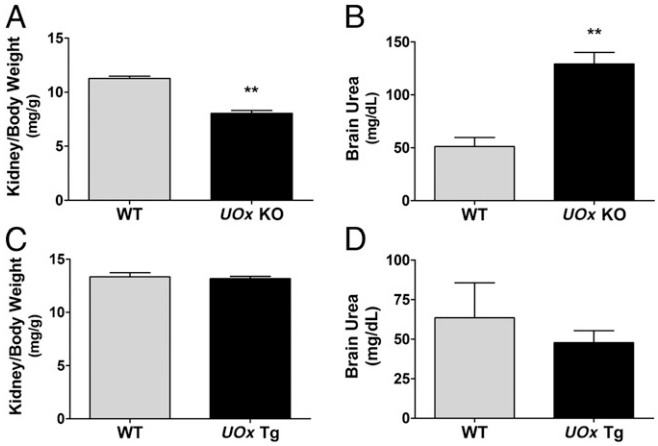

Fig. 2. Kidney to body weight ratios and urea levels in *UOx* KO and Tg mice. (*A*) *UOx* KO have significantly lower kidney to body weight ratio than WT mice (both kidneys from each animal; 4 mo old; $n = 11$ and 8 WT and *UOx* KO, respectively). (*B*) HPLC demonstrates a marked increase in brain urea level in *UOx* KO mice (3–4 mo old; $n = 5$, both WT and *UOx* KO). (*C*) Kidney to body weight ratio in UOx Tg mice (both kidneys from each animal. 6 mo old; $n = 11$ and 14 for WT and *UOx* Tg, respectively). (*D*) Brain urea is not changed in *UOx* Tg mice (4–5 mo old; $n = 5$, WT and *UOx* Tg). Data are expressed as mean ± SEM. $^{**}P < 0.01$ vs. WT.

analysis demonstrated significantly higher levels of residual dopamine (DA) ($P < 0.05$, Tukey's post hoc test) and its metabolite homovanillic acid (HVA) on the lesion side of *UOx* KO animals compared with their WT littermate controls ($P < 0.01$, Tukey's post hoc test) (Fig. 4*C*). Increased striatal levels of urate were confirmed in the KO animals compared with WT controls ($P < 0.01$, Tukey's post hoc test), in which the intrastriatal 6-OHDA infusion produced a long-lasting local increase in urate content compared with that of the unlesioned striatum (Fig. 4*D*). This 6-OHDA–induced increase in urate may reflect persistent changes in oxidative stress status or energy metabolism after 6-OHDA. 1-methyl-4-phenyl-1,2,3,6-tetrahydropyridine (MPTP), another commonly used parkinsonian toxin, has also been reported to increase striatal urate in mice (12). A representative set of sections stained for tyrosine hydroxylase (TH), a marker for dopaminergic neurons, showed few remaining TH-positive neurons in the substantia nigra (SN) on the lesion side in a WT mouse and preservation of TH positive neurons in a *UOx* KO mouse (Fig. 4*E*). Finally, stereological quantification of TH-positive nigral neurons indicated 46% survival of TH-positive neurons on the lesioned vs. unlesioned side in KO mice, a twofold increase over the percentage of surviving neurons in WT littermates (Fig. 4*F*) ($P < 0.05$, Tukey's post hoc test).

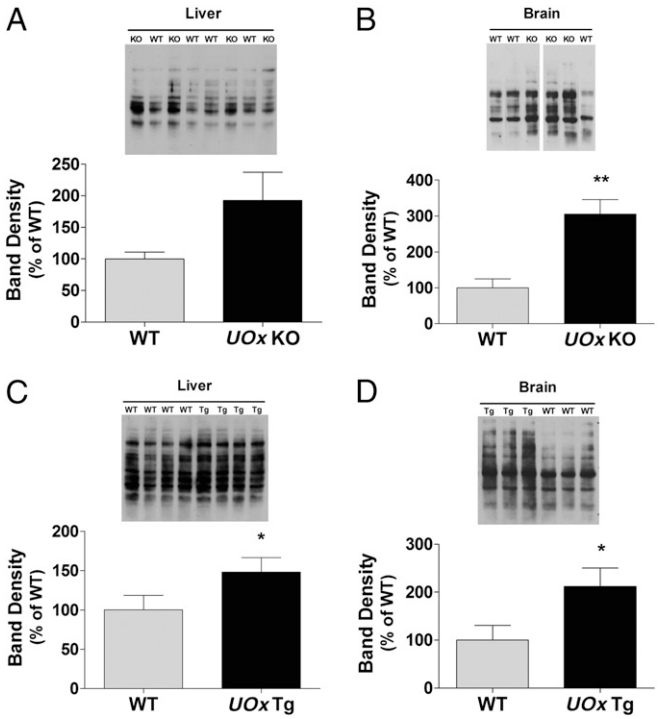

Fig. 3. *UOx* disruption or overexpression changes levels of protein carbonyls in mice. Protein carbonyls were assessed by Oxyblot. Band density was normalized with Ponceau staining of the proteins. (*A*) A trend toward increased levels of protein carbonyls in liver in *UOx* KO animals. (*B*) Protein carbonyls are higher in brain in *UOx* KO mice. Overexpression of *UOx* leads to increased protein carbonyl content in both liver (*C*) and brain (*D*) in Tg mice. Data are expressed as mean ± SEM $n = 6$, WT and *UOx* KO (3–4 mo old); $n = 5$, WT and *UOx* Tg (4–5 mo old). $^{*}P < 0.05$; $^{**}P < 0.01$ vs. WT.

***UOx* Tg Mice Are Susceptible to 6-OHDA Neurotoxicity.** The asymmetric turning behavior reflecting the extent of ipsilateral dopaminergic deficits was significantly exacerbated in *UOx* Tg mice at 3 and 4 wk after 6-OHDA infusion for both spontaneous ($P < 0.01$, *t* test) and amphetamine-induced ($P < 0.05$, *t* test) rotations in *UOx* Tg mice (average age, 5 mo) compared with WT non-Tg littermates (Fig. 5*A*). Consistent with the neurochemical phenotype of *UOx* Tg mice shown in Fig. 1*F*, their unlesioned striata had a significantly lower urate content than in WT non-Tg littermates. 6-OHDA lesioning induced an increase in local urate in WT mice, and even in the presence of excess UOx, in their Tg counterparts (Fig. 5*B*). DA and its metabolite 3,4-dihydroxyphenylacetic acid (DOPAC) in the striatum decreased by ~70% after 6-OHDA in WT non-Tg mice. In *UOx* Tg mice, DA content on the lesion side was further reduced to 13% of that of the nonlesion control side, a significant difference from WT littermates. DOPAC in the Tg mice was reduced to 20% of control nonlesion side, significantly lower than in WT mice ($P < 0.05$, DA and DOPAC, Tukey's post hoc test) (Fig. 5*C*). Quantitative stereological analysis demonstrated a significant decrease in the number of residual TH-positive nigral neurons on the lesion side in *UOx* Tg mice, compared with WT non-Tg littermates ($P < 0.01$, Tukey's post hoc test) (Fig. 5*D*). The difference was still significant statistically when expressed as percentage of control (CON) to normalize for the small difference on the control (unlesioned) side between the two groups of animals ($P < 0.01$, Tukey's post hoc test). The subtle reduction in TH-positive neurons but not in DA content in *UOx* Tg remains to be further characterized. Representative sections of the ventral mesencephalon stained for TH depicted the extensive disruption of dopaminergic neurons in the SN in a *UOx* Tg mouse at 5 wk after intrastriatal 6-OHDA (Fig. 5*E*).

Discussion

In contrast to the established and hypothesized deleterious effects of urate on human health, its putative protective effects against disease have taken on particular relevance for CNS function and disorders. Among neurodegenerative diseases, PD has been most closely linked to low urate by convergent epidemiological and clinical findings (5, 6). In pursuing their translation toward therapeutics it is important to understand whether and how urate may have disease-modifying effects in preclinical models of PD. By using complementary genetic approaches disrupting and overexpressing *UOx*, we have demonstrated that disruption of the *UOx* gene with a resultant rise in urate protects the nigrostriatal dopaminergic system, and conversely that transgenic overexpressson of *UOx* with a resultant fall in urate exacerbates dopaminergic neurodegeneration and resultant neurochemical and behavioral deficits in a 6-OHDA mouse model of PD.

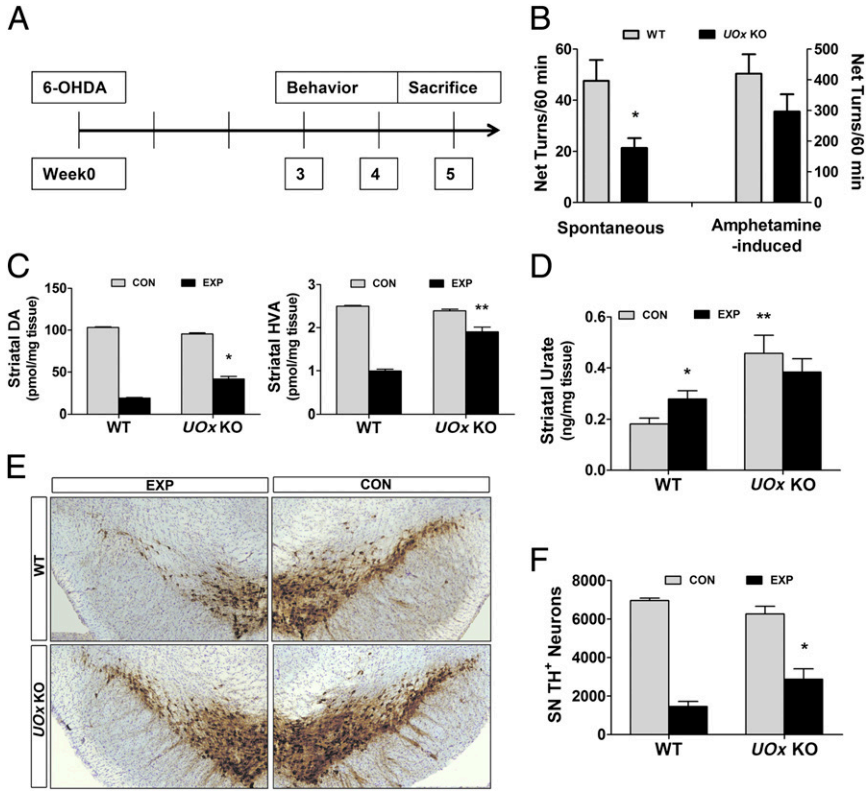

Fig. 4. *UOx* KO mice are more resistant to 6-OHDA neurotoxicity. (*A*) 6-OHDA (15 μg) was infused into the left striatum of *UOx* KO mice (average age, 3 mo). Spontaneous and 5 mg/kg amphetamine-induced rotational behavior were recorded at 3 and 4 wk after the lesion. Animals were killed at 5 wk after 6-OHDA lesion. (*B*) Spontaneous net ipsilateral rotations in *UOx* KO mice are attenuated (*$P < 0.05$ vs. WT), with a similar trend for attenuated amphetamine-induced net ipsilateral turns (WT $n = 11$; *UOx* KO $n = 9$). (*C*) *UOx* KO animals have significantly higher levels of DA and HVA on the experimental (lesion) side compared with their WT littermates (WT $n = 11$; *UOx* KO $n = 8$). *$P < 0.05$; **$P < 0.01$ vs. WT experimental side. (*D*) HPLC-electrochemical detection (ECD) confirms an increased level of urate in the *UOx* KO group. Injection of 6-OHDA induces an increase in urate in WT mice ($n = 11$ and 9 WT and *UOx* KO, respectively). *$P < 0.05$; **$P < 0.01$ vs. WT control side. (*E*) Preservation of SN dopaminergic neurons (TH positive) on the lesion side in a *UOx* KO mouse and disruption of SN TH neurons in a WT mouse. (*F*) Stereological quantification of TH neurons in the SN demonstrates more surviving dopaminergic neurons in the KO mice ($n = 8$ both WT and *UOx* KO groups). *$P < 0.05$ vs. WT experimental side. Data are expressed as mean ± SEM. CON, control nonlesion side; EXP, experimental lesion side.

Neuroprotective effects of urate have been reported in various in vitro and in vivo experimental models of neurological disorders, including ischemic brain injury (13, 14), multiple sclerosis (15), and spinal cord injury (16, 17). However, evidence regarding urate in PD models is sparse and largely restricted to cellular models of the disease. Urate blocked DA-induced apoptotic cell death, and it protected against 6-OHDA toxicity in PC12 cells (18, 19). In dopaminergic neurons, it reduced mitochondrial dysfunction and cell death occurring spontaneously in culture or induced by pesticides rotenone or iron ions (20, 21). We report here that *UOx* KO mice are more resistant to 6-OHDA neurotoxicity. *UOx* disruption with elevated urate levels can prevent DA loss, promote long-term survival of dopaminergic neurons, and preserve functional performances after 6-OHDA lesion.

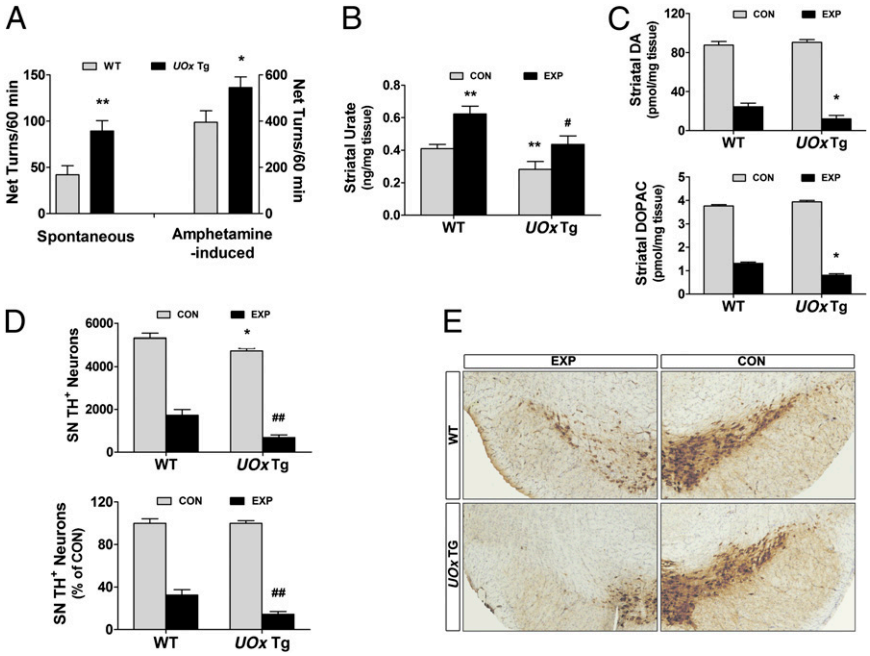

Fig. 5. *UOx* Tg mice are more susceptible to 6-OHDA neurotoxicity. *UOx* Tg mice (average age, 5 mo) received intrastriatal 6-OHDA infusion. Behavioral tests were performed and animals killed at time points indicated in Fig. 4*A*. (*A*) Marked increases in both spontaneous and amphetamine-induced net ipsilateral rotations in *UOx* Tg mice after 6-OHDA infusion compared with WT non-Tg mice ($n = 11$ WT; $n = 14$ *UOx* Tg). *$P < 0.05$; **$P < 0.01$ vs. WT. (*B*) *UOx* Tg mice had lower urate levels in the striatum, and 6-OHDA induces local increases in urate in both WT and Tg mice ($n = 11$ and 14 WT and *UOx* Tg, respectively). **$P < 0.01$ vs. WT nonlesion control side; $^{\#}P < 0.05$ vs. WT experimental side, and vs. *UOx* Tg control side. (*C*) Significant further reductions in DA and DOPAC on experimental side in *UOx* Tg animals after 6-OHDA lesion ($n = 11$ and 14 WT and *UOx* Tg, respectively). *$P < 0.05$ vs. WT experimental side. (*D*) A significant decrease in the number of nigral TH-positive neurons on the experimental side in *UOx* Tg mice, compared with WT littermates. The difference is still significant statistically when expressing as percentage of CON to normalize for the difference on control side between the two genotypes ($n = 6$ and 7 WT and *UOx* Tg, respectively). *$P < 0.05$ vs. WT nonlesion control side; $^{\#\#}P < 0.01$ vs. WT experimental side. (*E*) Few remaining TH-positive neurons in the SN in a *UOx* Tg mouse after intrastriatal 6-OHDA. Data are expressed as mean ± SEM. CON, control nonlesion side; EXP, experimental lesion side.

Conversely, Tg mice overexpressing *UOx* demonstrate enhanced susceptibility to 6-OHDA neurotoxicity. Lower urate levels have been associated with higher risk of PD, as well as more rapid clinical progression of PD (5, 6) and possibly other neurodegenerative diseases (22, 23). Similarly, lower urate levels have been consistently reported in PD patients compared with control subjects (24, 25). However, no experimental evidence has directly linked hypouricemia to neurodegeneration in vivo. Overexpression of *UOx* in mice leads to significant reduction in urate both in blood and in brain. The exacerbated neurotoxicity of 6-OHDA on the nigrostriatal dopaminergic pathway in *UOx* Tg mice entails greater DA depletion, more extensive neuron loss, and exacerbated asymmetry of movement. These findings in vivo are consistent with our recent report that this *UOx* transgene exacerbates dopaminergic neuron degeneration in a cellular model of PD (26).

Our findings thus provide a demonstration that genetic modulation of *UOx* modifies brain concentrations of urate and neurodegeneration in an established model of PD, supporting a contention that the known neuroprotective effects of urate itself may account for the complementary phenotypes of these opposing genetic manipulations in the 6-OHDA model of PD. However, altering *UOx* may have had other effects, particularly on purine metabolism, that could provide alternative explanations for the observed phenotypes. Blocking or accelerating purine catabolism at the level of UOx might also be expected to alter steady-state levels of its product allantoin as well as the multiple precursors of urate, including adenosine and inosine, which are themselves capable of modifying neuronal viability (27, 28). However, we have found that brain concentrations of major purine precursors upstream of urate from adenosine to xanthine are unaltered in *UOx* KO and Tg mice, arguing strongly against a proximal metabolic alteration as the basis of their phenotypes. Similarly, in *UOx* KO mice levels of brain allantoin were unaltered, confirming the absence of functional endogenous UOx in WT brain and supporting the hypothesis that the increased brain concentration of urate in *UOx* KO mice is the basis of their neuroprotective phenotype. By contrast, in *UOx* Tg mice allantoin was significantly increased in brain, raising the possibility of an alternative explanation for their exacerbated neurotoxicity other than the commensurate reduction in brain urate. However, the possibility that elevated allantoin mediates the *UOx* Tg phenotype presumes that allantoin can act as a neurotoxicant. However, the only available data of relevance indicate that allantoin actually displays neuroprotective properties in a 6-OHDA model of PD (29). Collectively, these data suggest that alterations in urate, rather the those in allantoin or another purine metabolite, are the basis for the observed *UOx* KO and Tg phenotypes.

Urate is a potent antioxidant, and antioxidant properties of urate have been proposed to mediate its neuroprotective effects in most aforementioned studies (13–21). We investigated oxidative stress status in *UOx* KO and Tg mice and found higher protein carbonyls, one of the most commonly used markers of oxidative stress, in both. Although an increase in basal levels of oxidative protein modification in *UOx* Tg animals is consistent with their lower levels of antioxidant urate, the converse hypothesis of lower levels of protein carbonyls in *UOx* KO mice is not supported. It is uncertain why protein carbonyls changed in the same direction despite urate level modulation in opposite directions. However, we are not the first to observe dissociation between urate and oxidative stress indices, protein carbonyl levels in particular. Clinical studies have revealed higher or unchanged protein carbonyls in patients with high urate, including refractory gout patients (30–32). Furthermore, urate has the capacity to act as a prooxidant under some circumstances (33–35).

In addition to this possible dual role of urate, it is particularly noteworthy that *UOx* KO mice develop nephropathy early in their lives despite pre- and perinatal allopurinol treatment. The severe kidney damage we and the others have documented (11, 36) in *UOx* KO mice may have confounded the testing of our hypothesis that elevated urate could confer antioxidant protection under basal conditions. Excessive oxidative stress has been linked to various renal pathologies (37), and urea, specifically, has been shown both in vitro and in vivo to induce reactive oxidative species (38). It is possible that an offsetting systemic effect of chronic nephropathy may predominate in determining the basal levels of oxidative stress in *UOx* KO mice. Therefore, despite the known oxidative mechanisms of 6-OHDA neurotoxicity (39) and antioxidant properties of urate, the basis for attenuated and exacerbated neurodegeneration in *UOx* KO and Tg mice, respectively, remains to be established.

Our complementary genetic approaches targeting *UOx* effectively manipulated urate in mice both peripherally and, perhaps more importantly in this study, in their brains. The findings that *UOx* KO (with higher urate) are more resistant to local 6-OHDA lesioning and that *UOx* Tg (with lower urate) are more susceptible to this neurotoxin support the possibility of a neuroprotective role for urate and PD. Together with previous epidemiological and clinical evidence (5, 6), these findings strengthen the rationale for investigating urate-elevating agents as potential therapeutic approaches to PD and possibly other neurodegenerative diseases. As proof-of-concept, our genetic study together with newly published pharmacological data (40) provides critical experimental evidence in vivo that urate may have beneficial CNS actions in the context of PD, and it provides a basis and justification for further mechanistic investigation. Nevertheless, further efforts to investigate the therapeutic potential of urate elevation—even within what is considered a "normal range"—must be tempered by known and potential risks of excessive urate.

Methods

Experimental Animals. *UOx* KO mice, originally constructed by Wu et al. (11) by homologous recombination disrupting exon 3 of the *UOx* gene, were obtained from the Jackson Laboratory. Our initial characterization indicated that whereas homozygous mice demonstrated significantly elevated urate in both serum and brain (Fig. 1), heterozygous *UOx* KO animals did not have a urate elevation phenotype (11). We therefore used only homozygous mice (generated by heterozygote × heterozygote crosses) for this study. Allopurinol (150 mg/L) was provided in the drinking water of breeders and pups until weaning for rescue from perinatal lethality of hyperuricemia (11). *UOx* Tg mice were obtained from Kenneth L. Rock, Department of Immunology, University of Massachusetts, Worcester, MA. *UOx* transgene expression is driven by a strong constitutive (β-actin) promoter (10). Hemizygous *UOx* Tg mice were used. Both *UOx* KO and Tg mice had been back-crossed to C57BL/6 (Jackson Laboratory) for at least eight generations. *UOx* KO, *UOx* Tg mice and their littermate controls were maintained in home cages at constant temperature with a 12-h light/dark cycle and free access to food and water. All animal protocols were approved by the Massachusetts General Hospital Animal Care and Use Committee.

Measurement of Urate and Urate Precursors. Animals were killed at indicated times via cervical dislocation. Whole blood was collected, and striatal tissues were dissected. Samples were prepared, and adenosine, inosine, hypoxanthine, xanthine, and urate concentrations were determined simultaneously using an HPLC method that we developed and recently reported (41).

Measurement of Allantoin. The urate metabolite allantoin was determined by Bioanalytical Systems. Animals were killed via cervical dislocation. Fresh frozen striatal tissues were weighed and homogenized in water. A volume of 100 μL was taken for extraction. Calibrator, quality control standard, and sample homogenates were extracted with acetonitrile in a 96-well plate after adding isotope-labeled allantoin as internal standard. LC-MS was used for detection.

Western Blot. For Western blot analysis of UOx, liver, heart, or brain tissues were obtained. Proteins were extracted and electrophoresed. After transferring, the membrane was treated with rabbit anti-UOx antibody (Santa Cruz Biotechnology, catalog no. SC33830) at 1:200, followed by secondary antibody (Thermo Scientific, catalog no. 32460). Densitometric analysis of band intensity was performed by using the Image J system (National Institutes of Health).

Protein Carbonylation. Protein carbonlys in liver and brain were detected using the Oxyblot Protein Oxidation Detection Kit (Millipore, catalog no. S7150) according to the manufacturer's instructions. Densitometric analysis of band intensity was performed by using the Image J system.

6-OHDA Lesion. Mice received a unilateral intrastriatal injection of 6-OHDA (42). Animals were pretreated with desipramine (Sigma-Aldrich). A total dose of 15 μg 6-OHDA was infused into the left striatum at the following coordinates: anterior–posterior (AP), +0.09 cm; medial–lateral (ML), +0.22 cm; dorsal-ventral (DV), −0.25 cm relative to bregma.

Rotational Behavior Assessment. Spontaneous and 5 mg/kg amphetamine-induced rotational behavior in mice was tested at 3–4 wk after the 6-OHDA lesion using an automated rotometry system (San Diego Instruments) as previously described (42). Results were expressed as ipsilateral net turns (net difference between ipsilateral and contralateral turns) per 60 min.

Measurement of DA and Metabolite. Five weeks after 6-OHDA lesion, mice were killed by rapid cervical dislocation, and their striata were dissected. DA and metabolites DOPAC and HVA were determined by standard HPLC with electrochemical detection, as previously described (42).

TH Immunohistochemistry and Stereological Cell Counting. Immunostaining for TH was performed as described previously (43). Five weeks after 6-OHDA lesioning mice were killed by rapid cervical dislocation. The hinder brain block containing midbrain was immediately fixed and cryoprotected. Every fourth section from a complete set of coronal midbrain sections was processed. The primary antibody was mouse monoclonal anti-TH (Sigma-Aldrich, catalog no. T1299) at 1:800. Stereologic analysis was performed with the investigator blinded to genotypes using the Bioquant Image Analysis System (R&M Biometrics) (43). For each animal, the SN on both sides of the brain was analyzed. For each section, the entire SN was identified and outlined as the region of interest. The number of TH-positive neurons in each counting frame (50 μm × 50 μm) was then determined under 40× objective by focusing down through the section using the optical dissector method. Our criterion for counting an individual TH-positive neuron was the presence of its nucleus either within the counting frame or touching the right or top frame lines (green), but not touching the left or bottom lines (red). The total number of TH-positive neurons for each side of the SN was calculated: total number = raw counts × 4 (every fourth section) × 6.25 (area of grid 125 μm × 125 μm/ area of counting frame 50 μm × 50 μm).

Statistic Analysis. All values are expressed as mean ± SEM. The difference between two groups was analyzed by Student *t* test. Multiple comparisons among groups were performed by one-way ANOVA and Tukey's post hoc test. All statistical analyses were performed using SigmaStat software (SPSS). $P < 0.05$ is considered statistically significant.

ACKNOWLEDGMENTS. The authors thank Kenneth L. Rock and Hajime Kono for generously providing *UOx* Tg mice and for advice on their use; and Alberto Serrano-Pozo for his assistance in stereological cell counting. This work is supported by the RJG Foundation, Michael J. Fox Foundation, American Federation for Aging Research Beeson Collaborative Program, and by National Institutes of Health Grants R21NS058324, K24NS060991, and DoD W81XWH-11-1-0150.

1. Wu XW, Lee CC, Muzny DM, Caskey CT (1989) Urate oxidase: primary structure and evolutionary implications. *Proc Natl Acad Sci USA* 86(23):9412–9416.
2. Johnson RJ, Lanaspa MA, Gaucher EA (2011) Uric acid: A danger signal from the RNA world that may have a role in the epidemic of obesity, metabolic syndrome, and cardiorenal disease: Evolutionary considerations. *Semin Nephrol* 31(5):394–399.
3. Ames BN, Cathcart R, Schwiers E, Hochstein P (1981) Uric acid provides an antioxidant defense in humans against oxidant- and radical-caused aging and cancer: A hypothesis. *Proc Natl Acad Sci USA* 78(11):6858–6862.
4. Álvarez-Lario B, Macarrón-Vicente J (2010) Uric acid and evolution. *Rheumatology (Oxford)* 49(11):2010–2015.
5. Constantinescu R, Zetterberg H (2011) Urate as a marker of development and progression in Parkinson's disease. *Drugs Today (Barc)* 47(5):369–380.
6. Chen X, Wu G, Schwarzschild MA (2012) Urate in Parkinson's disease: More than a biomarker? *Curr Neurol Neurosci Rep* 12(4):367–375.
7. Schapira AH, Tolosa E (2010) Molecular and clinical prodrome of Parkinson disease: Implications for treatment. *Nat Rev Neurol* 6(6):309–317.
8. ClinicalTrials.gov. Safety of Urate Elevation in Parkinson's Disease (SURE-PD). Available at http://clinicaltrials.gov/ct2/show/NCT00833690. Accessed December 2, 2012.
9. Usuda N, Reddy MK, Hashimoto T, Rao MS, Reddy JK (1988) Tissue specificity and species differences in the distribution of urate oxidase in peroxisomes. *Lab Invest* 58 (1):100–111.
10. Kono H, Chen CJ, Ontiveros F, Rock KL (2010) Uric acid promotes an acute inflammatory response to sterile cell death in mice. *J Clin Invest* 120(6):1939–1949.
11. Wu X, et al. (1994) Hyperuricemia and urate nephropathy in urate oxidase-deficient mice. *Proc Natl Acad Sci USA* 91(2):742–746.
12. Serra PA, et al. (2002) The neurotoxin 1-methyl-4-phenyl-1,2,3,6-tetrahydropyridine induces apoptosis in mouse nigrostriatal glia. Relevance to nigral neuronal death and striatal neurochemical changes. *J Biol Chem* 277(37):34451–34461.
13. Yu ZF, Bruce-Keller AJ, Goodman Y, Mattson MP (1998) Uric acid protects neurons against excitotoxic and metabolic insults in cell culture, and against focal ischemic brain injury in vivo. *J Neurosci Res* 53(5):613–625.
14. Romanos E, Planas AM, Amaro S, Chamorro A (2007) Uric acid reduces brain damage and improves the benefits of rt-PA in a rat model of thromboembolic stroke. *J Cereb Blood Flow Metab* 27(1):14–20.
15. Koprowski H, Spitsin SV, Hooper DC (2001) Prospects for the treatment of multiple sclerosis by raising serum levels of uric acid, a scavenger of peroxynitrite. *Ann Neurol* 49(1):139.
16. Du Y, Chen CP, Tseng CY, Eisenberg Y, Firestein BL (2007) Astroglia-mediated effects of uric acid to protect spinal cord neurons from glutamate toxicity. *Glia* 55(5): 463–472.
17. Scott GS, Cuzzocrea S, Genovese T, Koprowski H, Hooper DC (2005) Uric acid protects against secondary damage after spinal cord injury. *Proc Natl Acad Sci USA* 102(9): 3483–3488.
18. Zhu TG, et al. (2012) Protective effects of urate against 6-OHDA-induced cell injury in PC12 cells through antioxidant action. *Neurosci Lett* 506(2):175–179.
19. Jones DC, Gunasekar PG, Borowitz JL, Isom GE (2009) Dopamine induced apoptosis is mediated by oxidative stess and is enhanced by cyanide in differentiated PC12 cells. *J Neurochem* 74:2296–2304.
20. Guerreiro S, et al. (2009) Protection of midbrain dopaminergic neurons by the end-product of purine metabolism uric acid: Potentiation by low-level depolarization. *J Neurochem* 109(4):1118–1128.
21. Duan W, et al. (2002) Dietary folate deficiency and elevated homocysteine levels endanger dopaminergic neurons in models of Parkinson's disease. *J Neurochem* 80(1): 101–110.
22. Irizarry MC, et al. (2009) Plasma urate and progression of mild cognitive impairment. *Neurodegener Dis* 6(1-2):23–28.
23. Auinger P, Kieburtz K, McDermott MP (2010) The relationship between uric acid levels and Huntington's disease progression. *Mov Disord* 25(2):224–228.
24. Church WH, Ward VL (1994) Uric acid is reduced in the substantia nigra in Parkinson's disease: effect on dopamine oxidation. *Brain Res Bull* 33(4):419–425.
25. Bogdanov M, et al. (2008) Metabolomic profiling to develop blood biomarkers for Parkinson's disease. *Brain* 131(Pt 2):389–396.
26. Cipriani S, et al. (2012) Urate and its transgenic depletion modulate neuronal vulnerability in a cellular model of Parkinson's disease. *PLoS ONE* 7(5):e37331.
27. Schwarzschild MA, Agnati L, Fuxe K, Chen JF, Morelli M (2006) Targeting adenosine A2A receptors in Parkinson's disease. *Trends Neurosci* 29(11):647–654.
28. Burnstock G (2008) Purinergic signalling and disorders of the central nervous system. *Nat Rev Drug Discov* 7(7):575–590.
29. Terpstra B. Purine nucleoside mediated neuroprotection in the 6-hydroxydopamine rodent model of Parkinson's disease. Available at http://etd.ohiolink.edu/view.cgi?acc_num=ucin1298395215. Accessed December 2, 2012.
30. Hershfield MS, et al. (2010) Treating gout with pegloticase, a PEGylated urate oxidase, provides insight into the importance of uric acid as an antioxidant in vivo. *Proc Natl Acad Sci USA* 107(32):14351–14356.
31. Sinha S, Singh SN, Ray US (2009) Total antioxidant status at high altitude in lowlanders and native highlanders: Role of uric acid. *High Alt Med Biol* 10(3):269–274.
32. Tsukimori K, Yoshitomi T, Morokuma S, Fukushima K, Wake N (2008) Serum uric acid levels correlate with plasma hydrogen peroxide and protein carbonyl levels in preeclampsia. *Am J Hypertens* 21(12):1343–1346.
33. Bagnati M, et al. (1999) When and why a water-soluble antioxidant becomes prooxidant during copper-induced low-density lipoprotein oxidation: A study using uric acid. *Biochem J* 340(Pt 1):143–152.
34. Patterson RA, Horsley ET, Leake DS (2003) Prooxidant and antioxidant properties of human serum ultrafiltrates toward LDL: Important role of uric acid. *J Lipid Res* 44(3): 512–521.
35. Santos CX, Anjos EI, Augusto O (1999) Uric acid oxidation by peroxynitrite: Multiple reactions, free radical formation, and amplification of lipid oxidation. *Arch Biochem Biophys* 372(2):285–294.
36. Kelly SJ, et al. (2001) Diabetes insipidus in uricase-deficient mice: A model for evaluating therapy with poly(ethylene glycol)-modified uricase. *J Am Soc Nephrol* 12(5): 1001–1009.
37. Kao MP, Ang DS, Pall A, Struthers AD (2010) Oxidative stress in renal dysfunction: Mechanisms, clinical sequelae and therapeutic options. *J Hum Hypertens* 24(1):1–8.
38. D'Apolito M, et al. (2010) Urea-induced ROS generation causes insulin resistance in mice with chronic renal failure. *J Clin Invest* 120(1):203–213.
39. Jackson-Lewis V, Blesa J, Przedborski S (2012) Animal models of Parkinson's disease. *Parkinsonism Relat Disord* 18(Suppl 1):S183–S185.
40. Gong L, et al. (2012) Neuroprotection by urate on 6-OHDA-lesioned rat model of Parkinson's disease: Linking to Akt/GSK3β signaling pathway. *J Neurochem* 123(5): 876–885.
41. Burdett TC, et al. (2012) Efficient determination of purine metabolites in brain tissue and serum by high-performance liquid chromatography with electrochemical and UV detection. *Biomed Chromatogr*, 10.1002/bmc.2760.
42. Xiao D, et al. (2006) Forebrain adenosine A2A receptors contribute to L-3,4-dihydroxyphenylalanine-induced dyskinesia in hemiparkinsonian mice. *J Neurosci* 26(52): 13548–13555.
43. Kachroo A, et al. (2005) Interactions between metabotropic glutamate 5 and adenosine A2A receptors in normal and parkinsonian mice. *J Neurosci* 25(45):10414–10419.

European Neuropsychopharmacology (▮▮▮▮) ▮, ▮▮▮–▮▮▮

Appendix H

www.elsevier.com/locate/euroneuro

Conditional neural knockout of the adenosine A_{2A} receptor and pharmacological A_{2A} antagonism reduce pilocarpine-induced tremulous jaw movements: Studies with a mouse model of parkinsonian tremor

John D. Salamone[a,*], Lyndsey E. Collins-Praino[a], Marta Pardo[a,b], Samantha J. Podurgiel[a], Younis Baqi[c], Christa E. Müller[c], Michael A. Schwarzschild[d], Mercè Correa[a,b]

[a]*Behavioral Neuroscience Division, Department of Psychology, University of Connecticut, Storrs, CT 06269-1020, USA*
[b]*Department of Psychobiology, University Jaume I, Castelló, Spain*
[c]*Pharma-Zentrum Bonn, Pharmazeutisches Institut, Pharmazeutische Chemie, Universität Bonn, Bonn, Germany*
[d]*Department of Neurology, Massachusetts General Hospital, Boston, MA, USA*

Received 26 November 2011; received in revised form 31 July 2012; accepted 2 August 2012

KEYWORDS
Motor;
Parkinson's disease;
Parkinsonism;
Striatum;
Muscarinic receptor;
Acetylcholine

Abstract
Tremulous jaw movements are rapid vertical deflections of the lower jaw that resemble chewing but are not directed at any particular stimulus. In rats, tremulous jaw movements can be induced by a number of conditions that parallel those seen in human parkinsonism, including dopamine depletion, dopamine antagonism, and cholinomimetic drugs. Moreover, tremulous jaw movements in rats can be attenuated using antiparkinsonian agents such as L-DOPA, dopamine agonists, muscarinic antagonists, and adenosine A_{2A} antagonists. In the present studies, a mouse model of tremulous jaw movements was established to investigate the effects of adenosine A_{2A} antagonism, and a conditional neuronal knockout of adenosine A_{2A} receptors, on cholinomimetic-induced tremulous jaw movements. The muscarinic agonist pilocarpine significantly induced tremulous jaw movements in a dose-dependent manner (0.25–1.0 mg/kg IP). These movements occurred largely in the 3–7.5 Hz local frequency range. Administration of the adenosine A_{2A} antagonist MSX-3 (2.5–10.0 mg/kg IP) significantly attenuated pilocarpine-induced tremulous jaw movements. Furthermore, adenosine A_{2A} receptor knockout mice showed a significant reduction in pilocarpine-induced tremulous jaw movements compared to littermate controls. These results demonstrate the feasibility of using the tremulous jaw movement model in mice, and indicate that adenosine A_{2A} receptor antagonism and deletion are capable of reducing cholinomimetic-induced tremulous jaw movements in mice. Future

*Corresponding author.
E-mail address: john.salamone@uconn.edu (J.D. Salamone).

0924-977X/$ - see front matter © 2012 Published by Elsevier B.V.
http://dx.doi.org/10.1016/j.euroneuro.2012.08.004

Please cite this article as: Salamone, J.D., et al., Conditional neural knockout of the adenosine A_{2A} receptor and pharmacological A_{2A} antagonism reduce pilocarpine-induced tremulous jaw movements: Studies with a mouse model of parkinsonian tremor. European Neuropsychopharmacology (2012), http://dx.doi.org/10.1016/j.euroneuro.2012.08.004

studies should investigate the effects of additional genetic manipulations using the mouse tremulous jaw movement model.
© 2012 Published by Elsevier B.V.

1. Introduction

Resting tremor is a cardinal symptom of Parkinson's disease (Deuschl et al., 2001). Moreover, tremor and other parkinsonian symptoms can be induced by various drugs, including dopamine (DA) antagonists (Bezchlibnyk-Butler and Remington, 1994) and cholinomimetics (Song et al., 2008). Adenosine A_{2A} antagonists have emerged as a potential treatment of parkinsonian symptoms, including tremor (Schwarzschild et al., 2006; LeWitt et al., 2008). Adenosine A_{2A} receptors are highly expressed in neostriatum, and A_{2A} antagonists exert effects in animals that are consistent with antiparkinsonian actions (Ferré et al., 2008; Chen et al., 2001; Simola et al., 2004; Salamone et al., 2008; Collins et al., 2010). Clinical reports have indicated that adenosine A_{2A} antagonists significantly improve motor deficits, reduce OFF time, and increase ON time in parkinsonian patients (LeWitt et al., 2008).

One animal test that is useful for assessing the role of adenosine A_{2A} receptors in motor function is tremulous jaw movements (TJMs), an extensively validated rodent model of parkinsonian resting tremor (Simola et al., 2004; Miwa et al., 2009; Collins et al., 2010, 2011; for reviews, see Salamone et al., 1998; Collins-Praino et al., 2011). TJMs are rapid vertical deflections of the lower jaw that are not directed at any stimulus (Salamone et al., 1998), and occur in phasic bursts of repetitive jaw movement activity. TJMs have many of the neurochemical, anatomical, and pharmacological characteristics of parkinsonism, and meet a reasonable set of validation criteria for use as an animal model of parkinsonian tremor (Salamone et al., 1998; Collins-Praino et al., 2011). These movements are induced by conditions associated with parkinsonism, including neurotoxic or pharmacological depletion of striatal DA (Jicha and Salamone, 1991; Salamone et al., 2008), and DA antagonism (Ishiwari et al., 2005; Salamone et al., 2008). TJMs also are induced by cholinomimetic drugs, including muscarinic agonists such as pilocarpine and oxotremorine (Salamone et al., 1986, 1998; Collins et al., 2010), and anticholinesterases (Salamone et al., 1998; Simola et al., 2004; Collins et al., 2011). TJMs occur largely within the 3–7 Hz frequency range that is characteristic of parkinsonian resting tremor (Ishiwari et al., 2005; Collins et al., 2010), and can be attenuated by several classes of antiparkinsonian drugs, including DA agonists and anticholinergics (Salamone et al., 1998, 2005; Betz et al., 2009). Adenosine A_{2A} antagonists attenuate the TJMs induced by DA depletion, DA antagonism and cholinomimetics (Correa et al., 2004; Simola et al., 2004; Salamone et al., 2008; Betz et al., 2009; Collins et al., 2010, 2011; Pinna et al., 2010).

With the rising importance of genetic manipulations in mice (i.e. transgenic, knockout, knockin, etc.), it is necessary to investigate whether it is possible to extend well-validated behavioral paradigms currently being used in rats to mouse models. Although one previous study showed that muscarinic M4 receptor knockout mice showed significantly fewer cholinomimetic-induced TMMs than wild-type mice (Salamone et al., 2001), every other study of TJM activity has employed rats. Given the putative antiparkinsonian properties of adenosine A_{2A} receptor antagonists, it is of great interest to determine if adenosine A_{2A} receptor antagonism or genetic deletion reduces levels of TJM activity in mice. In order to investigate this research question, several experiments were necessary. The first experiment studied the ability of the muscarinic agonist pilocarpine to induce TJMs in the specific strain of mice being used for the knockout study (C57/BL6). The second experiment studied the local frequency range of the TJM "bursts" induced by pilocarpine using freeze-frame video analysis. Experiments 3 and 4 investigated the effects of the adenosine A_{2A} antagonist MSX-3 and genetic deletion of the adenosine A_{2A} receptor on pilocarpine-induced TJMs. It was hypothesized that A_{2A} knockout mice would show fewer TJMs than their wild-type littermates.

2. Experimental procedures

2.1. Animals

Male C57BL/6 mice (25; Harlan Laboratories, Indianapolis, IN, USA) were used for the first three studies. For the final study, a total of 24 neuronal A_{2A} receptor conditional knockout mice and their littermate controls (12 *CaMKIIα-cre*, A_{2A} *flox/flox* and 12 non-transgenic [no *cre*] A_{2A} *flox/flox* mice) congenic for the C57BL/6 background and with no prior drug experience were obtained from Massachusetts General Hospital (Boston, MA, USA; see Bastia et al., 2005 for details on the generation of these mice). Mice, weighed 15–40 g throughout the course of the experiment, had ad libitum access to lab chow and water, and were group-housed in a colony maintained at 23 °C with a 12-h light/dark cycle (lights on at 0700 h). Studies were conducted according to the University of Connecticut and NIH guidelines for animal care and use.

2.2. Drugs and selection of doses

Pilocarpine (Sigma Aldrich Chemical, St. Louis, MO, USA) was dissolved in 0.9% saline. The adenosine A_{2A} antagonist MSX-3 ((*E*)-phosphoric acid mono-[3-[8-[2-(3-methoxyphenyl)vinyl]-7-methyl-2,6-dioxo-1-prop-2-ynyl-1,2,6,7-tetra-hydropurin-3-yl]propyl] ester) was synthesized at the Pharmazeutisches Institut (Universität Bonn; Bonn, Germany), and dissolved in 0.9% saline. MSX-3 is a pro-drug of the active adenosine A_{2A} antagonist, MSX-2. Extensive pilot work was performed to determine doses, and the dose of 1.0 mg/kg pilocarpine used in experiments 2–4 was based upon the results of the first experiment.

2.3. Behavioral procedure: tremulous jaw movements

Observations took place in a 11.5 × 9.5 × 7.5 cm clear glass chamber with a mesh floor, which was elevated 26 cm from the table top. TJMs were defined as rapid vertical deflections of the lower jaw

Please cite this article as: Salamone, J.D., et al., Conditional neural knockout of the adenosine A_{2A} receptor and pharmacological A_{2A} antagonism reduce pilocarpine-induced tremulous jaw movements: Studies with a mouse model of parkinsonian tremor. European Neuropsychopharmacology (2012), http://dx.doi.org/10.1016/j.euroneuro.2012.08.004

that resembled chewing but were not directed at any particular stimulus (Salamone et al., 1998). Each individual deflection of the jaw was recorded using a mechanical hand counter by a trained observer, who was blind to the experimental condition of the mouse being observed. Separate studies with two observers demonstrated an inter-rater reliability of $r=0.98$ ($p<0.001$) using these methods in mice.

2.4. Experiments

Experiment 1: ability of pilocarpine to induce tremulous jaw movements
Eleven male C57BL/6 mice were used to assess the effect of pilocarpine on TJMs. Mice received IP injections of either 1.0 ml/kg saline or 0.25, 0.5, 0.75, or 1.0 mg/kg pilocarpine in a within-groups design, with all mice receiving all treatments in a randomly varied order (once per week; no treatment sequences were repeated). Five minutes after injection, mice were placed in the observation chamber and allowed 5 min to habituate, after which TJMs were counted for 10 min.

Experiment 2: freeze-frame video analysis of local frequency of the tremulous jaw movements induced by pilocarpine
Three male C57BL/6 mice received an IP injection of 1.0 mg/kg pilocarpine. After five minutes, mice were placed in a flat bottomed mouse restrainer (myNeuroLab.com, Richmond, IL) so that a consistent view of the orofacial area could be achieved. After habituating for 5 min, each mouse was recorded for 15 min using a FlipVideo UltraHD (Cisco Systems, Farmington, CT). The sections of video that allowed for clear observation of the orofacial area were subjected to a freeze-frame analysis (1 frame=1/30 s), in which the observer went frame-by-frame through each burst of jaw movements (i.e. each group of at least two jaw movements that were within 1.0 s of each other). The observer recorded the inter-movement interval for each pair of jaw movements within bursts, which was defined as the number of frames between each point at which the jaw was fully open during successive jaw movements. This information was used to determine the local frequency within bursts of jaw movements.

Experiment 3: ability of the adenosine A_{2A} antagonist MSX-3 to attenuate the tremulous jaw movements induced by pilocarpine
Eleven male C57BL/6 mice were used to assess the effects of the adenosine A_{2A} antagonist MSX-3 on the TJMs induced by 1.0 mg/kg pilocarpine. A within-groups design was utilized for this study, with all mice receiving all drug treatments in a randomly varied order (one treatment per week; no treatment sequences were repeated). On the test day each week, each mouse was given an IP injection of either 1.0 ml/kg saline or 2.5, 5.0, or 10.0 mg/kg MSX-3. After Ten minutes, all mice received an IP injection of 1.0 mg/kg pilocarpine. Five minutes after injections, mice were placed in the observation chamber and allowed 5 min to habituate, after which TJMs were counted for 10 min.

Experiment 4: ability of pilocarpine to induce tremulous jaw movements in mice with a knockout of the adenosine A_{2A} receptor
A total of 24 male C57BL/6 mice ($n=12$ postnatal neuronal A_{2A} receptor conditional KO mice (A_{2A} −/−); $n=12$ littermate controls (A_{2A} +/+)) were used to assess the effect of the knockout of the adenosine A_{2A} receptor on pilocarpine-induced TJMs. For this experiment, only homozygous A_{2A} KO mice and littermate controls were used. All mice received an IP injection of 1.0 mg/kg pilocarpine. Five minutes after IP injection, mice were placed in the observation chamber and allowed 5 min to habituate, after which TJMs were counted for 10 min by an observer blind to the condition of the mouse (i.e. littermate control vs. A_{2A} KO).

2.5. Data analyses

The data for experiments 1 and 3 were analyzed using a repeated measures analysis of variance (ANOVA). Average TJMs over the two five-min observation periods were calculated and then used in the ANOVA calculations (SPSS 12.0 for Windows). When there was a significant ANOVA, planned comparisons using the overall error term were used to assess the differences between each dose and the control condition; the total number of comparisons was restricted to the number of treatments minus one. The behavioral data from the knockout experiment (Experiment 4) was analyzed using Student's t-test for independent samples.

3. Results

3.1. Experiments 1 and 2: ability of pilocarpine to induce tremulous jaw movements.

There was a significant overall effect of pilocarpine treatment on TJM activity (Fig. 1A; $F(4, 40)=24.46$; $p<0.001$). All doses of pilocarpine significantly induced TJMs (planned comparisons, $p<0.001$) compared to the vehicle condition. Fig. 1B displays the results of the freeze-frame video analyses. A total of 509 jaw movements were analyzed. About 83.69% of these jaw movements took place within "bursts," defined as a group of at least two jaw movements that were within 1.0 s of each other. Data are shown as the number of inter-movement intervals (i.e. the number of 1/30 s frames that elapsed from one jaw movement to another) from jaw movements in bursts, assigned to four frequency bins. To interpret these data in terms of frequencies (i.e. jaw movements per second), the reciprocal of the inter-movement interval was calculated (e.g. 10/30 frames per second corresponds to 3 Hz; 4/30 frames per second to 7.5 Hz, etc.) The majority (77.60%) of the TJMs took place in the 3.0–7.5 Hz frequency range. There were no jaw movements in the 1–3 Hz or >10 Hz bins.

3.2. Experiments 3 and 4: ability of adenosine A_{2A} receptor antagonism and knockout attenuate the tremulous jaw movements induced by pilocarpine

The adenosine A_{2A} antagonist MSX-3 attenuated the TJMs induced by 1.0 mg/kg pilocarpine (Fig. 2A). There was a significant overall effect of MSX-3 treatment on pilocarpine-induced TJMs ($F(3,30)=35.88$; $p<0.001$), and the 2.5, 5.0 and 10.0 mg/kg doses of MSX-3 significantly reduced the pilocarpine-induced TJMs (planned comparisons, $p<0.05$). Fig. 2B shows that adenosine A_{2A} receptor neuronal knockout mice (A_{2A} −/−) showed significantly fewer pilocarpine-induced TJMs than their littermate controls ((A_{2A} +/+); $t=2.45$, df=22; $p<0.05$).

4. Discussion

These studies describe the development of a mouse model of TJM activity. Pilocarpine has consistently been shown to induce TJMs in rats (Salamone et al., 1986, 1998; Finn et al., 1997; Betz et al., 2007; Collins et al., 2010), so the first experiment investigated the ability of the pilocarpine to induce TJMs in C57BL/6 mice. Pilocarpine induced TJM

Please cite this article as: Salamone, J.D., et al., Conditional neural knockout of the adenosine A_{2A} receptor and pharmacological A_{2A} antagonism reduce pilocarpine-induced tremulous jaw movements: Studies with a mouse model of parkinsonian tremor. European Neuropsychopharmacology (2012), http://dx.doi.org/10.1016/j.euroneuro.2012.08.004

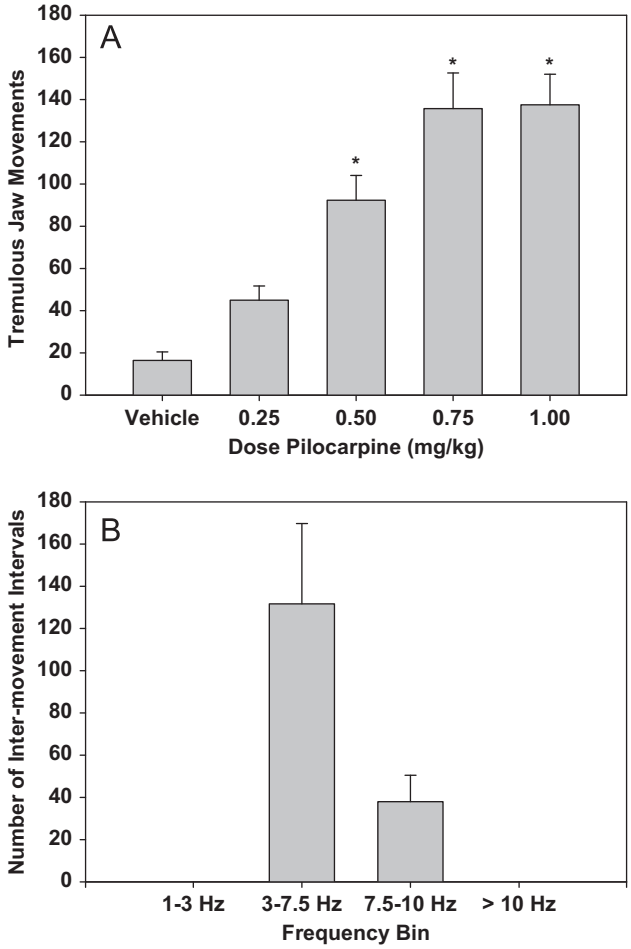

Fig. 1 (A) Effects of different doses of pilocarpine (IP) on tremulous jaw movements. Mean (±SEM) number of jaw movements in mice (n=11) treated with either saline vehicle or pilocarpine. **Significant difference from vehicle control ($p<0.05$). (B) This figure shows the results of the freeze-frame analysis of inter-movement intervals using the video analysis methods described above. Inter-movement times were determined by freeze-frame analysis of video obtained from three mice treated with 1.0 mg/kg pilocarpine, and were assigned to one of four local frequency bins. Distribution of the mean (±SEM) number of inter-movement intervals within each frequency bin is shown.

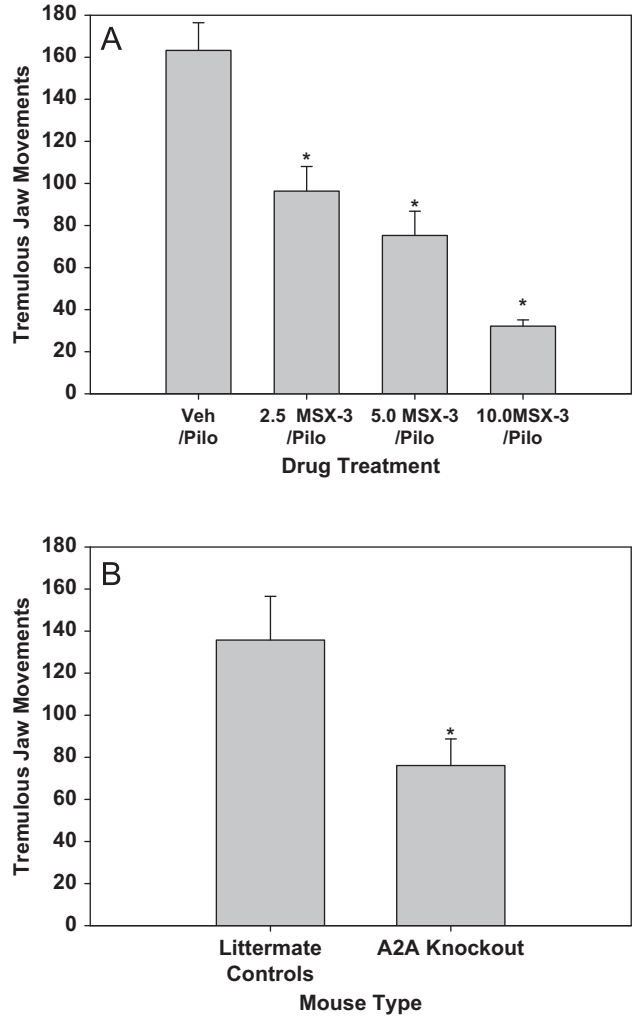

Fig. 2 (A) Effect of the adenosine A_{2A} antagonist MSX-3 on the tremulous jaw movements induced by 1.0 mg/kg pilocarpine. Mean (±SEM) number of jaw movements in mice (n=11) treated with pilocarpine plus vehicle (Veh/Pilo), and pilocarpine (Pilo) plus various doses (2.5, 5.0 and 10.0 mg/kg IP) of MSX-3. *Significant difference from pilocarpine plus vehicle control ($p<0.05$). (B) Effect of neuronal adenosine A_{2A} receptor knockout on the tremulous jaw movements induced by 1.0 mg/kg pilocarpine. Mean (±SEM) number of jaw movements in knockout mice (n=12) and littermate controls (n=12) treated with pilocarpine. *Significant difference from littermate controls ($p<0.05$).

activity in C57BL/6 mice at all doses tested (i.e. 0.25–1.0 mg/kg). This is consistent with the previous research indicating that the administration of pilocarpine induced TJMs in 129SvEv (50%) × CF1 (50%) mice (Salamone et al., 2001). Local frequency analysis of the pilocarpine-induced TJMs in mice indicated that pilocarpine-induced TJMs occurred largely in the 3–7.5 Hz frequency range, which is consistent with the findings from previous studies of the local frequency of TJMs induced by DA depletion, D2 antagonism, and administration of cholinomimetic drugs in rats (Ishiwari et al., 2005; Collins et al., 2010; Collins-Praino et al., 2011). Moreover, this 3–7.5 Hz frequency range is similar to that reported during resting tremor in parkinsonian patients (Deuschl et al., 2001). These findings are consistent with the hypothesis that pilocarpine-induced TJMs pilocarpine are potentially a useful mouse model of parkinsonian resting tremor. Also, the finding that pilocarpine is capable of significantly inducing TJMs in mice highlights the role that ACh plays in striatal motor functions related to parkinsonism. Cholinomimetic drugs, such as muscarinic agonists and anticholinesterases used for the treatment of Alzheimer's disease, have been shown to induce or exacerbate parkinsonian symptoms, including tremor, in humans (Song et al., 2008; Collins-Praino et al., 2011). Furthermore, muscarinic receptor antagonists have been used as treatments for the motor symptoms of parkinsonism (Bezchlibnyk-Butler and Remington, 1994).

Please cite this article as: Salamone, J.D., et al., Conditional neural knockout of the adenosine A_{2A} receptor and pharmacological A_{2A} antagonism reduce pilocarpine-induced tremulous jaw movements: Studies with a mouse model of parkinsonian tremor. European Neuropsychopharmacology (2012), http://dx.doi.org/10.1016/j.euroneuro.2012.08.004

Adenosine A_{2A} antagonists have emerged as a potential treatment of parkinsonian motor impairments. One clinical report suggested that tremor was particularly sensitive to the effects of adenosine A_{2A} antagonism (Bara-Jimenez et al., 2003). Adenosine A_{2A} receptors are highly expressed in neostriatum, and A_{2A} antagonists exert motor effects in rodents and primates that are consistent with antiparkinsonian actions (Ferré et al., 2008; Chen et al., 2001; Salamone et al., 2008; Collins et al., 2010). For that reason, the final two experiments investigated the ability of adenosine A_{2A} receptor antagonism or genetic deletion to attenuate pilocarpine-induced TJMs. The adenosine A_{2A} antagonist MSX-3 significantly attenuated pilocarpine-induced TJMs in mice, which is consistent with previous findings in rats (Correa et al., 2004; Simola et al., 2004; Salamone et al., 2008; Pinna et al., 2010; Collins et al., 2010, 2011). Furthermore, deletion of the adenosine A_{2A} receptor also resulted in significantly lower levels of pilocarpine-induced TJMs compared to wild-type mice. This is consistent with previous research showing that knockout of the adenosine A_{2A} receptor is capable of reversing the catalepsy induced by the DA D1 antagonist SCH 23390, the D2 antagonist haloperidol, and the muscarinic agonist pilocarpine (El Yacoubi et al., 2001). Moreover, genetic deletion of the adenosine A_{2A} receptor in mice has been shown to alter the locomotor response to adenosine antagonists (Yu et al., 2008), and to affect amphetamine sensitization (Chen et al., 2003), self-administration of cocaine and MDMA (Ruiz-Medina et al., 2011), aspects of cognition (Wei et al., 2011), and effort-related choice behavior (Pardo et al., 2012). Furthermore, mice lacking striatal adenosine A_{2A} receptors showed an absence of motor stimulation in response to adenosine A_{2A} antagonists (Yu et al., 2008; Wei et al., 2011).

The present results demonstrate the feasibility of using the TJM model in mice, and indicate that adenosine A_{2A} receptor antagonism and deletion are capable of reducing cholinomimetic-induced TJMs in mice. These findings add to growing evidence demonstrating that adenosine A_{2A} function is involved in regulating motor functions in animals that are potentially related to parkinsonism. Additional studies should further characterize the effects of adenosine A_{2A} receptor deletion on motor function, and should investigate the effects regionally-specific knockout of A_{2A} receptors (e.g. Lazarus et al., 2011).

Role of funding sources

This work was supported by grants to John Salamone from the University of Connecticut Research Foundation, which paid for all animals, supplies and equipment, except for the A_{2A} knockout mice and littermate controls, which were provided by a grant from Michael Schwarzschild from NIH (K24NS60991) and DoD (W81XWH-11-1-0150), Mercè Correa was supported by a grant from Fundació Bancaixa-UJI (P1.1B2010-43) and Caja Navarra, and Marta Pardo received a travel grant from Fundació Bancaixa-UJI.

Contributors

All authors contributed significantly to this manuscript. The work is part of the Ph.D. dissertations of L. Collins and M. Pardo. L. Collins, M. Pardo, S. Podurgiel and M. Correa performed the behavioral studies. Y. Baqi and C.E. Müller provided the MSX-3, and M. Schwarzschild provided the kockout mice. J. Salamone and M. Correa supervised the entire project.

Conflict of interest

There are no conflicts of interest connected to this work. In addition to the income received from my primary employer, compensation has been received from Merck-Serono and Pfizer within the last 3 years. There are no personal financial holdings that could be perceived as constituting a potential conflict of interest.

Acknowledgments

This work was supported by grants to John Salamone from the University of Connecticut Research Foundation, Michael Schwarzschild from NIH (K24NS60991) and DoD (W81XWH-11-1-0150), Mercè Correa from Fundació Bancaixa-UJI (P1.1B2010-43) and Caja Navarra, and Marta Pardo from Fundació Bancaixa-UJI.

References

Bara-Jimenez, W., Sherzai, A., Dimitrova, T., Favit, A., Bibbiani, F., Gillespie, M., Morris, M.J., Mouradian, M.M., Chase, T.N., 2003. Adenosine A(2A) receptor antagonist treatment of Parkinson's disease. Neurology 61, 293–296.

Bastia, E., Xu, Y.H., Scibelli, A.C., Day, Y.J., Linden, J., Chen, J.F., Schwarzschild, M.A., 2005. A crucial role for forebrain adenosine A(2A) receptors in amphetamine sensitization. Neuropsychopharmacology 30, 891–900.

Betz, A.J., McLaughlin, P.J., Burgos, M., Weber, S.M., Salamone, J.D., 2007. The muscarinic receptor antagonist tropicamide suppresses tremulous jaw movements in a rodent model of parkinsonian tremor: possible role of M4 receptors. Psychopharmacology 194, 347–359.

Betz, A.J., Vontell, R., Valenta, J., Worden, L., Sink, K.S., Font, L., Correa, M., Sager, T.N., Salamone, J.D., 2009. Effects of the adenosine A_{2A} antagonist KW-6002 (istradefylline) on pimozide-induced oral tremor and striatal c-Fos expression: comparisons with the muscarinic antagonist tropicamide. Neuroscience 163, 97–108.

Bezchlibnyk-Butler, K.Z., Remington, G.J., 1994. Antiparkinsonian drugs in the treatment of neuroleptic-induced extrapyramidal symptoms. Can. J. Psychiat 39, 74–84.

Chen, J.F., Moratalla, R., Impagnatiello, F., Grandy, D.K., Cuellar, B., Rubinstein, M., Beilstein, M.A., Hacket, E., Fink, J.S., Low, M.J., Ongini, E., Schwarzschild, M.A., 2001. The role of the D2 dopamine receptor (D2R) in A2A adenenosine-receptor (A2aR) mediated behavioral and cellular responses as revealed by A2A and D2 receptor knockout mice. Proc. Natl. Acad. Sci. 98, 1970–1975.

Chen, J.F., Fredduzzi, S., Bastia, E., Yu, L., Moratalla, R., Ongini, E., Schwarzschild, M.A., 2003. Adenosine A_{2A} receptors in neuroadaptation to repeated dopaminergic stimulation: implications for the treatment of dyskinesias in Parkinson's disease. Neurology 61, S74–S81.

Collins, L.E., Galtieri, D.J., Brennum, L.T., Sager, T.N., Hockemeyer, J., Müller, C.E., Hinman, J.R., Chrobak, J.J., Salamone, J.D., 2010. Cholinomimetic-induced tremulous jaw movements are suppressed by the adenosine A_{2A} antagonists MSX-3 and SCH58261, but not the adenosine A_1 antagonist DPCPX: possible relevance for drug-induced parkinsonism. Pharmacol. Biochem. Behav. 94, 561–569.

Collins, L.E., Paul, N.E., Abbas, S.F., Leser, C.E., Galtieri, D.J., Chrobak, J.J., Baqi, Y., Muller, C.E., Salamone, J.D., 2011. Oral tremor induced by galantamine in rats: a model of the parkinsonian side effects of cholinomimetics used to treat Alzheimer's disease. Pharmacol. Biochem. Behav. 99, 414–422.

Collins-Praino, L.E., Paul, N.E., Rychalsky, K.L., Hinman, J.R., Chrobak, J.J., Senatus, P.B., Salamone, J.D., 2011. Pharmacological and physiological characterization of the tremulous jaw movement model of parkinsonian tremor: potential insights into the pathophysiology of tremor. Front. Syst. Neurosci. 5, 49.

Correa, M., Wisniecki, A., Betz, A., Dobson, D.R., O'Neill, M.F., O'Neill, M.J., Salamone, J.D., 2004. The adenosine A_{2A} antagonist KF 17837 reverses the locomotor suppression and tremulous jaw movements induced by haloperidol in rats: possible relevance to parkinsonism. Behav. Brain Res. 148, 47–54.

Deuschl, G., Raethjen, J., Lindemann, M., Krack, P., 2001. The pathophysiology of tremor. A review. Muscle Nerve 24, 716–735.

El Yacoubi, M., Ledent, C., Parmentier, M., Costentin, J., Vaugeois, J.M., 2001. Adenosine A_{2A} receptor knockout mice are partially protected against drug-induced catalepsy. Neuroreport 12, 983–986.

Finn, M., Jassen, A., Baskin, P., Salamone, J.D., 1997. Tremulous characteristic of vacuous jaw movements induced by pilocarpine and ventrolateral striatal dopamine depletions. Pharmacol. Biochem. Behav. 57, 243–249.

Ferré, S., Quiroz, C., Woods, A.S., Cunha, R., Popoli, P., Ciruela, F., Lluis, C., Franco, R., Azdad, K., Schiffmann, S.N., 2008. An update on adenosine A_{2A}-dopamine D2 receptor interactions: implications for the function of G protein-coupled receptors. Curr. Pharm. Des. 14, 1468–1474.

Ishiwari, K., Betz, A., Weber, S., Felsted, J., Salamone, J.D., 2005. Validation of the tremulous jaw movement model for assessment of the motor effects of typical and atypical antipychotics: effects of pimozide (Orap) in rats. Pharmacol. Biochem. Behav. 80, 351–362.

Jicha, G., Salamone, J.D., 1991. Vacuous jaw movements and feeding deficits in rats with ventrolateral striatal dopamine depletions: possible model of parkinsonian symptoms. J. Neurosci. 11, 3822–3829.

Lazarus, M., Shen, H.Y., Cherasse, Y., Qu, W.M., Huang, Z.L., Bass, C.E., Winsky-Sommerer, R., Semba, K., Fredholm, B.B., Boison, D., Hayaishi, O., Urade, Y., Chen, J.F., 2011. Arousal effect of caffeine depends on adenosine A_{2A} receptors in the shell of the nucleus accumbens. J. Neurosci. 31, 10067–10075.

LeWitt, P.A., Guttman, M., Tetrud, J.W., Tuite, P.J., Mori, A., Chaikin, P., Sussman, N.M., 600-US-005 Study Group, 2008. Adenosine A_{2A} receptor antagonist istradefylline (KW-6002) reduces "off" time in Parkinson's disease: a double-blind, randomized, multicenter clinical trial (6002-US-005). Ann. Neurol. 63, 295–302.

Miwa, H., Kubo, T., Suzuki, A., Kondo, T., 2009. Effects of zonisamide on c-Fos expression under conditions of tacrine-induced tremulous jaw movements in rats: a potential mechanism underlying its anti-parkinsonian tremor effect. Parkinsonism Relat. Disord. 15, 30–35.

Pardo, M., Lopez-Cruz, L., Valverde, O., Ledent, C., Baqi, Y., Müller, C.E., Salamone, J.D., Correa, M., 2012. Adenosine A_{2A} receptor antagonism and genetic deletion attenuate the effects of dopamine D2 antagonism on effort-based decision making in mice. Neuropharmacology 62, 2068–2077.

Pinna, A., Schintu, N., Simola, N., Volpini, R., Pontis, S., Cristalli, G., Morelli, M., 2010. A new ethyladenine antagonist of adenosine A(2A) receptors: behavioral and biochemical characterization as an anti-parkinsonian drug. Neuropharmacology 58, 613–623.

Ruiz-Medina, J., Ledent, C., Carreton, O., Valverde, O., 2011. The A_{2A} adenosine receptor modulates the reinforcing efficacy and neurotoxicity of MDMA. J. Psychopharmacol. 25, 550–564.

Salamone, J.D., Lalies, M.D., Channell, S.L., Iversen, S.D., 1986. Behavioural and pharmacological characterization of the mouth movements induced by muscarinic agonists in the rat. Psychopharm. 88, 467–471.

Salamone, J.D., Mayorga, A.J., Trevitt, J.T., Cousins, M.S., Conlan, A., Nawab, A., 1998. Tremulous jaw movements in rats: a model of parkinsonian tremor. Prog. Neurobiol. 56, 591–611.

Salamone, J.D., Correa, M., Carlson, B., Wisniecki, A., Mayorga, A., Nisenbaum, E., Nisenbaum, L., Felder, C., 2001. Neostriatal muscarinic receptor subtypes involved in the generation of tremulous jaw movements in rodents. Implications for cholinergic involvement in parkinsonism. Life Sci. 68, 2579–2584.

Salamone, J.D., Carlson, B.B., Rios, C., Lentini, E., Correa, M., Wisniecki, A., Betz, A., 2005. Dopamine agonists suppress cholinomimetic-induced tremulous jaw movements in an animal model of Parkinsonism: tremorolytic effects of pergolide, ropinirole and CY 208-243. Behav. Brain Res. 156, 173–179.

Salamone, J.D., Betz, A.J., Ishiwari, K., Felsted, J., Madson, L., Mirante, B., Clark, K., Font, L., Korbey, S., Sager, T.N., Hockemeyer, J., Muller, C.E., 2008. Tremorolytic effects of adenosine A_{2A} antagonists: implications for parkinsonism. Front. Biosci. 13, 3594–3605.

Schwarzschild, M.A., Agnati, L., Fuxe, K., Chen, J.F., Morelli, M., 2006. Targeting adenosine A_{2A} receptors in Parkinson's disease. Trends Neurosci. 29, 647–654.

Simola, N., Fenu, S., Baraldi, P.G., Tabrizi, M.A., Morelli, M., 2004. Blockade of adenosine A_{2A} receptors anatagonizes parkinsonian tremor in the rat tacrine model by an action on specific striatal regions. Exp. Neurol. 189, 182–188.

Song, I.U., Kim, J.S., Ryu, S.Y., Lee, S.B., An, J.Y., Lee, K.S., 2008. Donepezil-induced jaw tremor. Parkinson. Rel. Disord. 14, 584–585.

Wei, C.J., Li, W., Chen, J.F., 2011. Normal and abnormal functions of adenosine receptors in the central nervous system as revealed by genetic knockout studies. Biochim. Biophys. Acta 1808, 1358–1379.

Yu, L., Shen, H.Y., Coelho, J.E., Araújo, I.M., Huang, Q.Y., Day, Y.J., Rebola, N., Canas, P.M., Rapp, E.K., Ferrara, J., Taylor, D., Müller, C.E., Linden, J., Cunha, R.A., Chen, J.F., 2008. Adenosine A_{2A} receptor antagonists exert motor and neuroprotective effects by distinct cellular mechanisms. Ann. Neurol. 63, 338–346.

Please cite this article as: Salamone, J.D., et al., Conditional neural knockout of the adenosine A_{2A} receptor and pharmacological A_{2A} antagonism reduce pilocarpine-induced tremulous jaw movements: Studies with a mouse model of parkinsonian tremor. European Neuropsychopharmacology (2012), http://dx.doi.org/10.1016/j.euroneuro.2012.08.004